Physics – Uspekhi **60** (8) 762 – 797 (2017)

REVIEWS OF TOPICAL PROBLEMS PACS numbers: 64.60.ae, 64.60.Cn, 64.60.Ht

Nonequilibrium critical behavior of model statistical systems and methods for the description of its features

V V Prudnikov, P V Prudnikov, M V Mamonova

DOI: https://doi.org/10.3367/UFNe.2017.02.038067

Contents

Abstract. This paper reviews features in critical behavior of far-from-equilibrium macroscopic systems and presents current methods of describing them by referring to some model statistical systems such as the three-dimensional Ising model and the two-dimensional *XY* model. The paper examines the critical relaxation of homogeneous and structurally disordered systems subjected to abnormally strong fluctuation effects involved in ordering processes in solids at second-order phase transitions. Interest in such systems is due to the aging properties and fluctuation–dissipation theorem violations predicted for and observed in systems slowly evolving from a nonequilibrium initial state. It is shown that these features of nonequilibrium behavior show up in the magnetic properties of magnetic superstructures consisting of alternating nanoscale-thick magnetic and nonmagnetic layers and can be observed not only near the film's critical ferromagnetic ordering temperature T_c, but also over the wide temperature range $T \leqslant T_c$.

Keywords: phase transitions and critical phenomena, nonequilibrium behavior, systems with slow dynamics, disordered systems, aging effects, fluctuation–dissipation relation, multilayer magnetic structures, Monte Carlo simulations

V V Prudnikov, P V Prudnikov, M V Mamonova
Dostoevsky Omsk State University,
prosp. Mira 55A, 644077 Omsk, Russian Federation
E-mail: prudnikv@univer.omsk.su

Received 14 September 2016
Uspekhi Fizicheskikh Nauk **187** (8) 817 – 855 (2017)
DOI: https://doi.org/10.3367/UFNr.2017.02.038067
Translated by Yu V Morozov; edited by A Radzig

1. Introduction

Systems with slow dynamics have recently evoked heightened interest on the part of both theorists and experimentalists [1–4] by virtue of aging properties characterized by fluctuation–dissipation theorem violations predicted for and observed in systems slowly evolving from a nonequilibrium initial state. Well-known examples of such systems with slow dynamics and manifestations of aging effects are such complex disordered systems as spin glasses [5–7]. Figure 1 demonstrates aging effects for $Ag_{0.973}Mn_{0.027}$ spin glass revealed in experiments. However, a number of analytical and numerical studies [8–11] have shown that such nonequilibrium behavior features can just as well occur in systems undergoing second-order phase transitions, because their critical dynamics are characterized by abnormally large relaxation times. To recall, the fluctuation–dissipation relation introduced earlier for spin glasses and linking the two-time spin response function with the two-time correlation function and generalizing the fluctuation–dissipation theorem for the case of nonequilibrium behavior is a new universal characteristic of critical behavior in various systems [8].

Importantly, specific features of nonequilibrium critical dynamics discovered thus far provide a basis for an adequate interpretation of experimental data obtained for multilayer Fe/Cr [12] and Co/Cr [13] structures. Suffice it to mention the recent paper [12] reporting the nonergodic behavior of a

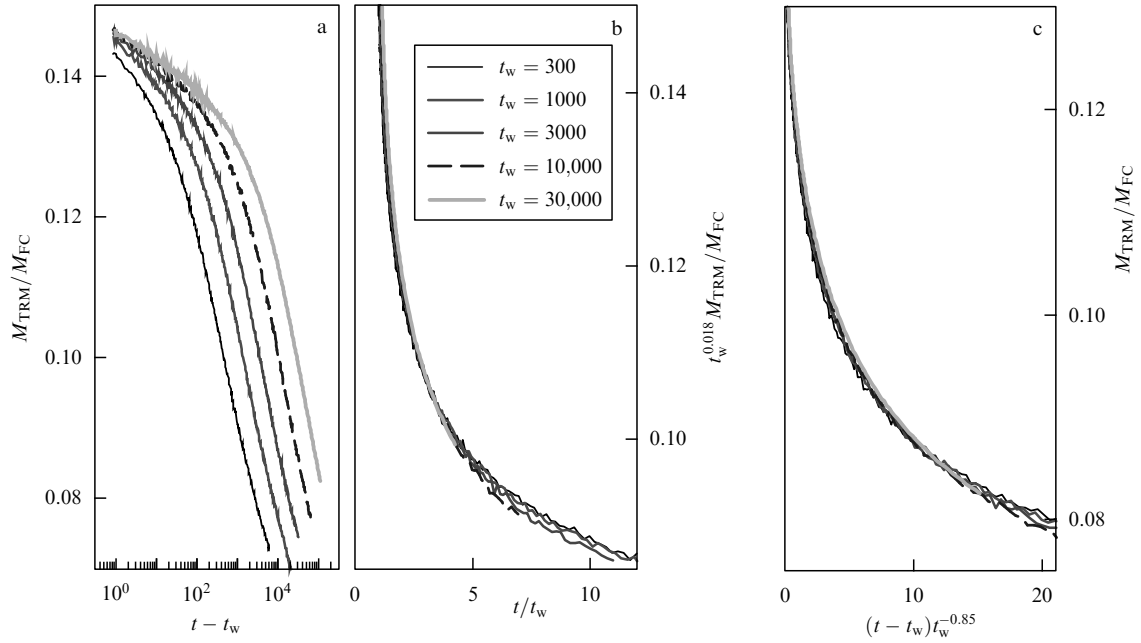

Figure 1. (a) Aging effects identified in the two-time dependence of thermoremanent magnetization M_{TRM} on observation time $t - t_w$ and waiting time t_w in $Ag_{0.973}Mn_{0.027}$ spin glass at $T = 0.87\,T_c$ during evolution from a high-temperature initial state. Times are measured in seconds. M_{FC} is the magnetization measured as the system moved from the paramagnetic to spin-glass state upon cooling in a weak magnetic field, T_c is the temperature of phase transition into the spin-glass phase. Verification results of the realization of two possible scaling forms: canonical aging (b) and subaging (c) for the $M_{TRM}/M_{FC}\,(t - t_w, t_w)$ function demonstrating characteristic 'collapse' of the values in the universal curve for different t_w. (Data according to M Ocio, J Hammann, E Vincent, borrowed from Ref. [2].)

multilayer Fe/Cr structure based on a periodic combination of ultrathin ferromagnetic iron films with nonmagnetic chromium films characterized by the dependence of magnetization of the sample on its magnetic prehistory.

As shown in Ref. [13], investigations into the relaxation of magnetization revealed magnetic aging effects in a Co/Cr-based magnetic superstructure. The nanoscale periodicity produces in such magnetic multilayer structures mesoscopic effects of spatial spin correlation with slow relaxation dynamics of magnetization upon quenching the system in a nonequilibrium state. Unlike bulk magnetic systems where slow dynamics and aging effects manifest themselves near the critical point, magnetic superstructures with nanoscale periodicity allow increasing the relaxation time owing to the effects related to the larger characteristic spin–spin correlation length. Due to this, aging and nonergodicity effects are possible to observe in multilayer magnetic structures within a wider temperature range than in bulk magnetic systems.

The present review considers the results of theoretical renormalization group and numerical studies reported recently for such universal quantities as the fluctuation–dissipation relation and critical parameters characterizing nonequilibrium critical dynamics of various statistical models. Particular emphasis is laid on the original data obtained by the authors in computer simulation of the three-dimensional Ising model and the two-dimensional XY model. Special attention is given to the results of numerical Monte Carlo (MC) simulations of the influence of structural defects on characteristics of the nonequilibrium critical behavior of spin systems. On the one hand, the relaxation dynamics of such systems are much easier to study than those of complex disordered systems, e.g., spin glasses; on the other hand, at the nonequilibrium stage of critical evolution these systems demonstrate aging effects analogous to those in spin glasses and deviation from unity of the limiting fluctuation–dissipation relation (FDR) as an indicator of the system departure from equilibrium.

The renormalization group [14, 15], numerical [16–19], and experimental [20] methods for investigations into critical dynamics of structurally disordered systems have made it possible to unambiguously establish that both uncorrelated structural defects and defects with long-range correlation effects present in a system are responsible for emerging new types of critical behavior and marked strengthening of critical slow-down effects, as opposed to those in 'pure' systems. Due to this, specific features of nonequilibrium behavior, such as aging effects, must certainly be much more pronounced in structurally disordered systems with new universal values of the fluctuation–dissipation relation.

Renormalization group calculations of FDR carried out in Refs [21, 22] in the framework of the ε-expansion method for dissipative models with the nonconserved order parameter in the lower orders of the theory showed that difficulties encountered in distinguishing fluctuation corrections in two-time dependences for the correlation function and the response function have thus far prevented any convincing characteristic of the influence of defects on the relative correspondence between the limiting FDR values for structurally disordered and 'pure' Ising models. Numerical studies by the inherently nonperturbative Monte Carlo method permitted clarifying this issue and distinguishing the influence of structural defects on aging effects and FDR contribution to the nonequilibrium critical behavior of the three-dimensional Ising model and the two-dimensional XY model.

The review presents, in addition, results of our numerical studies [23] on the nonequilibrium behavior and aging effects

in multilayer magnetic structures composed of ferromagnetic films separated by an interlayer of a nonmagnetic metal. Specific behavioral features of these structures revealed by the MC methods permit us not only to account for magnetic aging effects manifested as relaxation of thermoremanent magnetization in experiments with Co/Cr magnetic superstructures [13] but also to identify aging effects in the autocorrelation function nonequilibrium behavior during evolution of the system from different initial states. It has been shown that aging effects in multilayer magnetic structures are apparent within a wide temperature range and not only near the critical temperature, as in bulk systems. Certainly, these aging effects should be taken into consideration in practical applications of such multilayer magnetic nanostructures as spintronic devices with a giant magnetic resistance effect.

2. Basic concepts and model representations of the nonequilibrium behavior theory

Aging effects manifested at the nonequilibrium stage of relaxation of a slow-dynamics system are characterized by the presence of two-time dependences of such functions as correlation and response functions on waiting t_w and observation $t - t_w$ times; t_w is the time between a specimen preparation and the beginning of measurement of its characteristics. During the time period $t - t_w \ll t_{rel}$, where t_{rel} is the system's relaxation time, the temporal behavior of the system is influenced by its initial state and aging effects characterized by both translation symmetry breaking in time and a slow-down of relaxation and correlation processes with increasing 'age' t_w of the specimen.

It is supposed that the nonequilibrium behavior of a system is realized via its transition at the starting instant $t = 0$ from the initial state at temperature T_0 to the state with temperature T_s differing from T_0. The accompanying equilibration process is characterized by relaxation time $t_{rel}(T_s)$, and equilibrium corresponding to temperature T_s is reached in times $t \gg t_{rel}(T_s)$, while the system dynamics prove stationary and invariant with respect to time reversal. However, in times $0 < t \ll t_{rel}(T_s)$, the evolution of the system depends on its initial state. In this connection, the nonequilibrium behavior of the system depends on whether it evolves from a high-temperature ($T_0 > T_s$) or a low-temperature ($T_0 < T_s$) initial state.

At temperatures close to the temperature T_c of the second-order phase transition, the system's relaxation time t_{rel} is a diverging quantity: $t_{rel} \sim |T - T_c|^{-zv}$, where z and v are the dynamic critical exponent and correlation length exponent, respectively. Therefore, the system does not reach equilibrium at a critical point throughout the entire relaxation process; at $T_s \simeq T_c$ and for times $t \ll t_{rel}$, aging effects in the two-time dependence can be expected for the correlation function $C(t, t_w)$ and the external perturbation response function $R(t, t_w)$.

For a spin system with the spin density $S(x, t)$, the temporal correlation function is given by the expression

$$C(t, t_w) = \frac{1}{V}\int \langle S(x, t)S(x, t_w)\rangle \, d^d x - \frac{1}{V}\int \langle S(x, t)\rangle\langle S(x, t_w)\rangle \, d^d x , \quad (1)$$

and the response function for a weak external magnetic field $h(x, t)$ applied to the system at instant t_w by the relation

$$R(t, t_w) = \frac{1}{V}\int d^d x \left.\frac{\delta\langle S(x, t)\rangle}{\delta h(x, t_w)}\right|_{h=0} . \quad (2)$$

In formulas (1), (2), d is the space dimension, and $\mathbf{x}$ is the d-dimensional radius vector. In accordance with the causality principle, $R(t, t_w > t) = 0$.

According to the general picture of a relaxation process, one expects that for $t > t_w \gg t_{rel}(T_s)$ $C(t, t_w) = C^{eq}(t - t_w)$ and $R(t, t_w) = R^{eq}(t - t_w)$, where C^{eq} and R^{eq} are the corresponding equilibrium quantities. The fluctuation–dissipation theorem (FDT) relates the fluctuation spectrum of physical quantities in an equilibrium dissipative medium to its generalized susceptibilities, i.e., parameters characterizing its reaction to an external action.

The main feature of the nonequilibrium behavior of a slow-dynamics system is the breakdown of translational invariance in time due to the long-time influence of nonequilibrium initial states. It manifests itself first and foremost as two-time characteristics of the system, such as the correlation functions and response functions.

The nonequilibrium behavior of slow-dynamics systems is characterized not only by aging effects but also by violation of the FDT [1–4, 8], the consequences of which provide theoretical grounds of various experimental methods for the measurement of radiation scattering and absorption by matter. Under equilibrium conditions, the FDT should relate the correlation function with the linear response function conjugate to it:

$$R^{eq}(t - t_w) = \frac{1}{T_s}\frac{dC^{eq}(t - t_w)}{dt_w} . \quad (3)$$

In the case of nonequilibrium behavior of systems for $t, t_w \ll t_{rel}$, the generalized FDT assumes the form

$$R(t, t_w) = \frac{X(t, t_w)}{T_s}\frac{\partial C(t, t_w)}{\partial t_w} , \quad (4)$$

with the introduced quantity $X(t, t_w)$ being the fluctuation–dissipation ratio (FDR):

$$X(t, t_w) = \frac{T_s R(t, t_w)}{\partial_{t_w} C(t, t_w)} , \quad (5)$$

with $t > t_w$ as a measure of FDT violation. In equilibrium, the FDT states that $X(t > t_w \gg t_{rel}) = 1$. The asymptotic value of the FDR, viz.

$$X^\infty = \lim_{t_w\to\infty}\lim_{t\to\infty} X(t, t_w) , \quad (6)$$

can be used as a universal characteristic of the nonequilibrium behavior of a slow-dynamics system. Moreover, the value of $X^\infty \neq 1$ may provide an indication of the nonequilibrium behavior of the system. Also, X^∞ can be used to define effective nonequilibrium temperature $T_{eff} = T/X^\infty$ exhibiting certain properties of the equilibrium system temperature, i.e., characterizing the direction of thermal flows in the system and serving as a criterion for its thermalization [24].

Let us turn to the general properties of X^∞ and its dependence on the system's quenching temperature T_s. For those states of the system with temperature $T_s > T_c$, it follows from the FDT that $X^\infty(T_s > T_c) = 1$. On the other hand, the

Table 1. Limiting FDR values X^∞ for systems with a high-temperature initial state with $m_0 \ll 1$.

Model	Solution	X^∞			References
		$T_s < T_c$	$T_s = T_c$	$T_s > T_c$	
Free Gaussian field	Exact	—	1/2	1	[28]
d-dimensional spherical model	Exact	0	$1 - 2/d$	1	[27]
One-dimensional Ising model	Exact	—	1/2	1	[29]
Two-dimensional Ising model	MC MC MC		0.26(1) 0.340(5) 0.330(5)		[27] [30] [31, 32]
Two-dimensional Potts model with $q = 3$ spin states	MC		0.406(1)		[31, 32]
Two-dimensional Potts model with $q = 4$ spin states	MC		0.459(8)		[31, 32]
Three-dimensional Ising model	MC	0	≈ 0.40 *		[27]
Three-dimensional XY model	MC	0	0.43		[33]

* X^∞ value of ≈ 0.40 is reported in Ref. [27] as a result of preliminary numerical investigations of three-dimensional Ising model without demonstrations of the data obtained in Ref. [27] itself and in subsequent publications.

general scaling arguments in Ref. [25] suggest that for a low-temperature ordered phase with $T_s < T_c$, $X^\infty(T_s < T_c) = 0$. It is believed that these results are unrelated to specific properties of individual systems. In the case of $T_s = T_c$, however, there are no general arguments defining the value of $X^\infty(T_c)$, which necessitates its derivation for each individual statistical model. Table 1 contains X^∞ values for some statistical models, which were found either by exact solutions or in numerical studies by the MC methods (Ref. [26] presents a more comprehensive table for X^∞).

It follows from Table 1 that $X^\infty(T_s = T_c)$ depends on specific properties of the model and its spatial dimension d. At the same time, the authors of Refs [25, 27] argue, based on scaling arguments, that the limiting FDR $X^\infty(T_s = T_c)$ at the critical temperature must be a universal quantity associated with the universality class of the model's critical dynamics.

2.1 Nonequilibrium critical dynamics of systems evolving from a high-temperature initial state

2.1.1 Scaling forms for two-time dependences of the autocorrelation function and response function. It is presently well known that the two-time autocorrelation function and response function for system relaxation from a high-temperature initial state with $m_0 = 0$ (or $m_0 \ll 1$) satisfy the following scaling forms:

$$C(t, t_w) = A_C(t - t_w)^{a+1-d/z}\left(\frac{t}{t_w}\right)^{\theta-1} f_C\left(\frac{t_w}{t}\right),$$
$$R(t, t_w) = A_R(t - t_w)^{a-d/z}\left(\frac{t}{t_w}\right)^{\theta} f_R\left(\frac{t_w}{t}\right), \qquad (7)$$

where functions $f_C(t_w/t)$ and $f_R(t_w/t)$ are finite for $t_w \to 0$, $a = (2 - \eta - z)/z$, $\theta = \theta' - (2 - z - \eta)/z$, and θ' is the critical exponent characterizing the initial growth of magnetization [34]. A_R and A_C are nonuniversal amplitudes, the values of which are given by conditions $f_{R,C}(0) = 1$. Under these normalizing conditions, functions $f_{R,C}$ acquire universal properties. The given scaling forms suggest the universality of X^∞ expressed as the amplitude ratio: $X^\infty = A_R/[(1 - \theta)A_C]$ [25–27].

One of the unusual properties of the nonequilibrium critical behavior of systems relaxing from a high temperature initial state with $m_0 \ll 1$ is a rise in magnetization with growing observation time in accordance with the power-law function $M(t) \sim t^{\theta'}$ for times $t < t_{cr} \sim m_0^{-1/[\theta' + \beta/(z\nu)]}$ (an example of such magnetization behavior $M(t)$ for the three-dimensional Ising model with different spin concentrations is presented in Fig. 2).

Indeed, the singular part of the Gibbs potential $\Phi_{sing}(t, \tau, h, m_0)$ determining the system's state in the critical region is characterized, in accordance with the scaling theory, by generalized uniformity with respect to the main thermodynamic variables:

$$\Phi_{sing}(t, \tau, h, m_0) = b\Phi_{sing}(b^{a_t} t, b^{a_\tau}\tau, b^{a_h} h, b^{a_m} m_0), \qquad (8)$$

time t, reduced temperature τ, field h, and initial magnetization m_0; here, b is the similarity factor, and a_i are the similarity exponents. As a result, magnetization $M = -\delta\Phi/\delta h$ at the

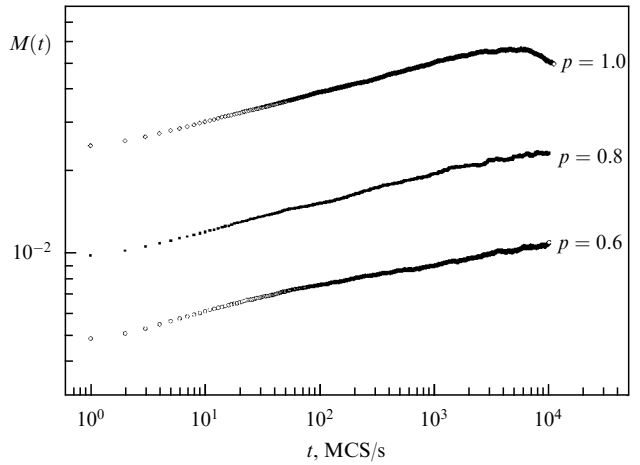

Figure 2. Time dependence of magnetization $M(t)$ at the nonequilibrium stage of evolution of the three-dimensional Ising model for different spin concentrations p at respective critical temperatures. MCS/s (Monte Carlo steps per spin).

critical point ($\tau = 0$, $h = 0$) is characterized by the following time dependence:

$$M(t, m_0) = t^{-(a_h+1)/a_t} F_m(m_0 t^{-a_m/a_t}), \tag{9}$$

where $F_m(m_0 t^{-a_m/a_t})$ is the scaling magnetization function. The expansion of the right-hand side of formula (9) in powers of small parameter $m_0 t^{-a_m/a_t}$ leads to the power-law dependence

$$M(t) \sim t^{-(a_h+a_m+1)/a_t} \sim t^{\theta'}. \tag{10}$$

All a_i but a_m can be related to the known critical exponents describing the system's behavior regardless of effects of the influence of nonequilibrium initial states. Therefore, the authors of Ref. [34] introduced a new independent dynamic critical exponent θ' that assumes a positive value, as shown in the renormalization group description of the nonequilibrium critical behavior of the system [34].

The nonequilibrium stage of the initial magnetization growth is followed for times $t \gg t_{\rm cr}$ by ordinary long-time dynamics of magnetization reduction with time according to the power-law $M(t) \sim t^{-\beta/(z\nu)}$. The critical exponents θ and θ' depending on the system's dynamic universality class of the critical behavior [35] were calculated by renormalization group methods for certain dynamic models, e.g., the model with a nonconserved order parameter [14, 16, 34, 36] (model A according to the Hohenberg–Halperin classification [35]), the model with the order parameter coupled to the conserved field (model C) [37], and the models with the order parameter coupled to hydrodynamic excitations having the character of precessional motion in magnets (models E, F, G, and J) [38].

The analysis of two-time dependences for autocorrelation and response functions [7] in the nonequilibrium process of system's relaxation allows three stages (regimes) of its execution to be distinguished. First is the quasiequilibrium stage of evolution for small waiting times, $t - t_{\rm w} \ll t_{\rm w}$ with $t_{\rm w} \gg 1$, when the dependence of the autocorrelation and response functions on waiting time is still unapparent and their changes have a stationary character: $C = C(t - t_w) \sim (t - t_{\rm w})^{-(d-2+\eta)/z}$ and $R = R(t - t_{\rm w}) \sim (t - t_{\rm w})^{-(d-2+\eta+z)/z}$. The second stage with manifestations of aging effects is realized for times $t - t_{\rm w} \sim t_{\rm w} \gg 1$. At this stage, the two-time dependence is quite apparent for autocorrelation and response functions characterized by the relations

$$\begin{aligned} C(t, t_{\rm w}) &\sim t_{\rm w}^{-2\beta/(\nu z)} \hat{F}_C\left(\frac{t}{t_{\rm w}}\right), \\ R(t, t_{\rm w}) &\sim t_{\rm w}^{-2\beta/(\nu z)-1} \hat{F}_R\left(\frac{t}{t_{\rm w}}\right), \end{aligned} \tag{11}$$

in which $\hat{F}_C(t/t_{\rm w})$ and $\hat{F}_R(t/t_{\rm w})$ are the scaling functions, and the relationship between critical exponents $2\beta/(\nu z) = d/z - a - 1$ is used. As a result, the curves for these functions on the observation timescale $t - t_{\rm w}$ do not coincide for different waiting times $t_{\rm w}$ and have, in accordance with Eqn (11), different slopes for each $t_{\rm w}$ value. For the third stage, with an essential nonequilibrium evolution of the system for observation times $t - t_{\rm w} \gg t_{\rm w} \gg 1$, scaling functions $\hat{F}_C(t/t_{\rm w})$ and $\hat{F}_R(t/t_{\rm w})$ in Eqn (11) are characterized by the decreasing power-law dependences

$$\hat{F}_C\left(\frac{t}{t_{\rm w}}\right) \sim \left(\frac{t}{t_{\rm w}}\right)^{-c_a}, \quad \hat{F}_R\left(\frac{t}{t_{\rm w}}\right) \sim \left(\frac{t}{t_{\rm w}}\right)^{-c_r}, \tag{12}$$

with the exponent $c_a = d/z - \theta'$ coincident with the exponent defining the time dependence of the autocorrelation function in the short-time regime ($t_{\rm w} \to 0$, $t \gg 1$) of the system's nonequilibrium critical behavior [16, 18, 39]. At this stage of short-time dynamics, aging effects are unapparent. The scaling analysis of the behavior of the response function $R(t, t_{\rm w})$ in this regime predicts that $c_r = c_a$.

2.1.2 Renormalization group description of the nonequilibrium critical behavior. Relaxation times of the order parameter $S(x, t)$ (spin density) near the critical point are very long; therefore, the nonequilibrium dynamics of the order parameter under these conditions are a random slow process. The nonequilibrium distribution function $P[S]$ of such processes must satisfy the Fokker–Planck equation

$$\begin{aligned} \partial_t P = &- \sum_{\alpha=1}^{n} \int \mathrm{d}^d x \, \frac{\delta\left(f_\alpha(x,t) P\right)}{\delta S_\alpha(x,t)} \\ &+ \sum_{\alpha,\beta}^{n} C_{\alpha\beta} \int \mathrm{d}^d x \, \frac{\delta^2 P}{\delta S_\alpha(x,t)\, \delta S_\beta(x,t)}. \end{aligned} \tag{13}$$

The dynamics of the order parameter is given by the Langevin equation

$$\partial_t S_\alpha(x, t) = f_\alpha(x, t) + \xi_\alpha(x, t), \tag{14}$$

where $S_\alpha(x, t)$ is the n-component order parameter. The random force ξ characterizing short-lived excitations in the system reflects the action of local microscopic degrees of freedom on the order parameter dynamics. Let the random force be white noise, namely

$$\begin{aligned} &\left\langle \xi_\alpha(x, t) \right\rangle_\xi = 0, \\ &\left\langle \xi_\alpha(x', t') \, \xi_\beta(x, t) \right\rangle_\xi = 2 C_{\alpha\beta} \delta(x - x') \delta(t' - t). \end{aligned} \tag{15}$$

The description of critical dynamics is not as universal as that of the equilibrium critical properties. We shall consider below the purely relaxation dynamics of the order parameter. This case is one of especially important, because it is realized in anisotropic spin systems and extensively studied in experiment. Moreover, it is this case of relaxation dynamics that is most successfully investigated numerically by MC methods with the use of the Metropolis algorithm generating single-spin flip dynamics [40].

Because the stationary solution of equation (13) must have the following limiting form

$$\lim_{t\to\infty} P\left[S(t)\right] = P_{\rm eq} \propto \exp\left(-H\right), \tag{16}$$

there appear limitations on the choice of $C_{\alpha\beta}$ and f_α, namely

$$\begin{aligned} C_{\alpha\beta} &= \lambda_{\alpha\beta} = \lambda \delta_{\alpha\beta}, \\ f_\alpha(x, t) &= -\lambda \, \frac{\delta H[S]}{\delta S_\alpha(x, t)}, \end{aligned} \tag{17}$$

where $H[S]$ is a Hamiltonian describing the critical behavior of the system. For example, the behavior of a structurally disordered system near the second-order phase transition temperature can be described by the effective model Ginzburg–Landau–Wilson Hamiltonian [41]

$$H_V[S] = \int \mathrm{d}^d x \left\{ \frac{1}{2} (\nabla S)^2 + \frac{1}{2} \left[\tau + V(x)\right] S^2 + \frac{g}{4!} S^4 \right\}, \tag{18}$$

where $\tau \propto (T - T_c)/T_c$ is the reduced temperature, and $V(x)$ is the potential of the random field of defects. The spatial distribution of the system of quenched uncorrelated point defects actually the Gaussian distribution $P[V]$ wholly determined by the first and second moments for random quantities $V(x)$:

$$\langle\langle V(x)\rangle\rangle = 0\,, \qquad \langle\langle V(x)V(y)\rangle\rangle = v\delta(x-y)\,, \tag{19}$$

where v is the positive constant proportional to the concentration of defects and the square of their potential. For 'pure' systems, one has $V(x) \equiv 0$.

Equations (14) and (15) with $C_{\alpha\beta}$ and f_α from formulas (17) and with the constant kinetic coefficient $\lambda > 0$ give the dynamic relaxation model A (according to the classification in Ref. [35]) defined by the equation

$$\partial_t S_\alpha(x,t) = -\lambda \frac{\delta H_V[S]}{\delta S_\alpha(x,t)} + \xi_\alpha(x,t)\,. \tag{20}$$

Let the realization of any order parameter configuration in a system at instant t be determined by the condition that, for a system with the initial magnetization m_0 at the starting moment $t = 0$, the distribution for the field of order parameter $S(x,0) = S_0(x)$ be characterized by the distribution function $P[S_0] \sim \exp(-H_0[S_0])$, with

$$H_0[S_0] = \int \mathrm{d}^d x\, \frac{\tau_0}{2}\big(S_0(x) - m_0\big)^2\,, \tag{21}$$

where $\tau_0^{-1/2}$ is the width of the initial magnetization distribution. This Gaussian distribution for the order parameter field can be realized for temperatures $T \gg T_c$ at which there are no long-range correlations for order parameter fluctuations yet.

In the framework of the field-theoretical description of critical phenomenon dynamics [41], an auxiliary field $\tilde{S}(x)$ is introduced that allows averaging over random forces $\xi(x,t)$ and describing critical dynamics equivalent to Langevin dynamics with the help of the generating functional $W[h,\tilde{h}]$ for dynamic correlation functions and response functions:

$$W[h,\tilde{h}] = \ln\left[\int \mathcal{D}(S,\mathrm{i}\tilde{S})P[V]\exp\big(-\mathcal{L}_V[S,\tilde{S},V] - H_0[S_0]\big) \times \exp\left(\int \mathrm{d}^d x \int_0^\infty \mathrm{d}t\,(\tilde{h}\tilde{S} + hS)\right)\right], \tag{22}$$

in which action functional $\mathcal{L}_V[S,\tilde{S},V]$ of the system is expressed as

$$\mathcal{L}_V[S,\tilde{S},V] = \int_0^\infty \mathrm{d}t \int \mathrm{d}^d x\, \tilde{S}\left(\frac{\partial S(x,t)}{\partial t} + \lambda \frac{\delta H_V[S]}{\delta S(x,t)} - \lambda\tilde{S}\right). \tag{23}$$

The expression for the generating functional (22) can be averaged over random fields $V(x)$ induced by structural defects, viz.

$$\int P[V]\exp\big(-\mathcal{L}_V[S,\tilde{S},V]\big) = \exp\big(-\mathcal{L}[S,\tilde{S}]\big)\,, \tag{24}$$

to obtain the action functional $\mathcal{L}[S,\tilde{S}]$ (translationally invariant and independent of random $V(x)$ fields) in the following form

$$\mathcal{L}[S,\tilde{S}] = \mathcal{L}_G[S,\tilde{S}] + \mathcal{L}_{\mathrm{int}}[S,\tilde{S}]\,, \tag{25}$$

$$\mathcal{L}_G = \int_0^\infty \mathrm{d}t \int \mathrm{d}^d x\, \tilde{S}_\alpha\big[\partial_t S_\alpha + \lambda(\tau - \Delta)S_\alpha - \lambda\tilde{S}_\alpha\big]\,, \tag{26}$$

$$\mathcal{L}_{\mathrm{int}} = g\,\frac{\lambda}{3!}\int \mathrm{d}^d x \int_0^\infty \mathrm{d}t\, \tilde{S}_\alpha S_\alpha S_\beta S_\beta - v\,\frac{\lambda^2}{2}\left(\int \mathrm{d}^d x \int_0^\infty \mathrm{d}t\, S_\alpha \tilde{S}_\alpha\right)^2. \tag{27}$$

The Gaussian part $\mathcal{L}_G$ describes free fields for which the problem of calculating the correlation functions is solved exactly. The constituent of the action functional $\mathcal{L}_{\mathrm{int}}$ with the nonzero interaction constant g characterizes interaction effects of order parameter fluctuations, while the constituent with constant v characterizes fluctuation interaction via the defect-induced field.

Magnetization, correlation and response functions can be obtained from the generating functional as derivatives taken over conjugate fields h and $\tilde{h}$:

$$\begin{aligned} M(x,t) &= \big\langle S(x,t)\big\rangle = \frac{\delta W[h,\tilde{h}]}{\delta h(x,t)}\bigg|_{h=0,\,\tilde{h}=0}\,, \\ C(x_1,t,\,x_2,t_{\mathrm{w}}) &= \big\langle S(x_1,t)S(x_2,t_{\mathrm{w}})\big\rangle \\ &= \frac{\delta^2 W[h,\tilde{h}]}{\delta h(x_1,t)\,\delta h(x_2,t_{\mathrm{w}})}\bigg|_{h=0,\,\tilde{h}=0}\,, \\ R(x_1,t,\,x_2,t_{\mathrm{w}}) &= \big\langle S(x_1,t)\tilde{S}(x_2,t_{\mathrm{w}})\big\rangle \\ &= \frac{\delta^2 W[h,\tilde{h}]}{\delta h(x_1,t)\,\delta \tilde{h}(x_2,t_{\mathrm{w}})}\bigg|_{h=0,\,\tilde{h}=0}\,. \end{aligned} \tag{28}$$

Let us consider the Gaussian (only quadratic) part of the generating functional and define correlation and response functions in the Gaussian approximation (bare functions). Next, the renormgroup perturbation theory is built up on the results of the Gaussian theory.

A convenient method for obtaining correlation and response functions in the Gaussian approximation is based on the solution of variational equations

$$\big[\partial_t + \lambda(\tau - \Delta)\big]S - 2\lambda\tilde{S} = \tilde{h}\,, \tag{29}$$

$$\big[-\partial_t + \lambda(\tau - \Delta)\big]\tilde{S} = h \tag{30}$$

under conditions

$$\tilde{S}(t=\infty) = 0\,, \quad S(t=0) - m_0 = \tau_0^{-1}\tilde{S}(t=0)\,. \tag{31}$$

Performing the Fourier transform and moving to the dependences of the functions on wave vectors $\mathbf{q}$ yield expressions for $\tilde{S}$ and S as functions of $\tilde{h}$ and h from equations (29) and (30):

$$\tilde{S}_q(t) = \int_0^\infty \exp\big[\lambda(q^2+\tau)(t-t')\big]h_q(t')\theta(t-t')\,\mathrm{d}t'\,, \tag{32}$$

$$S_q(t) = \int_0^\infty \mathrm{d}t'\,\exp\big[-\lambda(q^2+\tau)(t-t')\big]\theta(t-t') \times \big[\tilde{h}_q(t') + 2\lambda\tilde{S}_q(t') + \big(m_0 + \tau_0^{-1}\tilde{S}_q(0)\big)\delta(t')\big]\,. \tag{33}$$

Substituting expression (32) for $\tilde{S}_q(t)$ into (33) and varying $S_q(t)$ with respect to $\tilde{h}$ and h in accordance with formulas (28) lead, for a high-temperature initial state with

$m_0 = 0$ ($m_0 \ll 1$), to expressions for the free propagator $R_0(q, t, t_w)$ and correlator $C_0(q, t, t_w)$ as the bare response function and correlation function:

$$R_0(q, t, t_w) = \theta(t - t_w) \exp\left[-\lambda(q^2 + \tau)(t - t_w)\right], \quad (34)$$

$$C_0(q, t, t_w) = \frac{1}{\tau + q^2}\left\{ \exp\left[-\lambda(q^2 + \tau)|t - t_w|\right] + \left(\frac{\tau + q^2}{\tau_0} - 1\right) \exp\left[-\lambda(q^2 + \tau)(t + t_w)\right]\right\}. \quad (35)$$

In $C_0(q, t, t_w)$, the so-called equilibrium correlator $C_0^e(q, t - t_w)$ and the correlator characterizing the influence of the starting conditions, $C_0^i(q, t + t_w)$, can be distinguished:

$$C_0(q, t, t_w) = C^e(q, t - t_w) + C^i(q, t + t_w),$$

$$C_0^e(q, t - t_w) = \frac{1}{\tau + q^2} \exp\left[-\lambda(q^2 + \tau)|t - t_w|\right], \quad (36)$$

$$C_0^i(q, t + t_w) = \frac{1}{\tau + q^2}\left(\frac{\tau + q^2}{\tau_0} - 1\right) \exp\left[-\lambda(q^2 + \tau)(t + t_w)\right].$$

In formula (34) for $R_0(q, t, t_w)$, the θ-function reflects the property of causality, i.e., the requirement that a change in magnetization at the instant of time t be determined by a change in the external field at the preceding instant t_w for $t > t_w$.

Because τ_0 is finite (i.e., $\tau_0 \neq 0$), the term $\tau_0^{-1}(\tau + q^2)$ in formula (35) is much smaller than unity in the τ limit, $q \to 0$. Therefore, this item can be disregarded in the principal order of perturbation theory:

$$C_0(q, t, t_w) = C_0^D(q, t, t_w) + \tau_0^{-1} R_0(q, t, 0) R_0(q, t_w, 0), \quad (37)$$

where $C_0^D(q, t, t_w)$ is the Dirichlet correlator:

$$C_0^D(q, t, t_w) = \frac{1}{\tau + q^2}\left\{\exp\left[-\lambda(q^2 + \tau)|t - t_w|\right] - \exp\left[-\lambda(q^2 + \tau)(t + t_w)\right]\right\}. \quad (38)$$

The condition $\tau_0 = \infty$ is called the Dirichlet boundary condition. A Dirichlet correlator constituent equaling $C_0^i(q, t + t_w)$ is responsible for the breakdown of translational invariance in time.

The FDR in momentum space is given by the expression

$$X(q, t, t_w) = \frac{T_s R(q, t, t_w)}{\partial_{t_w} C(q, t, t_w)}. \quad (39)$$

In the Gaussian approximation, one obtains

$$X_0(q, t, t_w) = \frac{T_s R_0(q, t, t_w)}{\partial_{t_w} C_0(q, t, t_w)} = \left\{1 + \exp\left[-2\lambda(q^2 + \tau)t_w\right]\right\}^{-1}. \quad (40)$$

When a system does not reside in a critical point with $\tau \sim T - T_c \neq 0$, the limiting FDR value is $X^\infty = \lim_{t_w \to \infty} \lim_{t \to \infty} X_0(q, t, t_w) = 1$ for all values of wave vectors q, in agreement with the opinion that all the high-temperature phase modes have a finite equilibration time. The exponentially fast equilibration accounts for the fulfilment of the FDT. In a critical point and $\tau = 0$, the limiting FDR value is unity as before for the order parameter modes with $q \neq 0$, whereas for the mode with $q = 0$ it is $X^\infty = \lim_{t_w \to \infty} \lim_{t \to \infty} X_0(q = 0, t, t_w) = 1/2$. This means that only the zero order-parameter mode with $q = 0$ is characterized by aging effects at the critical point; in other words, it does not relax to equilibrium state and the FDT for this mode is violated.

In the Gaussian approximation, the main characteristic quantities of the nonequilibrium critical behavior for model A with relaxation dynamics and a nonconserved order parameter are the dynamic critical exponent $z = 2$ and the critical exponent $\theta' = 0$ of the nonequilibrium initial increase in magnetization, with the limiting FDR equal to $X^\infty = 1/2$. Strong fluctuation effects accompanying second-order phase transitions result in fluctuation corrections to these values. Following standard methods [41, 42], fluctuation corrections to expressions for correlation and response functions can be obtained by perturbative expansion of the functional weight $\exp\left[-(\mathcal{L}[S, \tilde{S}] + H_0[S_0])\right]$ in powers of coupling constant g being present at vertex $g(\lambda/3!)\tilde{S}_\alpha S_\alpha S_\beta S_\beta$ in the action functional $\mathcal{L}_{int}[S, \tilde{S}]$ (27), and describing fluctuation interaction in a pure system, as well as in powers of coupling constants g and v in the respective vertices of the action functional $\mathcal{L}_{int}[S, \tilde{S}]$ in expression (27), which describe fluctuation interaction in a system containing defects.

It was shown for the first time in Ref. [34] that the critical evolution of a system from an initial high-temperature nonequilibrium state with low magnetization $m_0 = m(0) \ll 1$ results in the universal scaling behavior for magnetization $M(t)$ at the short-time stage of its critical evolution and is characterized by the power-law increase in magnetization with time: $M(t) \sim t^{\theta'}$. The authors proposed the renormgroup description of nonequilibrium critical relaxation and presented scaling forms for magnetization, the correlation function, and dynamic susceptibility. They also computed the exponent θ' using ε-expansion technique in the two-loop approximation.

To recall, the short-time stage of the nonequilibrium evolution of a system corresponds to the limit $t - t_w \gg t_w$ in scaling two-time forms (7) for correlation and response functions. Further computer simulation studies [39] of nonequilibrium critical relaxation of the three-dimensional Ising model in the short-time regime confirmed theoretical predictions of the power-law evolution of magnetization in ferromagnetic systems, but the value of $\theta' = 0.108(2)$ found in this study proved to be at variance with the theoretical value of $\theta' = 0.130$ [34] obtained by direct substitution of parameter $\varepsilon = 1$ in the case of three-dimensional systems or with $\theta' = 0.138$ obtained by the Padé–Borel method for summation of a very short series of the perturbation theory in ε.

The authors of Ref. [14] were the first to calculate the critical exponent θ' of short-time evolution in the following three-loop approximation of the renormalization group theory in the framework of the ε-expansion method:

$$\theta' = \frac{n + 2}{4(n + 8)} \varepsilon\left[1 + \frac{6\varepsilon}{(n + 8)^2}\left(n + 3 + (n + 8)\ln\frac{3}{2}\right) - \frac{7.2985}{(n + 8)^4} \varepsilon^2 (n^3 + 17.3118n^2 + 153.2670n + 383.5519)\right] + O(\varepsilon^4), \quad (41)$$

and to demonstrate excellent agreement with the results of computer simulation applying the Padé–Borel method to sum up a three-term series of the theory at $\varepsilon = 1$ with $\theta' = 0.1078(22)$ for the Ising model with $n = 1$, and $\theta' = 0.1289(23)$ for the XY model with $n = 2$. Reference [14]

also reports the calculation of the dynamic critical exponent z:

$$z = 2 + \frac{\varepsilon^2}{2}\left(6\ln\frac{4}{3} - 1\right)\frac{n+2}{(n+8)^2} \times \left[1 + \varepsilon\left(\frac{6(3n+14)}{(n+8)^2} - 0.4384812\right)\right]. \quad (42)$$

The authors of Ref. [14] pointed out that the additional vertex function $\Gamma^{\rm eq}_{1,0}$ governing fluctuation corrections to the dynamic response function, which are associated with the influence of initial nonequilibrium states, and localized at the 'surface' of initial states with time $t = 0$ emerges in pure systems only starting from the three-loop approximation in the theory of nonequilibrium critical processes. These fluctuation corrections reflect the influence of initial nonequilibrium states and must be taken into consideration in order to adequately describe relaxation processes and obtain by applying the ε-expansion method values consistent with the results of computer simulation for the critical exponent θ' determining evolution of the system in the short-time regime.

Reference [15] reports on evaluating the influence of nonequilibrium initial states on the critical evolution of structurally disordered systems with quenched uncorrelated defects. The field-theoretical description of the nonequilibrium critical behavior of three-dimensional systems was realized for the first time and the critical exponent θ' of short-time evolution was calculated in the two-loop approximation without ε-expansion. It was shown that the additional vertex function $\Gamma^{\rm eq}_{1,0}$ localized at the initial state 'surface' and conditioning fluctuation corrections in the dynamic response function due to the influence of initial nonequilibrium states emerges already starting from the two-loop approximation. Numerical values of dynamic critical exponents obtained by summation of asymptotic series were compared with results of computer simulation of the nonequilibrium critical behavior of the three-dimensional disordered Ising model in the short-time regime [15]. It was demonstrated that the values of critical exponents $z = 2.198(2)$, $\theta' = 0.120(8)$ calculated on a basis of the renormalization group description better agree with the results $z = 2.191(42)$, $\theta' = 0.127(16)$ of computer simulation than those obtained by applying ε-expansion method with $\theta' = 0.0867$ [36].

Renormalization group investigations into aging effects in the nonequilibrium critical behavior of both 'pure' and structurally disordered systems with purely dissipative dynamics described by model A [35] were conducted in Refs [21, 22], respectively, applying the ε-expansion method. In these studies, the asymptotic FDR values X^∞ were calculated for 'pure' systems with the n-component order parameter [21], which gave in the two-loop approximation the following expression:

$$\frac{(X^\infty)^{-1}}{2} = 1 + \frac{n+2}{4(n+8)}\,\varepsilon + \varepsilon^2\frac{n+2}{(n+8)^2}\left[\frac{n+2}{8} + \frac{3(3n+14)}{4(n+8)} + c\right] + O(\varepsilon^3) \quad (43)$$

with the numerical parameter $c = -0.0415\ldots$ (the analytical expression for c is reported in paper [21]). For the diluted Ising model, the following expression was derived in the one-loop approximation [22]:

$$X^\infty = \frac{1}{2} - \frac{1}{4}\sqrt{\frac{6\varepsilon}{53}} + O(\varepsilon). \quad (44)$$

The following fluctuation–dissipation ratios were found based on relation (43): $X^\infty_{\rm 3DIs} = 0.429(6)$ for the three-dimensional Ising model ($\varepsilon = 1$, $n = 1$); $X^\infty_{\rm 3D}{}_{XY} = 0.416(8)$ for the XY model ($\varepsilon = 1$, $n = 2$), and $X^\infty_{\rm 2DIs} = 0.30(5)$ for the two-dimensional Ising model ($\varepsilon = 2$, $n = 1$). These values are in excellent agreement with the results of MC research presented in Table 1. The value of $X^\infty_{\rm 3DRIM} \simeq 0.416$ was obtained for the disordered three-dimensional Ising model. The authors of Ref. [22] emphasize that the comparison of these X^∞ values calculated in the first-order perturbation theory with the results for the 'pure' model does not allow the character and peculiarities of the influence of defects on the FDR to be elucidated; calculations in higher orders are needed for this purpose. Moreover, Refs [43–45] showed that expansion series in powers of $\sqrt{\varepsilon}$ are not well suited for $d = 3$ substitution in real three-dimensional systems. The results of MC research on nonequilibrium critical dynamics in 'pure' and structurally disordered three-dimensional Ising models are presented in Sections 3 and 4.

2.2 Nonequilibrium critical dynamics of systems evolving from a low-temperature initial state

2.2.1 Scaling forms for the autocorrelation function and the response function. Given that the initial state of a system is characterized by magnetization $m_0 \neq 0$ (a low-temperature initial state) with its subsequent quenching at $T_{\rm s} = T_{\rm c}$, the renormalization group analysis of nonequilibrium critical dynamics for the systems described by the totally dissipative model A predicts that magnetization, the correlation function, and the response function exhibit the following scaling behaviors [34, 46]:

$$\begin{aligned} M(t, t_{\rm m}) &= A_M t^{-\beta/(z\nu)} F_M\left(\frac{t}{t_{\rm m}}\right), \\ C(t, t_{\rm w}, t_{\rm m}) &= A_C (t - t_{\rm w})^{a+1-d/z}\left(\frac{t}{t_{\rm w}}\right)^{\theta-1} F_C\left(\frac{t_{\rm w}}{t}, \frac{t}{t_{\rm m}}\right), \\ R(t, t_{\rm w}, t_{\rm m}) &= A_R (t - t_{\rm w})^{a-d/z}\left(\frac{t}{t_{\rm w}}\right)^{\theta} F_R\left(\frac{t_{\rm w}}{t}, \frac{t}{t_{\rm m}}\right). \end{aligned} \quad (45)$$

Modification of these relationships in comparison with scaling forms (7) is conditioned by the introduction of a new timescale $t_{\rm m}$ determined by initial magnetization m_0 and related to m_0 by the universal dependence

$$t_{\rm m} = B_m m_0^{-\kappa}, \quad (46)$$

in which B_m is the nonuniversal amplitude, and exponent $\kappa > 0$ is expressed via static and dynamic critical exponents: $\kappa = 1/(\theta + a + \beta/(\nu z)) = 1/(\theta' + \beta/(\nu z))$.

As a result, functions $C(t, t_{\rm w}, t_{\rm m})$ and $R(t, t_{\rm w}, t_{\rm m})$ become the homogeneous in the extended sense functions of three timescales: $t - t_{\rm w}$, $t_{\rm w}$, and $t_{\rm m}$. Specifically, when $t_{\rm w} < t \ll t_{\rm m}$ (which is always fulfilled in the case of initial magnetization $m_0 = 0$), the scaling relations (45) for C and R reduce to those in formulas (7) with $F_{C,R}(x, 0) = f_{C,R}(x)$. Otherwise, for $t_{\rm m} \ll t_{\rm w} < t$, the scaling relations (45) assume the following form [46]:

$$\begin{aligned} C(t, t_{\rm w}) &= \bar{a}_C (t - t_{\rm w})^{a+1-d/z}\left(\frac{t}{t_{\rm w}}\right)^{\bar{\theta}-1} \bar{F}_C\left(\frac{t_{\rm w}}{t}\right), \\ R(t, t_{\rm w}) &= \bar{a}_R (t - t_{\rm w})^{a-d/z}\left(\frac{t}{t_{\rm w}}\right)^{\bar{\theta}} \bar{F}_R\left(\frac{t_{\rm w}}{t}\right), \end{aligned} \quad (47)$$

where the new exponent $\bar{\theta} = -\beta\delta/(vz) = -(1 + a + \beta/(vz))$, while $\bar{F}_{C,R}$ are universal scaling functions related to $F_{C,R}(x, y)$ behavior at large values of argument y. In the aging regime realized for times $t - t_w \sim t_w \gg t_m$, the two-time dependence of the correlation function and the response function is described by the relations

$$C(t, t_w) \sim t_w^{-2\beta/(vz)} \tilde{F}_C\left(\frac{t}{t_w}\right), \qquad R(t, t_w) \sim t_w^{-2\beta/(vz)-1} \tilde{F}_R\left(\frac{t}{t_w}\right), \tag{48}$$

with scaling functions $\tilde{F}_{C,R}(t/t_w)$ that decay at long observation times, $t - t_w \gg t_w \gg t_m$, following the power-law time dependence

$$\tilde{F}_{C,R}\left(\frac{t}{t_w}\right) \sim \left(\frac{t}{t_w}\right)^{-\phi} \tag{49}$$

characterized by exponent $\phi = d/z - a + \beta\delta/(vz)$.

2.2.2 Renormalization group description. In the renormalization group description of nonequilibrium behavior of systems evolving from an initial low-temperature state with a nonzero average value of the order parameter $\langle S(x,t)\rangle = M(t)$, it is convenient to write the action functional given by relations (25)–(27) in terms of fluctuations with respect to $S(x,t) - M(t)$ values. To conserve the former notations for variables $S(x,t)$ and $\tilde{S}(x,t)$ in relations (25)–(27) and assign to them the same sense of mean zero-value fields, we perform $S(x,t), \tilde{S}(x,t) \to S(x,t) + M(t), \tilde{S}(x,t)$ transformation in expressions (25)–(27). By redefining $m^2(t) = gM^2(t)/2$, the Gaussian constituent of the action functional (26) can be represented as

$$\mathcal{L}_G = \int_0^\infty dt \int d^d x\, \tilde{S}_\alpha \left[\partial_t S_\alpha + \lambda(\tau - \Delta + m^2) S_\alpha - \lambda \tilde{S}_\alpha + \sqrt{\frac{2}{g}}\,\partial_t m + \lambda\sqrt{\frac{2}{g}}\, m\left(\tau + \frac{m^2}{3}\right)\right], \tag{50}$$

where the set of items

$$\sqrt{\frac{2}{g}}\,\partial_t m + \lambda\sqrt{\frac{2}{g}}\, m\left(\tau + \frac{m^2}{3}\right) \equiv h_{\text{eff}} \tag{51}$$

has the sense of an effective magnetic field acting on the order parameter $S(x,t)$. Notice that the effect of the nonzero mean value of the order parameter $m(t)$ is equivalent to the time-dependent shift of the phase transition temperature: $\tau \to \tau + m^2(t)$. Therefore, when the system asymptotically approaches the critical point $\tau = 0$ for large times, it effectively passes in the short-time regime into the high-temperature magnetically disordered phase.

The introduction of the bare response function and correlation function to the Gaussian approximation by the method described in Section 2.1.2 yields the following expressions for them in the momentum space:

$$R_0(q, t, t_w) = \theta(t - t_w) \times \exp\left[-\lambda(q^2 + \tau)(t - t_w) + \int_{t_w}^{t} dt'\, m^2(t')\right], \tag{52}$$

$$C_0(q, t, t_w) = 2\lambda \int_0^\infty dt'\, R_0(q, t, t') R_0(q, t_w, t'). \tag{53}$$

The law of magnetization evolution $m(t)$ needed to find R_0 and C_0 is derived from the equation of motion $\langle \delta\mathcal{L}_G/\delta\tilde{S}\rangle = 0$, which leads at $\langle S(x,t)\rangle = 0$ and $\langle \tilde{S}(x,t)\rangle = 0$ to the equation

$$\partial_t m(t) + \lambda m(t)\left(\tau + \frac{m^2(t)}{3}\right) = 0. \tag{54}$$

As a result, the influence of the effective magnetic field h_{eff} (51) on the order parameter in the Gaussian component of the action functional (50) disappears due to relevant equation (54) for the time-dependent behavior of magnetization $m(t)$.

At the critical point with $\tau = 0$, equation of motion (54) takes the form

$$\partial_t m(t) + \lambda \frac{m^3(t)}{3} = 0 \tag{55}$$

having the solution

$$m^2(t) = m_0^2\left(1 + \frac{2\lambda m_0^2 t}{3}\right)^{-1}. \tag{56}$$

The last expression is consistent with the scaling behavior of magnetization $M(t)$ in relation (45). A comparison of formulas (45), (46), and (56) taking into account that $m(t) = \sqrt{g/2}M(t)$ leads in the Gaussian approximation to $t_m = 3/(2\lambda m_0^2) = B_m m_0^{-\kappa}$ with $\kappa = 2$ and $A_M = 1$, $B_m = \sqrt{2/3}$. For $t \gg t_m$, one has $m(t) \sim (2t/3)^{-1/2}$; therefore, nonzero initial values of magnetization m_0 prove unessential at the long-time stage of system's evolution; in the best case, they can serve as corrections to the leading terms in the scaling behavior of thermodynamic and correlation functions.

Substituting relation (56) into (52) and (53) yields the following expressions for the bare response function and the correlation function at the critical point ($\tau = 0$):

$$R_0(q, t, t_w, t_m) = \theta(t - t_w)\left(\frac{t_w + t_m}{t + t_m}\right)^{3/2} \exp\left[-\lambda q^2 (t - t_w)\right], \tag{57}$$

$$C_0(q, t, t_w, t_m) = \frac{2\lambda \exp\left[-\lambda q^2 (t + t_w)\right]}{\left[(t + t_m)(t_w + t_m)\right]^{3/2}} \times \int_0^{t_w} dt'\, (t' + t_m)^3 \exp(2\lambda q^2 t'). \tag{58}$$

At $q = 0$, relations (57) and (58) assume the form

$$R_0(q = 0, t, t_w, t_m) = \theta(t - t_w)\left(\frac{t_w + t_m}{t + t_m}\right)^{3/2}, \tag{59}$$

$$C_0(q = 0, t, t_w, t_m) = \frac{\lambda}{2} \frac{(t_w + t_m)^4 - t_m^4}{\left[(t + t_m)(t_w + t_m)\right]^{3/2}}. \tag{60}$$

By comparing expressions (59) and (60) at $t_m = 0$ with the scaling forms (47) for the response and correlation functions, it is easy to find that in the Gaussian approximation the exponents $z = 2$, $a = 2$, $\bar{\theta} = -3/2$ correspond to the mean-field values of critical exponents $\delta = 3$, $\nu = \beta = 1/2$, and $\eta = 0$ and that $\bar{a}_R = 1$, $\bar{a}_C = \lambda/2$, $\bar{F}_R(x) = 1$, and $\bar{F}_C(x) = 1$.

Now, let us determine the FDR in the Gaussian approximation. To this effect, we differentiate (58) with respect to t_w

and represent the results in the form

$$\partial_{t_w} C_0(q,t,t_w,t_m) = 2\lambda R_0(q,t,t_w,t_m) - \left(q^2 + m^2(t_w)\right) C_0(q,t,t_w,t_m)\,. \quad (61)$$

The FDR at the critical point is then expressed as

$$X_0(q,t,t_w,t_m) = \frac{R_0(q,t,t_w,t_m)}{\partial_{t_w} C_0(q,t,t_w,t_m)} = \frac{1}{2\lambda}\left[1 - \left(q^2 + m^2(t_w)\right)\frac{C_0(q,t,t_w,t_m)}{2\lambda R_0(q,t,t_w,t_m)}\right]^{-1}. \quad (62)$$

It follows from formulas (57), (58), and (62) that $X_0(q,t,t_w,t_m)$ actually depends on two variables, $x = t_w/t_m = 2t_w m_0^2/3$ and $y = q^2 t_w$, and is unrelated to t, i.e., $X_0(q,t,t_w,t_m) \equiv X_0(t_w/t_m, q^2 t_w)$, which is a distinctive feature of the FDR in the Gaussian approximation. Function $X_0(x=0,y)$ corresponds to the critical evolution of the system from a high-temperature initial state and $X_0(x=0,y=0) = 1/2$, and with an increase in $y = q^2 t_w$ $X_0(x=0,y)$ tends toward unity: $X_0(x=0,y\to\infty) = 1$, which suggests FDT violation for the zero mode with $q = 0$ in the large waiting time limit of $t_w \to \infty$, whereas the remaining modes of spin density $S(q \neq 0, t)$ arrive in this limit at the equilibrium state with $X_0^\infty = 1$.

For the zero mode with $q = 0$ $(y = 0)$, the FDR as a function of variable $x = t_w/t_m = 2t_w m_0^2/3$ is characterized by the relation

$$X_0(x, y=0) = \frac{4}{5}\left[1 + \frac{3}{5}\frac{1}{(1+x)^4}\right]^{-1}. \quad (63)$$

Its value grows monotonically from $X_0(x=0,y=0) = 1/2$ at $x = 0$ to $X_0(x\to\infty, y=0) = 4/5$ as $x \to \infty$. Thus, the FDR for the global order parameter (complete magnetization) in the long-time limit reaches the value of $X_0^\infty = 4/5$ if initial magnetization $m_0 \neq 0$ in the case of evolution from a magnetized low-temperature state, and $X_0^\infty = 1/2$ if initial magnetization $m_0 = 0$ in the case of evolution from a high-temperature state. The value of $X_0^\infty = 4/5$ invariably remains independent of a concrete $m_0 \neq 0$ value.

It should be also noted that for time intervals with $t_w \gg t - t_w \gg 1$ the quasiequilibrium regime is realized in which $C_0(q=0,t,t_w) \sim (t-t_w)^{-(d-2)/2} = C_0(t-t_w)$ and $R_0(q=0,t,t_w) = R_0(t-t_w)$ behave as equilibrium functions.

Characteristics of nonequilibrium critical behavior considered in preceding paragraphs in the Gaussian approximation acquire fluctuation corrections in real systems. The respective fluctuation corrections to expressions for correlation functions and response functions can be obtained by perturbative expansion of the functional weight $\exp\{-(\mathcal{L}[S,\tilde{S}] + H_0[S_0])\}$ in powers of coupling constant g describing the interaction of fluctuations in a pure system, and in powers of coupling constants g and v in expression (27) describing fluctuation interaction in a system containing defects.

Reference [46] reports a renormalization group study of the nonequilibrium critical behavior of a d-dimensional Ising model with purely dissipative dynamics undergoing relaxation from a magnetized initial state. The correlation function and the response function were calculated using the first-order ε-expansion in the framework of the field-theoretical approach. Aging effects were revealed for these functions and the universal limiting FDR was calculated:

$$X^\infty = \frac{4}{5}\left(\frac{73}{600} - \frac{\pi^2}{100}\right)\varepsilon + O(\varepsilon^2)\,. \quad (64)$$

Expression (64) gives $X_{3DIs}^\infty \simeq 0.78$ for the three-dimensional Ising model ($\varepsilon = 1$, $n = 1$), and $X_{2DIs}^\infty \simeq 0.75$ for the two-dimensional Ising model ($\varepsilon = 2$, $n = 1$). These findings were confirmed in part in Ref. [46] reporting numerical MC research on the nonequilibrium critical behavior for a two-dimensional Ising model that yielded $X_{MC}^\infty = 0.73(1)$.

In Section 3, we present results of our numerical MC simulations of the nonequilibrium critical behavior of a 'pure' three-dimensional Ising model described by dissipative model A for its evolution from both a high-temperature initial state with low magnetization $m_0 \ll 1$ and a low-temperature initial state with $m_0 = 0$, laying emphasis on aging effects and their characteristics. Moreover, we calculated the limiting FDR and evaluated the influence of structural defects on aging effects and FDT violations in the nonequilibrium critical behavior of the three-dimensional Ising model undergoing relaxation from the high-temperature initial state.

3. Investigations into aging effects and fluctuation–dissipation theorem violation in the behavior of the 'pure' three-dimensional Ising model

A simple but not trivial model whose nonequilibrium critical behavior exhibits aging effects is the three-dimensional Ising model. Its dynamics determined in simulations by the Metropolis single-spin flip and thermal bath [47] algorithms are purely dissipative and correspond to relaxation model A [35]. The Hamiltonian of the model given on a cubic lattice and taking into account the influence of a local magnetic field h_i has the form

$$H = -J\sum_{\langle i,j\rangle} S_i S_j - \sum_i h_i S_i\,, \quad (65)$$

where $J > 0$ is the integral of the short-range exchange interaction between S_i spins fixed at crystal lattice sites and assuming the values of $S_i = \pm 1$.

The nonequilibrium evolution of a macroscopic grid system of N spins is simulated by the statistical MC method. For example, the dynamic single-spin flip process examined using the thermal bath algorithm [47] is characterized by the probability of ith spin transition into a new state, $S_i \to S_i'$:

$$W_{sp}(S_i \to S_i') = \frac{\exp\left(-\beta H(S_i')\right)}{\sum_{S_j}\exp\left(-\beta H(S_j)\right)}\,, \quad (66)$$

where summation over S_j in the denominator is performed for all possible states of spin S_i before the spin flip. The time unit of the dynamic process is one Monte Carlo step per spin (MCS/s), which designates the sequence of N different spin flips at lattice sites. For an Ising model with two possible spin states $S_j = \pm 1$, the probability of a spin flip can be represented in the form

$$W_{sp}(S_i \to S_i') = \frac{\exp\left(-\beta H(S_i')\right)}{\exp\left(\beta H(S_i)\right) + \exp\left(-\beta H(S_i)\right)}\,, \quad (67)$$

with realization of the so-called Glauber dynamics.

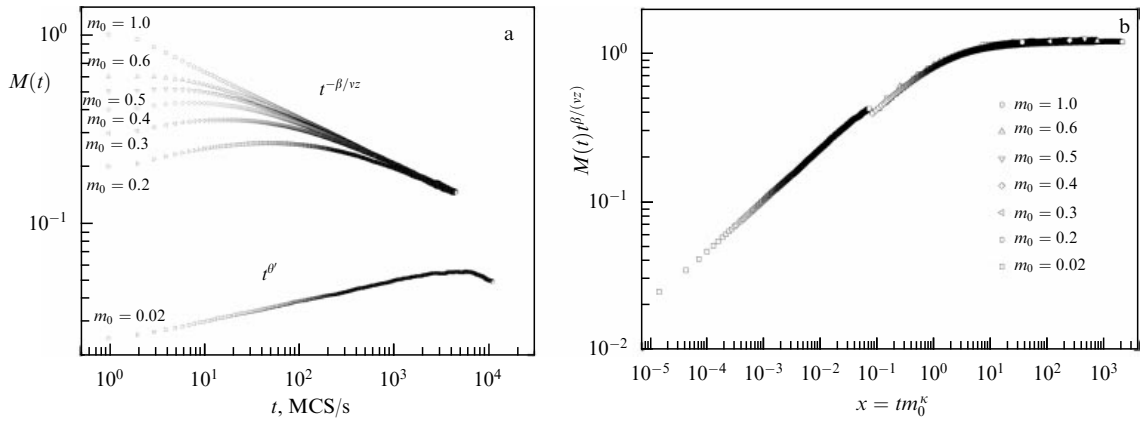

Figure 3. Time dependence of magnetization $M(t)$ (a) and its scaling functions $F_M(t/t_{\rm m}) = M(t)t^{\beta/(z\nu)}$ (b) for different initial states of m_0 shown in the panels.

References [48–50] report simulations of the nonequilibrium critical behavior of a system with Ising spins on a cubic lattice having the linear dimension $L = 128$ with imposed periodic boundary conditions at $T_{\rm c} = 4.5114(1)$ [51]. The authors calculated the magnetization

$$M(t) = \left\langle \frac{1}{L^3} \sum_{i=1}^{L^3} S_i(t) \right\rangle \tag{68}$$

and two-time autocorrelation function

$$C(t, t_{\rm w}) = \left\langle \frac{1}{L^3} \sum_{i=1}^{L^3} S_i(t) S_i(t_{\rm w}) \right\rangle - M(t) M(t_{\rm w}) , \tag{69}$$

where angular brackets denote statistical averaging over different realizations of initial spin configurations and MC runs. To calculate $C(t, t_{\rm w})$, averaging was done over 3000 runs for each $t_{\rm w}$ value.

In a study of critical relaxation of systems from the initial high-temperature state with magnetization $m_0 = 0.02$, the response function and FDR were calculated using relations as follows [32, 52, 53]:

$$R(t, t_{\rm w}) = \frac{1}{TL^3} \sum_{i=1}^{L^3} \left\langle S_i(t) \left[S_i(t_{\rm w} + 1) - S_i^W(t_{\rm w} + 1) \right] \right\rangle , \tag{70}$$

where $S_i^W = \tanh\left(J \sum_{m \neq i} S_m / T\right)$, and

$$X(t, t_{\rm w}) = \frac{\sum_{i=1}^{N} \left\langle S_i(t) \left[S_i(t_{\rm w} + 1) - S_i^W(t_{\rm w} + 1) \right] \right\rangle}{\sum_{i=1}^{N} \left\langle S_i(t) \left[S_i(t_{\rm w} + 1) - S_i(t_{\rm w}) \right] \right\rangle} . \tag{71}$$

In simulation of system's dynamics with the use of the thermal bath algorithm, these relations make it possible to obtain the response function and then FDR without the introduction of a magnetic field. A detailed method for derivation of these expressions is described in Ref. [54]. When calculating $R(t, t_{\rm w})$ and $X(t, t_{\rm w})$, the values obtained were averaged over 90,000 MC runs for each $t_{\rm w}$, because $R(t, t_{\rm w})$ and $X(t, t_{\rm w})$, unlike the autocorrelation function, are characterized by greater fluctuation effects and their determination and averaging require much more extensive statistics.

When modeling critical relaxation of the system from an initial low-temperature state with magnetization $m_0 = 1$, an integral characteristic (dynamic susceptibility) [46, 52] was calculated:

$$\chi(t, t_{\rm w}) = \int_0^{t_{\rm w}} {\rm d}t' \, R(t, t') = \frac{1}{T_{\rm c} N} \sum_{i=1}^{N} \left\langle S_i(t) \Delta S_i(t_{\rm w}) \right\rangle , \tag{72}$$

with the response function defined by relation (2) and the $\Delta S_i(t_{\rm w})$ function calculated during simulation within a time interval from $t = 0$ to $t = t_{\rm w}$:

$$\Delta S_i(t_{\rm w}) = \sum_{s=0}^{t_{\rm w}} \left[S_i(s) - S_i^W(s) \right] . \tag{73}$$

In the limit of large observation times, one has

$$T_{\rm c} \chi(C) = \int_0^C X(q) \, {\rm d}q .$$

Then, the limiting FDR can be defined as

$$X^{\infty} = \lim_{C \to 0} \frac{\partial T_{\rm c} \chi(t, t_{\rm w})}{\partial C(t, t_{\rm w})} . \tag{74}$$

Reference [55] reports a study of nonequilibrium critical relaxation of magnetization $M(t)$ in the 'pure' Ising model for different initial states m_0 (Fig. 3a) that demonstrated essential qualitative and numerical differences in magnetization relaxation from the initial high-temperature state with $m_0 \ll 1$ and the perfectly ordered low-temperature state with $m_0 = 1$, the intermediate cases possessing $m_0 = 0.2 - 0.6$.

Thus, in the case of a high-temperature initial state with $m_0 = 0.02 \ll 1$, the stage of nonequilibrium evolution was characterized by a rise in magnetization described by the power-law dependence $M(t) \sim t^{\theta'}$ with $\theta' = 0.111(4)$, where θ' is the independent dynamic critical exponent [14, 17, 34]. For times $t > t_{\rm cr} \sim m_0^{-1/[\theta' + \beta/(z\nu)]}$, this evolution stage is replaced by a regime characterized by the power-law time dependence of magnetization $M(t) \sim t^{-\beta/(z\nu)}$.

If a system evolves from the initial ordered state with $m_0 = 1$, the time dependence of magnetization at a critical point is directly determined by the power-law dependence $M(t) \sim t^{-\beta/(z\nu)}$ with exponent $\beta/(z\nu) = 0.241(8)$. Intermediate cases with $m_0 = 0.2 - 0.5$ are characterized by the short stage of magnetization growth following the $M(t) \sim t^{\theta'}$ law with the subsequent transition into a longer relaxation stage, $M(t) \sim t^{-\beta/(z\nu)}$, whereas magnetization behavior for

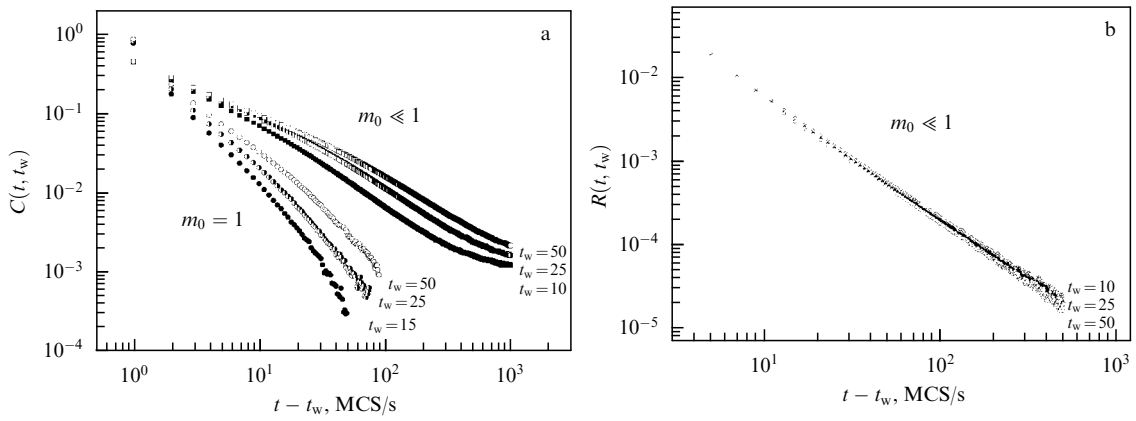

Figure 4. Dependences of the correlation function $C(t, t_w)$ (a) and the response function $R(t, t_w)$ (b) on observation time $t - t_w$ for different initial nonequilibrium states.

$0.5 < m_0 < 1.0$ at short observation times is associated with the onset of the transient regime with t_{cr} at the very first steps of modeling that passes into the relaxation stage described as $M(t) \sim t^{-\beta/(z\nu)}$.

Figure 3a also demonstrates that relaxation curves for the systems evolving from initial states with $m_0 < 1$ asymptotically tend toward the relaxation curve of a system evolving from the low-temperature initial state with $m_0 = 1$. In this case, the process of critical relaxation of magnetization $M(t)$ from the high-temperature initial state with $m_0 = 0.02 \ll 1$ is faster than relaxation from other initial states with $m_0 \neq 0$.

Figure 3b shows results of numerical verification of the prediction of the scaling time dependence of $M(t)$ as a function of initial values of magnetization m_0 specified by relation (45). The presented tm_0^{κ} dependences of $t^{\beta/(z\nu)}M(t)$ at the critical exponents $\beta/\nu = 0.516(2)$ [56], $z = 2.024(6)$ [57], and $\theta' = 0.106(4)$ [39] for the three-dimensional Ising model suggest a 'collapse' of the data at $\kappa \simeq 2.77$ for $M(t)$ obtained for different m_0 in a single curve with universal scaling dependence $F_M(tm_0^{\kappa})$. In this case, the section of the curve corresponding to the increase in the scaling function (linear on the double logarithmic scale) and described by the power-law dependence $F_M(x) \sim x^{1/\kappa}$ corresponds to the stage of growing magnetization $M(t) \sim t^{\theta'}$, whereas the horizontal section of scaling function $F_M(x)$ corresponds to the stage of a critical decay of magnetization as $M(t) \sim t^{-\beta/(z\nu)}$.

The results of MC simulations of two-time dependences of the autocorrelation function $C(t, t_w)$ and the response function $R(t, t_w)$ on observation time $t - t_w$ at different waiting times t_w and initial nonequilibrium states ($m_0 \ll 1$ and $m_0 = 1$) are presented in Fig. 4. Dependences $C(t, t_w)$ and $R(t, t_w)$ graphically demonstrate manifestations of aging effects at times $t - t_w \simeq t_w$ characterized by the slowing down of correlation time and the weakening of the system's response to the external field with increasing its 'age' t_w.

In the aging regime, the two-time dependences for the autocorrelation function $C(t, t_w)$ and the response function $R(t, t_w)$ are defined by the scaling relations (11) and (12) (see Section 2.1.1). These relations fairly well describe the results of simulations as viewed in Fig. 5. Specifically, $(t - t_w)/t_w$ dependences of $t_w^{2\beta/(z\nu)}C(t, t_w)$ and $t_w^{2\beta/(z\nu)+1}R(t, t_w)$ demonstrate a collapse of the data obtained for different t_w in the universal curves corresponding to the scaling functions $\hat{F}_C(t/t_w)$ and $\hat{F}_R(t/t_w)$ in relations (11). According to

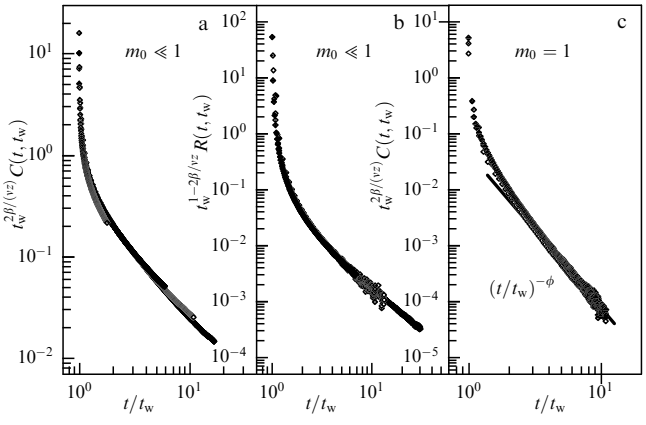

Figure 5. Scaling collapse of the correlation function $C(t, t_w)$ (a), response function $R(t, t_w)$ (b) in the case of a high-temperature initial state with $m_0 \ll 1$, and the correlation function $C(t, t_w)$ (c) for a low-temperature initial state with $m_0 = 1$.

formulas (12), these scaling functions in time intervals $(t - t_w)/t_w \gg 1$ are characterized by a power-law dependence on t/t_w. The computed exponents $c_a = 1.333(40)$ and $c_r = 1.357(18)$ are in excellent agreement with each other within the calculation accuracy and with exponent $c_a = 1.362(19)$ obtained by the short-time dynamics method in Ref. [39].

The short-time dynamics regime for an initial perfectly ordered state with $m_0 = 1$ for the autocorrelation function $C(t, t_w)$ is characterized, according to dependence (49), by exponent ϕ. The analysis of the two-time dependence of $t_w^{2\beta/(z\nu)}C(t, t_w)$ on $(t - t_w)/t_w$ (Fig. 5c) for the time interval $(t - t_w)/t_w \gg 1$ gave the exponent $\phi = 2.742(32)$, in excellent agreement with the theoretically predicted value of $\phi = 1 + d/z + \beta/(z\nu) = 2.737(8)$ calculated with the use of critical exponents $\beta = 0.325(1)$, $\nu = 0.630(1)$ [56], and $z = 2.024(6)$ [57].

In the aging regime, taking account of the influence of different initial states with $0 \leqslant m_0 \leqslant 1$, the time dependence of the autocorrelation function is characterized by the scaling relation

$$C(t, t_w, t_m) \sim t_w^{-2\beta/(z\nu)}\tilde{F}_C\left(\frac{t}{t_w}, \frac{t}{t_m}\right). \qquad (75)$$

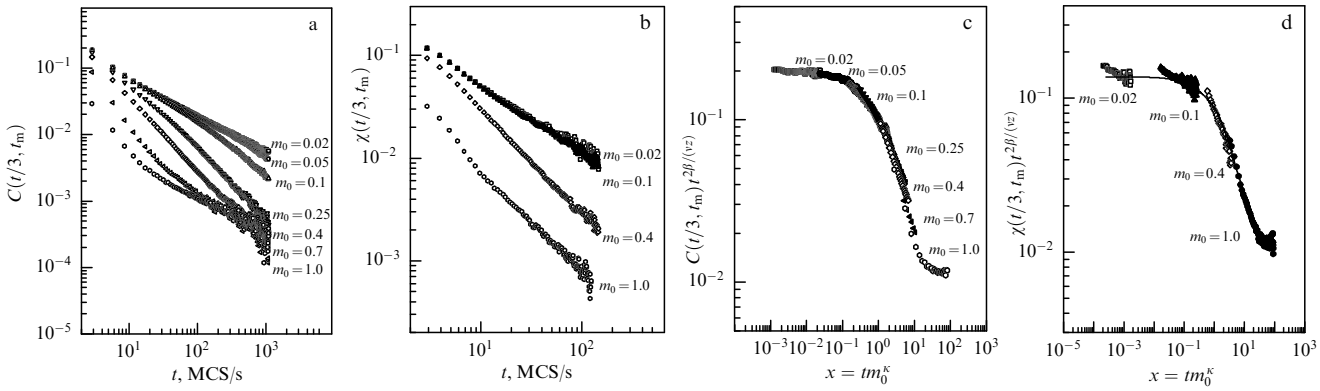

Figure 6. Dependences of autocorrelation function $C(t, t_w = t/3, t_m)$ (a) and dynamic susceptibility $\chi(t, t_w = t/3, t_m)$ (b) on observation time t, and of functions $t^{2\beta/(z\nu)}C(t, t_m)$ (c) and $t^{2\beta/(z\nu)}\chi(t, t_m)$ (d) on variable $x = tm_0^\kappa$ for different initial magnetizations m_0.

A similar scaling form for the time dependence of dynamic susceptibility can be obtained applying the integral relation (72) and the scaling time dependence (48) for the response function. This approach leads to the result:

$$\chi(t, t_w, t_m) \sim t_w^{-2\beta/(z\nu)} \tilde{F}_\chi\left(\frac{t}{t_w}, \frac{t}{t_m}\right). \tag{76}$$

To reveal the dependence of the autocorrelation function and dynamic susceptibility on the initial magnetization m_0 predicted by relations (75) and (76), it is convenient to choose as the waiting time a quantity proportional to the observation time, e.g., $t_w = t/3$. Then, the scaling forms predicted for these functions by relations (75) and (76) will look like

$$\begin{aligned} C\left(t, t_w = \frac{t}{3}, t_m\right) &= t^{-2\beta/(z\nu)} G_C(tm_0^\kappa), \\ \chi\left(t, t_w = \frac{t}{3}, t_m\right) &= t^{-2\beta/(z\nu)} G_\chi(tm_0^\kappa). \end{aligned} \tag{77}$$

The dependences of functions $C(t, t_w = t/3, t_m)$ and $\chi(t, t_w = t/3, t_m)$ on observation time t obtained in our studies for different initial magnetizations m_0 are plotted in Figs 6a, b. Figures 6c, d illustrate dependences of scaling function $G_C(tm_0^\kappa) = t^{2\beta/(z\nu)}C(t, t_w = t/3, t_m)$ and $G_\chi(tm_0^\kappa) = t^{2\beta/(z\nu)}\chi(t, t_w = t/3, t_m)$ on variable $x = tm_0^\kappa$ at $\kappa \simeq 2.77$. All these figures demonstrate a collapse of the data on C and χ at different m_0 in the universal curves corresponding to the scaling functions $G_C(tm_0^\kappa)$ and $G_\chi(tm_0^\kappa)$. These results thus confirm the complex generalized homogeneous dependence of the correlation function and the response function (45) on time-related variables t, t_w, and t_m.

Let us turn to determining the FDR for different initial states. For the high-temperature initial state with $m_0 \ll 1$, Fig. 7 presents the FDR calculated by formula (71) in the form of the functional dependence of $X(t, t_w)$ on $t_w/(t - t_w)$ for $t - t_w \gg t_w$. The linear approximation of dependence $X(t, t_w)$ as $t_w/(t - t_w) \to 0$ yielded $X(t_w)$ values for each t_w. Extrapolation of $X(t_w \to \infty)$ was applied to the $X(t_w)$ values obtained for different waiting times, which allowed determining the sought limiting FDR value X^∞ (see Fig. 16 in Section 4.1.2.). These procedures brought forth the value of $X^\infty = 0.380(13)$, which agrees poorly with the field-theoretical value of $X^\infty_{3DIs} = 0.429(6)$ calculated in Ref. [21], but satisfactorily corresponds to $X^\infty \approx 0.40$ reported in Ref. [27] as a result of preliminary numerical assessment of the three-dimensional Ising model.

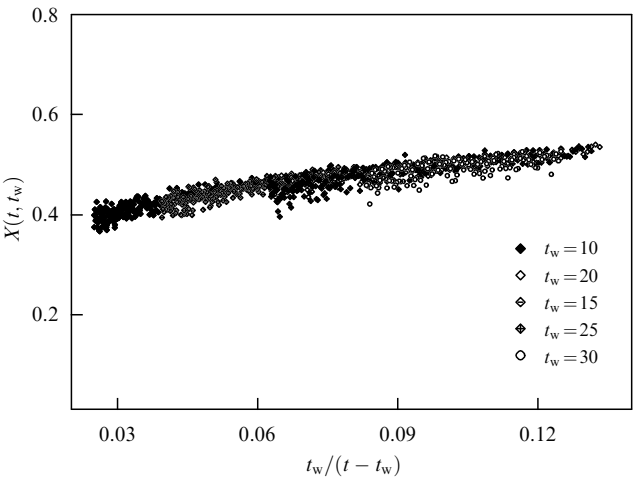

Figure 7. Fluctuation–dissipation relation $X(t, t_w)$ as a function of $t_w/(t - t_w)$ for $t - t_w \gg t_w$ for the high-temperature initial state with $m_0 \ll 1$.

For the initial totally ordered state with magnetization $m_0 = 1$, the FDR limiting value is $X^\infty = 0.784(7)$ calculated from the limiting dependence $T_c\chi(C)$ (Fig. 8a) on the basis of relation (74). This X^∞ value is in excellent agreement with the field-theoretical value of $X^\infty \simeq 0.78$ computed in Ref. [46].

It is shown in Section 2.2.2 that the renormalization group description of the nonequilibrium critical behavior of systems in the Gaussian approximation for dissipative model A predicts a change in the FDR as a function of $x = t_w/t_m$ for initial states with $m_0 \neq 0$ from $1/2$ at $x = 0$ to $4/5$ at $x \to \infty$, with the limiting FDR value $X^\infty = 4/5$ being independent of $m_0 \neq 0$. To evaluate fluctuation effects on the FDR as $m_0 \neq 0$, time dependences of dynamic susceptibility $\chi(t, t_w, t_m)$ and autocorrelation function $C(t, t_w, t_m)$ were calculated at $t_w = t/3$ for the initial states with $m_0 = 0.1$ and $m_0 = 0.4$.

The calculated parametric dependence of $T_c\chi$ on C presented in Fig. 8b gives the limiting FDR value X^∞ as $C \to 0$ in accordance with relation (74). Thus, for the initial state with $m_0 = 0.1$, the result for $X^\infty = 0.402(12)$ is consistent with the high-temperature $X^\infty = 0.380(13)$, while $X^\infty = 0.788(5)$ obtained for the initial state with $m_0 = 0.4$ agrees with the low-temperature value of $X^\infty = 0.784(7)$.

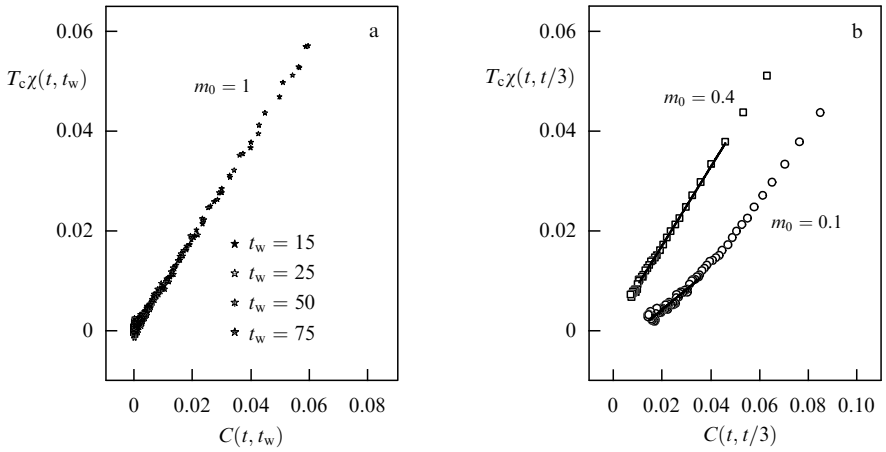

Figure 8. Quantity $T_c\chi(t, t_w)$ as a function of $C(t, t_w)$ for a low-temperature initial state with $m_0 = 1$ for different waiting times t_w (a) and in the case of relaxation from initial states with $m_0 = 0.4$, 0.1 (b).

It can be concluded that the nonequilibrium critical behavior of the three-dimensional Ising model with arbitrary initial values of magnetization m_0 can be categorized into two universality classes corresponding to high-temperature and low-temperature initial states with the limiting FDR values $X^\infty = X^\infty(m_0 = 0) = 0.380(13)$ for $m_0 \lesssim 0.1$ and $X^\infty = X^\infty(m_0 = 1) = 0.784(7)$ for $m_0 \gtrsim 0.4$.

The above results of numerical research give evidence of FDT violation in the case of nonequilibrium critical behavior of the three-dimensional Ising model. The limiting FDR values X^∞ differ from unity and depend on their belonging to one of the two universality classes of nonequilibrium critical behavior corresponding to the high-temperature and low-temperature initial states of the system, respectively. The threshold value of initial magnetization m_0^{th} separating these two classes lies in the range of $0.1 < m_0^{\text{th}} < 0.4$.

4. Influence of structural defects on characteristics of the nonequilibrium critical behavior of the three-dimensional Ising model

In carrying out studies on the influence of structural disorder on second-order phase transitions, researchers face two problems, namely: do the critical exponents of a 'pure' magnet change upon dilution with nonmagnetic impurities and, if so, are the new critical exponents universal, i.e., independent of defect concentration up to the percolation threshold? The answer to the first question was given in Ref. [58] showing that critical exponents of systems with quenched structural defects are altered in comparison with those of their defect-free analogs, given that the critical exponent of the heat capacity of the 'pure' system is positive. This criterion is met only by three-dimensional systems whose critical behavior is described by the Ising model.

Investigations into the critical behavior of diluted Ising type magnets with the use of renormalization group methods, MC numerical simulations, and experimental techniques are reported in numerous publications [41, 43, 45, 59–64]. They confirm the existence of a new universality class of critical behavior exhibited by diluted Ising type magnets, but the dependence of asymptotic values of critical exponents on the degree of their dilution and the influence of crossover effects in weakly and strongly disordered systems await elucidation and remain subjects of ardent discussion.

It is worthwhile to note that analytical renormalization group methods applied to study the critical behavior of impurity systems are suitable only for weakly diluted magnetic materials with concentration of defects $(1 - p) \ll 1$, where p is the spin concentration. As a system becomes increasingly more diluted with nonmagnetic impurity atoms at spin concentrations $p_c^s < p < p_c^{\text{imp}} = 1 - p_c^s$, where p_c^s and p_c^{imp} are the spin and impurity percolation thresholds, respectively (for cubic lattices with nearest neighbor interactions one has $p_c^s \simeq 0.31$, $p_c^{\text{imp}} \simeq 0.69$), the impurities aggregate into a binding cluster coexisting for $T \leqslant T_c$ with the spin binding cluster at spin concentrations up to p_c^s and form a fractal-like structure with effective long-range spatial correlation in impurity distribution [65].

A change in effects of order parameter fluctuation scattering from impurity atoms must give rise to new fixed points for the vertices of interaction between order parameter fluctuations. Therefore, the region with $p_c^s < p < p_c^{\text{imp}}$ is characterized by a new type of critical behavior of three-dimensional Ising models, corresponding to the region of the strong structural disorder.

Such universal characteristics of the critical behavior as critical exponents obtained for the structurally disordered Ising model with the use of the renormalization group description at a fixed system dimension $d = 3$ and various methods for summation of series in the theory are defined by the values of exponents $\nu = 0.678(10)$, $\beta = 0.349(5)$, $\gamma = 1.330(17)$, $\omega = 0.25(10)$ [68], $z = 2.179(1)$ [57], $\theta' = 0.120$ [17] (the values for static and dynamic exponents were obtained with the highest currently attainable accuracy) and fairly well agree with experimental findings for Ising type magnets $Fe_pZn_{1-p}F_2$ at a spin concentration $p = 0.9$: $\nu = 0.70(2)$, $\gamma = 1.34(6)$ [64], $\beta = 0.350(9)$, $z = 2.18(10)$ [20, 63]. Experimental studies of strongly disordered magnetic materials yielded $\nu = 0.73(3)$, $\gamma = 1.44(6)$ [61] for $Fe_pZn_{1-p}F_2$ at $p = 0.6$, and $\nu = 0.75(5)$, $\gamma = 1.57(16)$ [62] for $Mn_pZn_{1-p}F_2$ at $p = 0.5$.

Results of numerical MC research on the critical behavior of the structurally disordered three-dimensional Ising model are rather contradictory: some of them confirm the independence of critical exponents on defect concentration up to the percolation threshold with $\nu = 0.684(5)$, $\beta = 0.355(3)$, $\gamma = 1.342(10)$ [69], $z = 2.62(7)$ [70], $z = 2.35(2)$ [71], $\theta' = 0.10(2)$ [72, 73] obtained by adjusting intermediate

values and amplitudes in the scaling dependence of thermodynamic characteristics calculated for different spin concentrations with the use of the fitted exponent of the correction to the scaling $\omega = 0.370(63)$ [69], $\omega = 0.50(13)$ [70], $\omega_2 = 0.82(8)$ [71], while others suggest the existence of two universal classes of critical behavior for weakly disordered systems with $\nu = 0.68(2)$, $\beta = 0.34(2)$ [74], $z = 2.38(1)$ [75], $\nu = 0.682(3)$, $\beta = 0.344(3)$ [76, 77], $\nu = 0.683(4)$, $\beta = 0.310(3)$, $\gamma = 1.299(3)$ [60], $\nu = 0.696(3)$, $\gamma = 1.345(4)$, $\omega = 0.23(13)$ [16], $z = 2.20(7)$ [66, 67], $z = 2.191(21)$, $\omega = 0.256(55)$, $\theta' = 0.127(16)$ [17] and strongly disordered systems with $\nu = 0.72(2)$, $\beta = 0.33(2)$, $\gamma = 1.51(3)$ [74], $z = 2.53(3)$ [75], $\nu = 0.717(7)$, $\beta = 0.313(12)$ [76, 77], $\nu = 0.725(6)$, $\beta = 0.349(4)$, $\gamma = 1.446(4)$ [60], $\nu = 0.725(4)$, $\gamma = 1.415(11)$, $\omega = 0.28(15)$ [16], $z = 2.58(9)$ [66, 67], $z = 2.663(30)$, $\omega = 0.286(10)$, $\theta' = 0.167(18)$ [41, 78, 79].

The essentially nonperturbative numerical MC studies of two-time characteristics of nonequilibrium critical behavior of the structurally disordered three-dimensional Ising model reviewed below give a more definite answer concerning the relative correspondence between limiting FDR values X^{∞} for structurally disordered and 'pure' Ising models and make it possible to evaluate the influence of structural defects on aging effects and X^{∞} values in the nonequilibrium critical behavior of the three-dimensional Ising model with spin concentrations in both weak and strong disorder regions.

4.1 Evolution from a high-temperature initial state

This section presents results of research on aging effects in the nonequilibrium critical behavior of the structurally disordered Ising model evolving from a high-temperature initial state [48–50, 54, 80, 81]. Two strategies were employed to determine the response function and FDR.

One concerns the introduction of the influence from an infinitesimally small random magnetic field, the calculation of the two-time dependence of magnetic susceptibility of the system as its response to the random magnetic field induced at the instant of time t_w, and the FDR determination through the relationship between dynamic susceptibility and the autocorrelation function [48, 50, 80]. This strategy for modeling the evolution of a macroscopic spin system uses the Metropolis algorithm.

The other approach [48–50, 54, 81] does not require the introduction of an external magnetic field but makes use of a computation method based on applying the thermal bath algorithm to express the response function to the external field via the special two-time correlation function (70). Details of this approach were highlighted in Section 3.

The Hamiltonian of a structurally disordered Ising model is given by the expression

$$H = -J \sum_{\langle i,j \rangle} p_i p_j S_i S_j \,, \tag{78}$$

where summation is taken over the nearest neighbors, and $S_i = \pm 1$, p_i are occupation numbers indicating the presence of quenched structurally uncorrelated disorder in the system: $p_i = 1$ for the i site with a spin, and $p_i = 0$ for the site with a nonmagnetic impurity atom.

4.1.1 Simulation with a test magnetic field. Results of numerical studies. The autocorrelation function

$$C(t, t_w) = \left[\left\langle \frac{1}{pL^3} \sum_{i=1}^{pL^3} p_i \, S_i(t) S_i(t_w) \right\rangle \right] \tag{79}$$

and magnetic susceptibility

$$\chi(t, t_w) = \overline{\left[\left\langle \frac{1}{h^2 pL^3} \sum_{i=1}^{pL^3} p_i \, h_i(t_w) S_i(t) \right\rangle \right]} \tag{80}$$

were calculated, where p is the spin concentration in the cubic lattice with linear dimension L, angular brackets denote statistical averaging over realizations of the initial state, square brackets stand for averaging over various configurations of the defect distribution in the lattice, and the macron indicates averaging over realizations of a random magnetic field. Notice that dynamic susceptibility is an integral characteristic related to the response function by the expression

$$\chi(t, t_w) = \int_{t_w}^{t} \mathrm{d}t' \, R(t, t') \,. \tag{81}$$

To calculate dynamic susceptibility $\chi(t, t_w)$ at the instant t_w, the Hamiltonian is supplemented by perturbation $\delta H = -\sum_i h_i S_i$, where the random magnetic field is given by bimodal distribution $\pm h$ at the sites of the crystal lattice [9]. Field amplitude h was chosen to be small enough ($h = 0.01$) to avoid the nonlinear effects of the field.

The system was modelled on a spin lattice with a linear size $L = 128$ at spin concentrations $p = 0.8$ and 0.6 and the respective critical temperatures $k_B T_c/J = 3.4995(2)$ and 2.4241(1) [16, 17]. The initial high-temperature state, $T \gg T_c$, of the system with low magnetization $m_0 \ll 1$ ($m_0 = 0.01$ for $p = 0.8$, and $m_0 = 0.005$ for $p = 0.6$) was formed to be essentially nonequilibrium for the critical regime of interest at $T = T_c$. The system's behavior was examined at times up to 10,000 MCS/s for waiting times $t_w = 50$, 250, 500, and 1000 MCS/s. The resulting dependences were computed by averaging over 1000 impurity configurations; for each of them, averaging was performed over 20 realizations of the initial state, and 10 realizations of a random magnetic field.

Figure 9 shows on the double logarithmic scale the plots of calculated temporal evolution of the autocorrelation function for systems with $p = 0.8$ and 0.6 and different waiting times. The graphs clearly demonstrate the possibility of distinguishing a few regimes in the two-time behavior of the autocorrelation function. For example, the behavior for $t - t_w \ll t_w$ does not exhibit any dependence on the waiting time, in which case $C(t, t_w) = C(t - t_w)$, thus suggesting realization of the quasiequilibrium regime with the power-law time dependence $C(t - t_w) \sim (t - t_w)^{-(d-2+\eta)/z}$.

For observation $(t - t_w)$ and waiting (t_w) times long enough but comparable $(t - t_w \sim t_w \gg 1)$, the behavior of $C(t, t_w)$ exhibits an essential dependence of waiting time t_w that characterizes aging effects, i.e., the slowing down of the temporal correlation decline with an increase in the system's 'age' t_w. An approximation of the autocorrelation function at this stage with $T = T_c$ by the power-law dependence $C(t, t_w) \sim (t - t_w)^{-\lambda}$ yielded λ values for different t_w. The λ values presented in Table 2 give evidence of the slowing down of system evolution with growing t_w, and simultaneous enhancement of aging effects with increasing concentration of defects.

For the stage with $t - t_w \sim t_w \gg 1$, two-time dynamic functions can be characterized by the following depen-

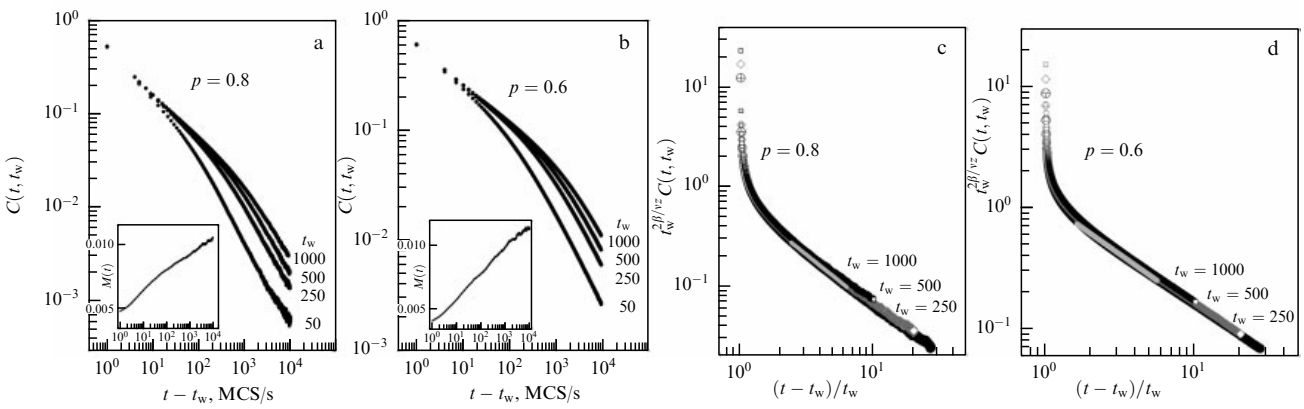

Figure 9. Dependence of autocorrelation function $C(t, t_w)$ on observation time $t - t_w$ on the double logarithmic scale at spin concentrations (a) $p = 0.8$ and (b) $p = 0.6$ for different waiting times t_w. Demonstration of realization of the scaling dependence for autocorrelation function (82) at different times t_w for spin concentrations (c) $p = 0.8$ and (d) $p = 0.6$.

Table 2. Critical λ values for systems with spin concentrations $p = 0.8$ and 0.6.

t_w	λ	
	$p = 0.8$ $t - t_w = 160-1600$	$p = 0.6$ $t - t_w = 300-1200$
50	0.938(34)	0.746(32)
250	0.739(40)	0.604(45)
500	0.644(25)	0.531(40)
1000	0.569(30)	0.467(36)

dences [27]:

$$C(t, t_w) \sim t_w^{-(d-2+\eta)/z} F_C\left(\frac{t}{t_w}\right), \qquad R(t, t_w) \sim t_w^{-1-(d-2+\eta)/z} F_R\left(\frac{t}{t_w}\right). \tag{82}$$

The behavior of scaling functions $F_C(t/t_w)$ and $F_R(t/t_w)$ is well known for the stage of essentially nonequilibrium evolution of the system, realized for times $t \gg t_w \gg 1$. At this stage, the scaling functions are expressed as

$$F_C\left(\frac{t}{t_w}\right) \approx A_C\left(\frac{t}{t_w}\right)^{-c_a}, \qquad F_R\left(\frac{t}{t_w}\right) \approx A_R\left(\frac{t}{t_w}\right)^{-c_r} \tag{83}$$

with exponent $c_a = c_r = d/z - \theta'$. Here, the critical exponent θ' defines growing magnetization $M(t) \sim t^{\theta'}$ during nonequilibrium critical evolution of the system from the initial state with $m_0 \ll 1$ (see inserts to Figs 9a, b).

To confirm the scaling dependence of the autocorrelation function (82), the t/t_w dependence of $t_w^{(1+\eta)/z} C(t, t_w)$ was constructed. The result is presented in Figs 9c, d demonstrating the collapse of the data obtained for different t_w in the universal curves corresponding to $p = 0.8$ and $p = 0.6$ and fitting the scaling function $F_C(t/t_w)$ in formulas (82). The critical exponents $z = 2.191(21)$ and $1 + \eta = 2\beta/\nu = 1.016(32)$ were used in the case of a weakly disordered system with $p = 0.8$ [17], and $z = 2.663(30)$ and $1 + \eta = 0.924(80)$ for a strongly disordered system with $p = 0.6$ [41, 78].

An analysis of the t/t_w dependence of $t_w^{(1+\eta)/z} C(t, t_w)$ was employed to calculate the c_a exponent for scaling function (83): $c_a(p = 0.8) = 1.237(22)$ and $c_a(p = 0.6) = 0.982(30)$. The c_a value for the weakly disordered system with $p = 0.8$ is in excellent agreement (within the calculation accuracy)

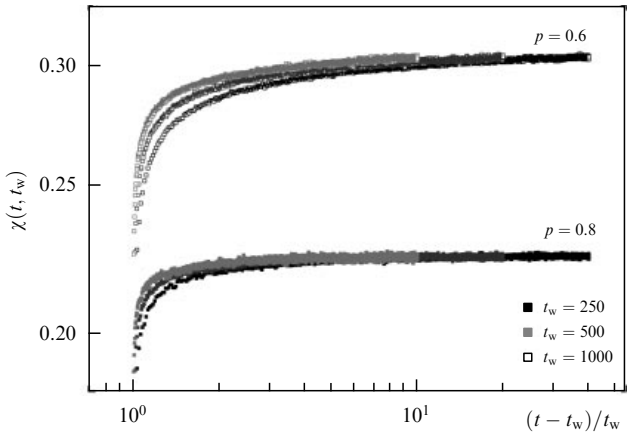

Figure 10. Dependence of generalized susceptibility $\chi(t, t_w)$ on t/t_w at spin concentrations $p = 0.8$ and $p = 0.6$ for different waiting times t_w.

with $c_a = 1.242(10)$ obtained in Ref. [17] applying the short-time dynamics method and taking advantage of leading scaling corrections, but poorly agrees with $c_a = 1.05(3)$ found in studies on the nonequilibrium critical dynamics in the disordered Ising model [72, 73]. We discussed the causes of such a discrepancy in Ref. [17].

Figure 10 plots the t/t_w two-time dependence of generalized susceptibility $\chi(t, t_w)$ for systems with spin concentrations $p = 0.8$ and $p = 0.6$ for different waiting times t_w. It can be seen that at the stage of evolution with $t - t_w \sim t_w \gg 1$, as for the autocorrelation function, the t_w dependence of $\chi(t, t_w)$ characteristic of aging effects (slow-down of system's relaxation with age t_w) is manifested, whereas at the stage with $t \gg t_w \gg 1$ the universal scaling dependence in the form of $F_\chi(t/t_w) \sim (t/t_w)^{c_\chi}$ takes place.

The scaling behavior of dynamic functions $C(t, t_w)$ and $R(t, t_w)$ in the $t - t_w \gg t_w \gg 1$ regime defined by relation (82) leads to the functional dependence of FDR $X(t, t_w)$ only on t/t_w [31, 32]:

$$X(t, t_w) = \frac{TR(t/t_w)}{(\partial/\partial t_w) C(t/t_w)} \sim \frac{F_R(t/t_w)}{(2\beta/\nu z) F_C(t/t_w) + (t/t_w) F_C'(t/t_w)}. \tag{84}$$

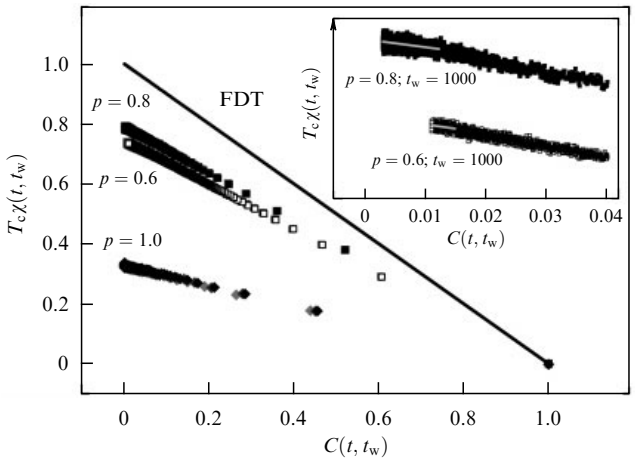

Figure 11. Parametric dependences of $T_c\chi(t, t_w)$ on $C(t, t_w)$ at $t_w = 1000$ MCS/s for spin concentrations of $p = 1.0$, 0.8, and 0.6 in comparison with the dependence in the case of fulfillment of the FDT.

Such behavior of $X(t, t_w)$ is confirmed by renormalization group calculations [21].

Representation (84) allowed limiting FDR values to be obtained in Refs [31, 32] by means of linear approximation by $t_w/t \to 0$ of the set of data obtained for certain two-dimensional spin systems (Ising model, Potts model with the number of states $q = 4$, and clock-models with $q = 3$) taking advantage of their weak dependence on t_w. In the case of the three-dimensional Ising model, our data demonstrate the well-apparent t_w dependence; therefore, we first applied the procedure for obtaining $X^\infty(t_w) = \lim_{t\to\infty} X(t, t_w)$ and then found the sought limiting FDR value $X^\infty = \lim_{t_w\to\infty} X^\infty(t_w)$.

Belonging to the universality class of both 'pure' and disordered systems is manifested as the universality of the values of critical exponents and critical amplitude ratios. According to formulas (82) and (83), the limiting FDR value assumes the form

$$X^\infty = \lim_{t_w\to\infty}\lim_{t\to\infty} X(t, t_w) = \frac{A_R}{A_C}\left(c_a - \frac{2\beta}{\nu z}\right)^{-1} \qquad (85)$$

and becomes a new universal characteristic of the critical behavior.

FDR values can be obtained on the basis of time dependences we calculated for the autocorrelation function $C(t, t_w)$ and susceptibility $\chi(t, t_w)$ (see Fig. 10), if quantity $T_c\chi(t, t_w)$ is expressed in accordance with Eqns (2) and (81) as a function of $C(t, t_w)$:

$$T_c\chi(t, t_w) = \int_{t_w}^{t} X(t, t')\,\frac{\partial C(t, t')}{\partial t'}\,dt' = \int_{C(t,t_w)}^{1} X(C)\,dC\,. \qquad (86)$$

To accomplish this, the $C(t, t_w)$ dependence of $T_c\chi(t, t_w)$ is represented in the form of a certain curve (Fig. 11) with the asymptotic curvature determining $X^\infty(t_w)$:

$$X^\infty(t_w) = -\lim_{C\to 0}\frac{d(T_c\chi)}{dC}\,. \qquad (87)$$

The sought limiting FDR value X^∞ is obtained by finding $X^\infty(t_w)$ for different waiting times, then carrying out linear approximation, and finally extrapolating the result: $X^\infty(t_w \to \infty)$.

Table 3. Limiting FDR values X^∞ for systems with spin concentrations $p = 1.0$, 0.8, and 0.6.

t_w	X^∞	t_w	X^∞	
	$p = 1.0$		$p = 0.8$	$p = 0.6$
10	0.586(24)	250	0.708(15)	0.726(13)
25	0.460(52)	500	0.544(23)	0.583(14)
50	0.437(63)	1000	0.494(17)	0.519(29)
$\to\infty$	0.390(12)	$\to\infty$	0.415(18)	0.443(6)

Figure 11 shows parametric dependences of $T_c\chi(t, t_w)$ on $C(t, t_w)$ at $t_w = 1000$ MCS/s for spin concentrations $p = 1.0$, 0.8, and 0.6. The solid straight line corresponds to the quasi-equilibrium behavior of the system satisfying the FDT and $X(t, t_w) = 1$. Dependences of $T_c\chi(t, t_w)$ on $C(t, t_w)$ demonstrate FDT violation for the nonequilibrium critical behavior of both 'pure' and disordered Ising models. These dependences and FDRs were calculated at waiting times $t_w = 250$, 500, and 1000 MCS/s for structurally disordered systems, and $t_w = 10$, 25, and 50 MCS/s for the 'pure' system. Table 3 presents $X^\infty(t_w)$ values obtained for different waiting times.

$X^\infty(t_w)$ values are calculated according to procedure (87) in the $C(t, t_w) \to 0$ limit corresponding to the stage with $t \gg t_w \gg 1$. Therefore, the inset to Fig. 11 shows those portions of $C(t, t_w)$ dependences of $T\chi(t, t_w)$ that meet these criteria and on which $X^\infty(t_w)$ values were determined.

Importantly, in numerical research on nonequilibrium critical behavior, the duration of the nonequilibrium stage of evolution for three-dimensional lattices even of such a large size as $L = 128$ in pure systems reaches 1000 MCS/s compared with 10,000 MCS/s in structurally disordered systems with $L = 128$ (as confirmed in the insets to Fig. 9). This allows studies to be carried out for the analysis of aging effects and limiting FDR values in structurally disordered systems at much longer waiting times t_w than in 'pure' systems, enhancing the significance of the characteristics thus obtained for the critical state of a system with abnormally large amplitudes and long-lived order parameter fluctuations.

Figure 12 plots the calculated $X^\infty(1/t_w)$ dependence and its extrapolation to the X^∞ value as $t_w \to \infty$. The limiting FDR values $X^\infty = 0.415(18)$ and $X^\infty = 0.443(6)$ obtained for the system with spin concentrations $p = 0.8$ and $p = 0.6$, respectively, suggest FDT violation in the nonequilibrium

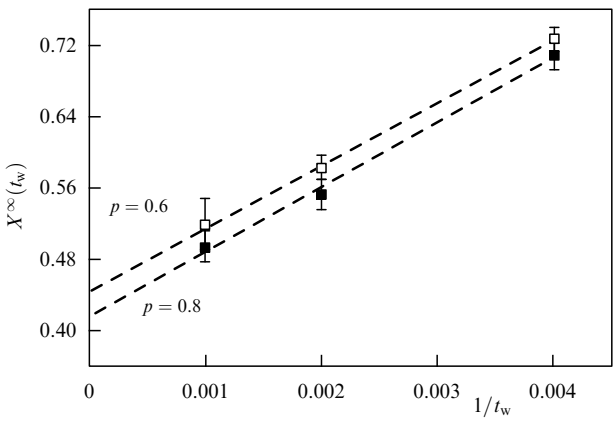

Figure 12. Finding the FDR by approximation of limiting $X^\infty(t_w)$ values as $t_w^{-1} \to 0$ for $p = 0.8$ and 0.6.

critical behavior of structurally disordered systems described by the three-dimensional Ising model. They also indicate that the presence of defects in strongly disordered systems with $p = 0.6$ is associated with a higher X^∞ value than in weakly disordered systems with $p = 0.8$.

It can be concluded based on the tentative limiting X^∞ value $\simeq 0.4$ found in numerical studies on the nonequilibrium critical behavior of a 'pure' three-dimensional Ising model [27] and our examination of this model yielding $X^\infty = 0.390(12)$ that the presence of structural defects is responsible for a new universality class of the critical behavior for the three-dimensional Ising model characterized, inter alia, by limiting FDR values $X^\infty_{\text{disorder}} > X^\infty_{\text{pure}}$.

It is worthwhile to mention that Ref. [21] presents the renormalization group description of the nonequilibrium critical behavior of dissipative systems with the nonconserved order parameter, for which the FDR was calculated making use of the ε-expansion in the second order of the theory. The FDR obtained as a series in ε looked like expression (43). For the three-dimensional Ising model with $\varepsilon = 1$ and $n = 1$, summation of Padé approximants gave $X^\infty = 0.429(6)$ (the series is unsummable by Padé–Borel or Padé–Borel–Leroy method). In Ref. [22], X^∞ was calculated in the one-loop approximation for a weakly diluted Ising model that led, in accordance with expression (44) at $\varepsilon = 1$, to $X^\infty = 0.416$.

The authors of Ref. [22] pointed out that these results obtained in the first order of the theory for the disordered Ising model do not allow deducing peculiarities of the influence of defects on FDR by comparing them with the results for a pure model; calculations in higher orders are needed for this purpose. Nevertheless, the value of $X^\infty = 0.422(14)$ we obtained for a weakly disordered system with spin concentration $p = 0.8$ agrees with the results of the renormalization group description to within statistical accuracy.

The reported numerical studies demonstrate through the behavior of two-time functions striking peculiarities of the nonequilibrium behavior of slow-dynamics systems, such as the influence of initial states for times shorter than the system's relaxation time, manifestations of aging effects at observation times close to the waiting time, and identification of the FDR, the introduction of which generalizes the FDT for the case of nonequilibrium behavior with the possibility of introducing the effective system's temperature as $T_{\text{eff}} = T/X(t, t_{\text{w}})$ [24]. These peculiarities need to be taken into consideration when setting conditions for an experimental study on the behavior of slow-dynamics systems and the analysis of the results obtained.

4.1.2 Simulation by the thermal bath method. Results and their analysis. In this section, FDT violations in a structurally disordered Ising model were investigated by the thermal bath method, allowing the response function to be obtained in the course of simulating the system's dynamics without introducing a magnetic field by expressing it via a special two-time correlation function given by expression (70) and the FDR in accordance with expression (71). For structurally disordered systems, expressions (70) and (71) are modified taking into account the introduction of randomly distributed nonmagnetic impurity atoms and the necessity of additional averaging over different configurations of quenched defect distribution over the lattice. As a result, the following expressions are used in calculating these quantities:

$$R(t, t_{\text{w}}) = \frac{1}{TN_{\text{s}}} \sum_{i=1}^{N_{\text{s}}} \Big[\big\langle p_i S_i(t) \big(S_i(t_{\text{w}} + 1) - S_i^W(t_{\text{w}} + 1) \big) \big\rangle \Big] , \tag{88}$$

$$X(t, t_{\text{w}}) = \frac{TR(t, t_{\text{w}})}{\partial_{t_{\text{w}}} C(t, t_{\text{w}})} = \frac{\sum_{i=1}^{N_{\text{s}}} \big[\big\langle p_i S_i(t) \big(S_i(t_{\text{w}} + 1) - S_i^W(t_{\text{w}} + 1) \big) \big\rangle \big]}{\sum_{i=1}^{N_{\text{s}}} \big[\big\langle p_i S_i(t) \big(S_i(t_{\text{w}} + 1) - S_i(t_{\text{w}}) \big) \big\rangle \big]} , \tag{89}$$

where $S_i^W = \tanh \big(J \sum_{m \neq i} p_m S_m / T \big)$, $N_{\text{s}} = pL^3$ is the number of spins in the lattice.

We undertook simulation of the nonequilibrium critical behavior of both 'pure' and structurally disordered Ising models with spin concentrations $p = 1.0$, 0.95, 0.8, 0.6, and 0.5 on a 3D cubic lattice with the linear size $L = 128$ [81].

The study was designed to elucidate the evolution of the system from a specially formed high-temperature initial state for $T_0 \gg T_{\text{c}}$ with low magnetization $m_0 \ll 1$ ($m_0(p = 1) = 0.02$, $m_0(p = 0.95; 0.8) = 0.01$, and $m_0(p = 0.6; 0.5) = 0.005$). The system's dynamics was realized after preparing the initial configuration at the following critical temperatures:

$$T_{\text{c}}(p = 1) = 4.5114(1) , \quad T_{\text{c}}(p = 0.95) = 4.26267(4) ,$$
$$T_{\text{c}}(p = 0.8) = 3.4995(2) , \quad T_{\text{c}}(p = 0.6) = 2.4241(1) ,$$
$$T_{\text{c}}(p = 0.5) = 1.84509(6) ,$$

corresponding to the spin concentrations being considered [16, 17]. The behavior of the systems was examined for times up to 10,000 MCS/s. The 'pure' system was modelled with statistical averaging over 94,000 runs. For modeling the structurally disordered Ising model, the calculated values were averaged over 6,200 impurity configurations and 15 runs for each configuration.

Figures 13a, b illustrate on the double logarithmic scale the resulting dependences of the autocorrelation function $C(t, t_{\text{w}})$ and the response function $R(t, t_{\text{w}})$ on observation time $t - t_{\text{w}}$ for a set of different waiting times t_{w}. Manifestation of aging effects via dependences of functions $C(t, t_{\text{w}})$ and $R(t, t_{\text{w}})$ on the system's 'age' t_{w} is quite apparent (correlation effects slow down with age and the response of the system to external perturbations decreases); in addition, relaxation of the system slows down with a rise in defect concentration (and decrease in spin concentration p), while aging effects become stronger.

In the aging regime realized at observation times $t - t_{\text{w}} \sim t_{\text{w}}$, in which the two-time dependence of functions $C(t, t_{\text{w}})$ and $R(t, t_{\text{w}})$ is most pronounced, the scaling dependence of these functions on waiting times t_{w} and t is given by relations (11) and characterized only by scaling functions $\hat{F}_C(t/t_{\text{w}})$ and $\hat{F}_R(t/t_{\text{w}})$ that depend only on the ratio between these times. To confirm the scaling dependence of the autocorrelation function and the response function (11), we constructed t/t_{w} dependences of $t_{\text{w}}^{2\beta/(z\nu)} C(t, t_{\text{w}})$ and $t_{\text{w}}^{1+2\beta/(z\nu)} R(t, t_{\text{w}})$ with values of the critical exponents $z = 2.191(21)$, $2\beta/\nu = 1.016(32)$ for $p = 0.95$, 0.8 [17] and $z = 2.663(30)$, $2\beta/\nu = 0.924(80)$ for $p = 0.6$, 0.5 [41, 78]. The result is shown in Fig. 14, demonstrating the collapse of the data obtained for various t_{w} in universal curves corresponding to spin concentrations $p = 1.0$, 0.95, 0.8, 0.6, and 0.5 characterized by the scaling functions $\hat{F}_C(t/t_{\text{w}})$ and $\hat{F}_R(t/t_{\text{w}})$ in relations (11).

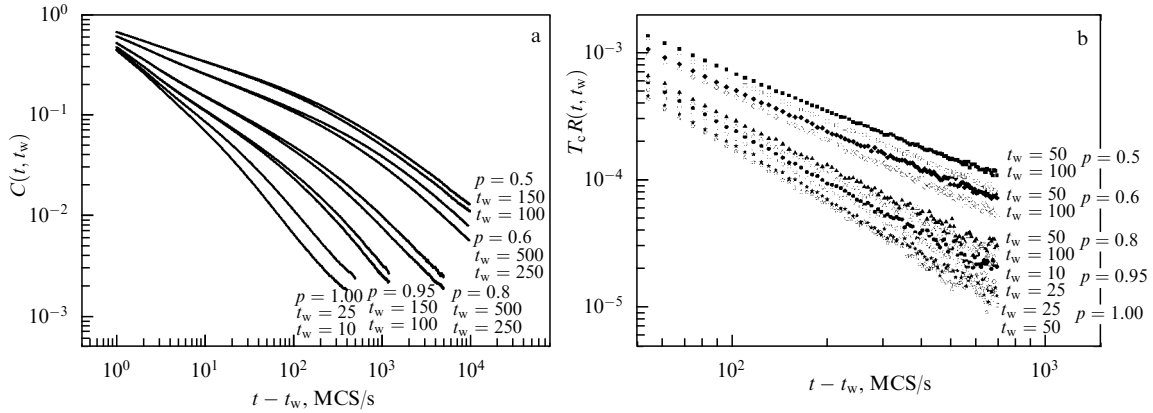

Figure 13. Dependences of correlation function $C(t, t_w)$ (a) and response function $R(t, t_w)$ (b) on observation times $t - t_w$ for various spin concentrations p and waiting times t_w.

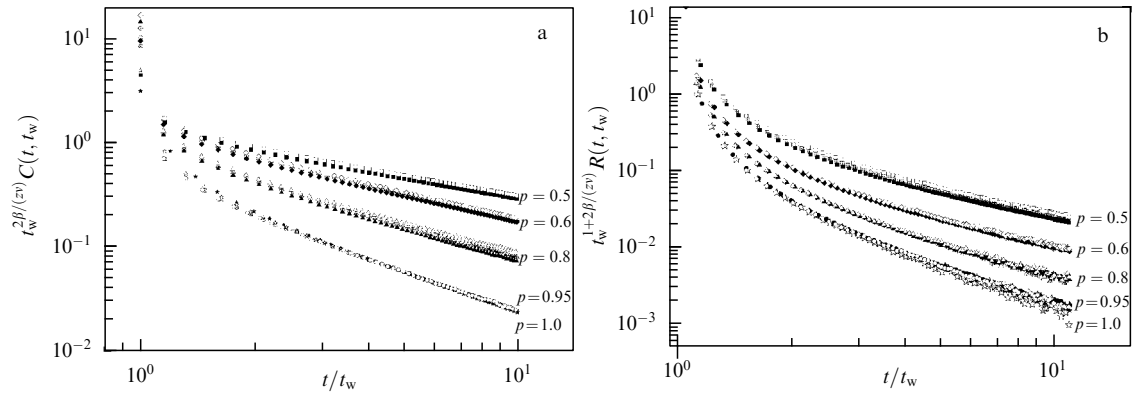

Figure 14. Scaling dependences of the correlation function $C(t, t_w)$ (a) and the response function $R(t, t_w)$ (b) for different spin concentrations with a characteristic collapse of the data for various t_w in universal curves.

It should be noted that systems with different spin concentrations p are characterized by various scaling functions $\hat{F}_{C,R}(t, t_w, p)$. For times $t \gg t_w$, these functions exhibit the power-law dependence: $\hat{F}_{C,R}(t/t_w) \approx A_{C,R}(t/t_w)^{-c_{a,r}}$. At this stage of system's evolution, the influence of aging effects is unapparent and exponents $c_{a,r}$ are related to the known dynamic critical exponents z and θ' [17]: $c_a = c_r = d/z - \theta'$.

Table 4 collates the values of c_a and c_r computed in Ref. [81] for different spin concentrations p. The values of c_a and c_r are in excellent agreement with one another for each fixed spin concentration p and separately for weakly disordered spin systems with $p = 0.95$, 0.8 and strongly disordered systems with $p = 0.6$, 0.5, but differences between the values for the weakly and strongly disordered systems and for the 'pure' Ising model are much greater than statistical errors of their determination. The data in Table 4 agree with the values of $c_a = 1.362(19)$ for a 'pure' Ising model, $c_a = 1.242(10)$ for a weakly disordered system with $p = 0.8$, and $c_a = 0.941(21)$ for a strongly disordered system with $p = 0.6$ obtained in Refs [17, 39, 78] by the short-time dynamics method.

Figure 15 demonstrates FDR values calculated based on relation (89) as the dependence of $X(t, t_w)$ on $t_w/(t - t_w)$ for $t - t_w \gg t_w$ for systems with different spin concentrations. The linear approximation of $X(t, t_w)$ dependence as $t_w/(t - t_w) \to 0$ gave the $X(t_w, p)$ value for each t_w and the respective spin concentration p. The linear approximation of $X(t_w, p)$ values thus obtained for different waiting times

Table 4. Values of scaling function exponents c_a, c_r and limiting FDR values X^∞ for different spin concentrations.

p	c_a	c_r	X^∞
1.0	1.333(40)	1.357(18)	0.380(13)
0.95	1.230(28)	1.264(40)	0.413(7)
0.8	1.237(22)	1.251(22)	0.413(11)
0.6	0.982(30)	0.950(8)	0.446(8)
0.5	0.896(64)	0.955(33)	0.441(13)

followed by their extrapolation as $t_w \to \infty$ yielded the sought limiting FDR value X^∞. Approximation and extrapolation procedures are illustrated by Fig. 16. They permitted obtaining $X^\infty(p)$ values collated in Table 4 for different spin concentrations p.

The values of $X^\infty \neq 1$ suggest FDT violation in the nonequilibrium critical behavior of 'pure' and structurally disordered systems described by the three-dimensional Ising model and the influence of a defect presence for increased $X^\infty(p)$. Similar to exponents c_a and c_r, these $X^\infty(p)$ values can be regarded as universal characteristics of three classes of nonequilibrium critical behavior for 'pure', weakly, and strongly disordered three-dimensional Ising systems [66, 67].

Analyzing the results of numerical studies gives evidence that structural defects are responsible for new universal FDR values, with $X^\infty(p)$ for strongly disordered systems being higher than $X^\infty(p)$ for weakly disordered systems, and even

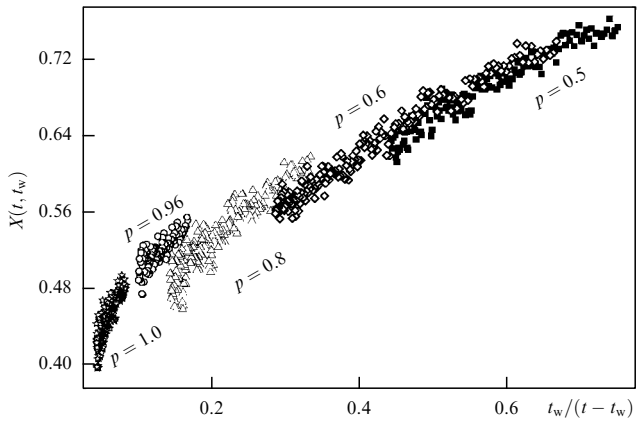

Figure 15. Functional dependence of FDR $X(t, t_w)$ on $t_w/(t - t_w)$ for $t - t_w \gg t_w$ and different spin concentrations.

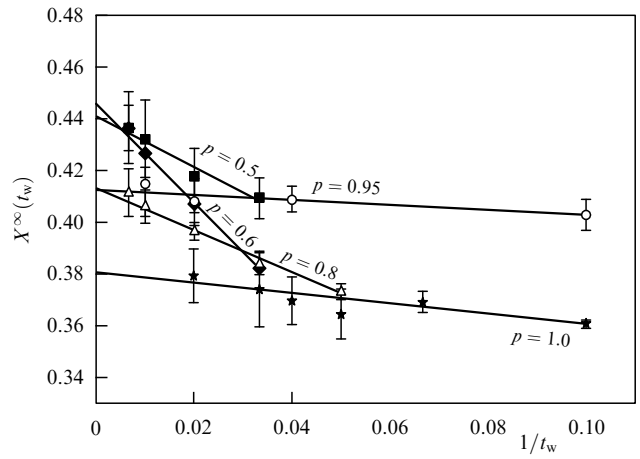

Figure 16. Functional dependences of limiting FDR values $X(t_w, p)$ on $1/t_w$ for different spin concentrations. $X^\infty(p)$ values are derived in the $1/t_w \to 0$ limit by linear approximation.

higher than $X^\infty(p = 1)$ for the 'pure' three-dimensional Ising model.

$X^\infty(p)$ values found for the weakly disordered three-dimensional Ising model with $p = 0.95$ and 0.8 fairly well agree with $X^\infty_{\text{3DRIM}} \simeq 0.416$ [see formula (44)] obtained by renormalization group computations with the use of ε-expansion in Ref. [22]. However, $X^\infty(p)$ values (see Table 4) for the strongly disordered Ising model with $p = 0.6$ and 0.5 are at variance with $X^\infty_{\text{3DRIM}} \simeq 0.416$ within the calculation accuracy. Also noticeable is the fact that $X^\infty(p = 1) = 0.380(13)$ obtained for the 'pure' Ising model differs from $X^\infty_{\text{3DIS}} = 0.429(6)$ calculated with the use of ε-expansion in Ref. [21] [see formula (43) and the discussion at the end of Section 2.1.2] but is close to $X^\infty(p = 1) \simeq 0.40$ reported in paper [27] as a result of preliminary calculations for the 'pure' three-dimensional Ising model.

An important feature of numerical studies of the nonequilibrium critical behavior applying the MC methods is the duration of the nonequilibrium evolution stage of the 'pure' Ising model for three-dimensional lattices of even such a large size as $L = 128$ does not exceed 1000 MCS/s, in contrast to 10,000 MCS/s (i.e., an order of magnitude longer) for diluted systems with $p = 0.8$ and $L = 128$. For this reason, aging effects and FDT violations are possible to examine in structurally disordered systems at considerably longer waiting times than t_w in 'pure' systems, which increases the significance of the resultant characteristics of the critical behavior of systems with intrinsically high amplitudes and long-lived order parameter fluctuations.

Importantly, the choice of experimental conditions and analysis of critical behavior data for different systems require that not only the influence of critical slow-down effects but also that of aging effects be taken into consideration, bearing in mind that the latter markedly strengthen the former with increasing specimen 'age' and are responsible for the influence of the system's initial states on the values of thermodynamic and correlation functions. Both the presence of structural defects in the system and the elevation of their concentration lead to an appreciable increase in aging effects.

4.2 Evolution from a low-temperature initial state. Superaging effects

To elucidate peculiarities of nonequilibrium critical behavior in a three-dimensional Ising spin system evolving from a low-temperature initial state with $m_0 = 1$ and to evaluate the influence of structural defects on these features, we applied a method (see Refs [55, 82]) allowing us to calculate the response function without the application of an external magnetic field by computing generalized susceptibility in the form of the integral response function (thermostatic susceptibility):

$$\chi(t, t_w) = \int_0^{t_w} dt' \, R(t, t') = \frac{1}{TN_s} \sum_{i=1}^{N_s} \left[\left\langle p_i S_i(t) \Delta S_i(t_w) \right\rangle \right], \quad (90)$$

with the response function given by relation (2) and function $\Delta S_i(t_w)$ found by modeling the system's states from the starting instant $t = 0$ till waiting time t_w. This function is defined by the relation

$$\Delta S_i(t_w) = \sum_{s=0}^{t_w} \left[S_i(s) - S_i^W(s) \right], \quad (91)$$

where $S_i^W = \tanh\left(J \sum_{m \neq i} p_m S_m / T\right)$.

On the other hand, taking the response function in expression (90) in the form (4) yields

$$T\chi(t, t_w) = \int_0^{t_w} X(t, t') \, \frac{\partial C(t, t')}{\partial t'} \, dt' = \int_0^{C(t, t_w)} X(C) \, dC. \quad (92)$$

As a result, the FDR will be defined by the relationship

$$X(t, t_w) = \lim_{C \to 0} T \, \frac{\partial \chi(t, t_w)}{\partial C(t, t_w)}, \quad (93)$$

which can be used to find the limiting FDR value (6).

In Refs [55, 82], the three-dimensional Ising model was modelled with spin concentrations $p = 1.0$, 0.95, 0.8, 0.6, 0.5 on a cubic lattice of linear size $L = 128$ at respective critical temperatures $T_c(p)$: $T_c(1.0) = 4.5114(1)$ [51], $T_c(0.95) = 4.26267(4)$, $T_c(0.8) = 3.4995(2)$, $T_c(0.6) = 2.4241(1)$, $T_c(0.5) = 1.84509(6)$ [16]. At the early stage of system's evolution, the correlation length is still rather small and the finiteness of the size of the model being simulated turns out unessential. Therefore, the employment of the lattice with a large enough linear size $L = 128$ allows finite-dimensional effects to be disregarded in view of their smallness in comparison to effects associated with the simulation of equilibrium critical phenomena [16].

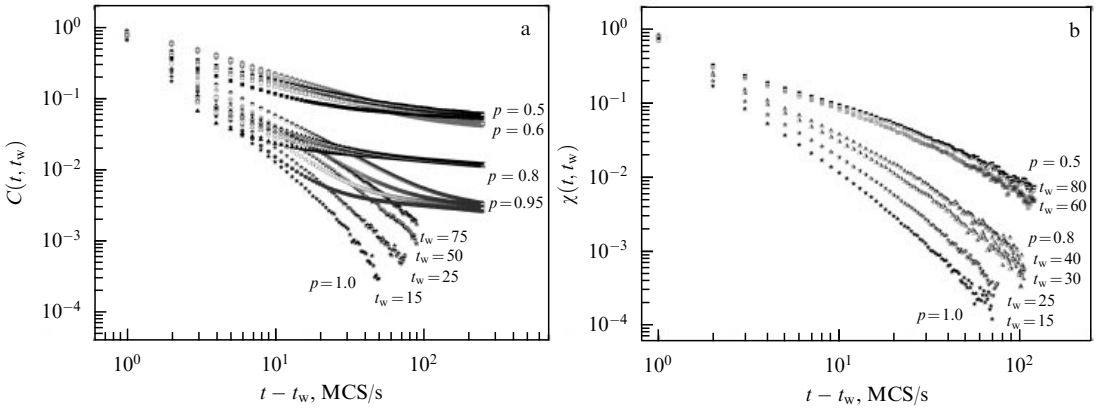

Figure 17. Nonequilibrium dependences of autocorrelation function $C(t, t_w)$ (a) and dynamic susceptibility $\chi(t, t_w)$ (b) on observation time $t - t_w$ for different spin concentrations p and waiting times t_w.

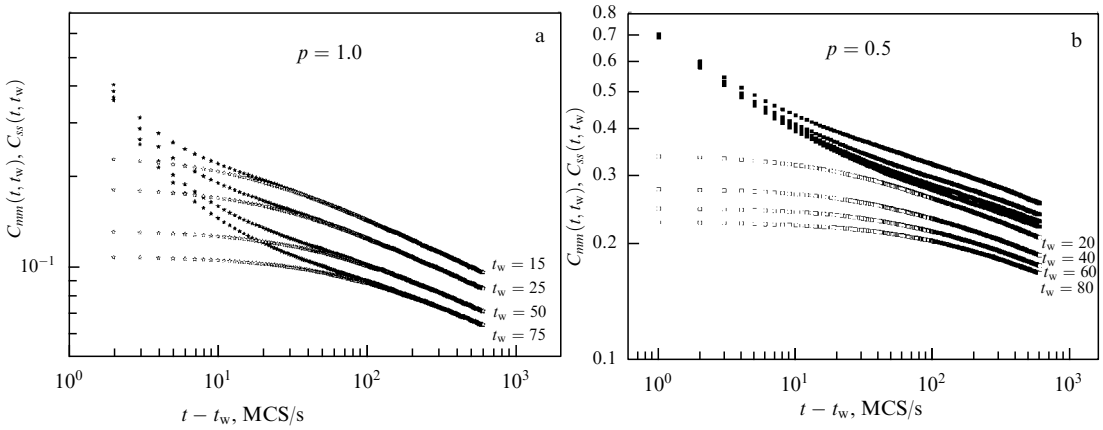

Figure 18. Comparison of time-dependent contributions to autocorrelation function $C_{ss}(t, t_w) \sim [\langle S(t)S(t_w)\rangle]$ and $C_{mm}(t, t_w) \sim [\langle S(t)\rangle\langle S(t_w)\rangle]$ for spin concentrations $p = 1.0$ (a) and $p = 0.5$ (b).

The two-time dependences of the autocorrelation function

$$C(t, t_w) = \left[\left\langle \frac{1}{N_s}\sum_{i=1}^{N_s} p_i S_i(t) S_i(t_w)\right\rangle\right] - \left[\left\langle \frac{1}{N_s}\sum_{i=1}^{N_s} p_i S_i(t)\right\rangle\left\langle \frac{1}{N_s}\sum_{i=1}^{N_s} p_i S_i(t_w)\right\rangle\right] \quad (94)$$

and susceptibility $\chi(t, t_w)$ (90) on observation time $t - t_w$ were calculated for the time set t_w at the above-given spin concentrations p. The behavior of the systems was examined for times up to 10,000 MCS/s. The 'pure' system with $p = 1.0$ was modelled by statistical averaging over 90,000 runs, and the structurally disordered Ising model by averaging the calculated values over 6000 impurity configurations and 15 runs for each configuration.

The calculated results are presented in Fig. 17. Aging effects manifested themselves via dependences of $C(t, t_w)$ and $\chi(t, t_w)$ on the system's age t_w at observation times $t - t_w \sim t_w$ and were characterized by the slowing down of age-driven correlation and relaxation processes. Figure 17 also indicates that aging effects grow as defect concentration increases and spin concentration p decreases. The influence of defects is most developed through a strong slowing down of correlation effects in structurally disordered systems, as opposed to those in a 'pure' system.

We attribute these marked changes in the behavior of the autocorrelation function to the pinning of domain walls on structural defects, which is associated with a nonequilibrium alteration of the system's domain structure during transition from a single-domain state at $T_0 = 0$ to the multidomain fluctuation structure arising at critical temperature T_c. This inference follows from the plots for two [$C_{ss}(t, t_w)$ and $C_{mm}(t, t_w)$] constituents of the correlation function (94) represented in Fig. 18 for a 'pure' system and a system with spin concentration $p = 0.5$. Evidently, the values of $C_{ss}(t, t_w)$ and $C_{mm}(t, t_w)$ constituents in the 'pure' system begin to coincide for observation times $t - t_w \geqslant t_w$, which leads to their cancellation in the complete autocorrelation function. In contrast, the plots of these constituents in structurally disordered systems tend to draw together for times $t - t_w \geqslant t_w$ and undergo parallel changes, but full cancellation fails to be achieved; moreover, the difference increases with time t_w and defect concentration $c_{imp} = 1 - p$.

In the aging regime, the time dependence of the autocorrelation function and dynamic susceptibility is characterized by scaling relations (48) and (62) with scaling functions $\tilde{F}_{C,\chi}(t/t_w)$ demonstrating an $\tilde{F}_{C,\chi}(t/t_w) \sim (t/t_w)^{-\phi}$ power-law behavior at the long-time stage of system relaxation with $t - t_w \gg t_w \gg t_m$ and $\phi = 1 + d/z + \beta/(z\nu)$. To confirm the scaling forms for the autocorrelation function and susceptibility, the dependences of $t_w^{2\beta/(z\nu)} C(t, t_w)$ and $t_w^{2\beta/(z\nu)}\chi(t, t_w)$ on $(t - t_w)/t_w$ were constructed with following

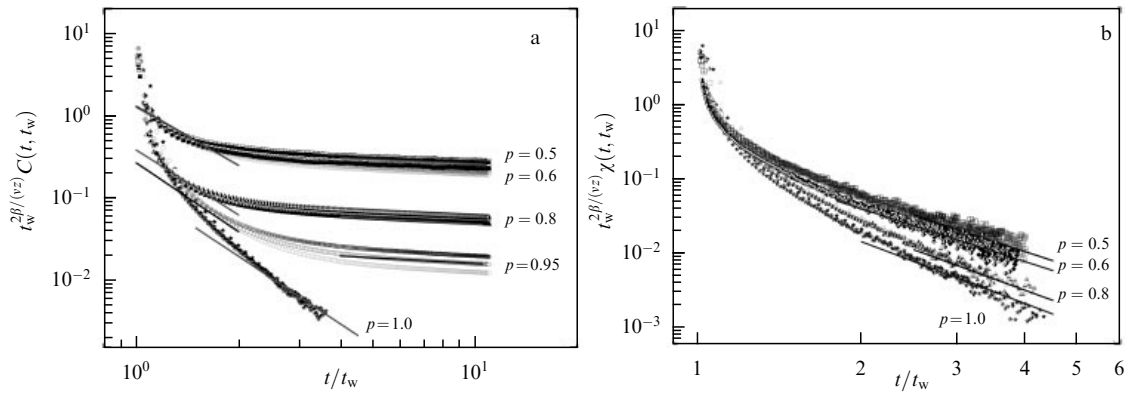

Figure 19. Scaling dependences for the autocorrelation function $t_w^{2\beta/(vz)}C(t, t_w)$ (a) and susceptibility $t_w^{2\beta/(vz)}\chi(t, t_w)$ (b) on t/t_w demonstrating a collapse of the data obtained for different t_w.

critical exponents: $2\beta/\nu = 1.032(5)$ [56], $z = 2.024(6)$ [57] for $p = 1.0$; $2\beta/\nu = 1.016(32)$, $z = 2.191(21)$ [17] for $p = 0.95$ and 0.8; $2\beta/\nu = 0.924(80)$, $z = 2.663(30)$ [41] for $p = 0.6$ and 0.5. The result is presented in Fig. 19 demonstrating 'collapse' of the data obtained for different t_w at the respective spin concentrations p in universal curves characterized by scaling functions $\tilde{F}_C(t/t_w)$ and $\tilde{F}_\chi(t/t_w)$.

The exponents $\phi_c = 2.742(32)$ and $\phi_\chi = 2.756(56)$ were found for time intervals with $(t - t_w)/t_w \gg 1$ for a 'pure' system at $p = 1.0$; within calculation errors, they agree with each other and with the theoretically predicted exponent $\phi = 1 + d/z + \beta/(vz) = 2.737(8)$. However, the exponents for the autocorrelation function and susceptibility determined in the $(t - t_w)/t_w \gg 1$ interval for structurally disordered systems with $p < 1$ are significantly different due to the strong influence of structural defects on the system's correlation properties at the nonequilibrium stage of evolution. Therefore, exponent $c_a = \beta/(z\nu)$ entering the dependence

$$\tilde{F}_C\left(\frac{t}{t_w}\right) \sim \left(\frac{t}{t_w}\right)^{-c_a} \tag{95}$$

and characterizing long-time relaxation of magnetization $M(t) \sim t^{-\beta/(z\nu)}$ at $T = T_c$ should be taken for structurally disordered systems to describe the power-law behavior of the scaling function $\tilde{F}_C(t/t_w)$. Indeed, the following c_a values were found: $c_a = 0.232(7)$ at $p = 0.95$, $c_a = 0.229(10)$ at $p = 0.8$, $c_a = 0.175(6)$ at $p = 0.6$, and $c_a = 0.175(10)$ at $p = 0.5$; they are consistent, within the calculation errors, with $\beta/(z\nu)$ values at the respective spin concentrations. At the same time, the calculated values of $\phi_\chi = 2.63(4)$ for $p = 0.95$, $\phi_\chi = 2.61(4)$ for $p = 0.8$, $\phi_\chi = 2.33(3)$ for $p = 0.6$, and $\phi_\chi = 2.31(3)$ for $p = 0.5$ for the scaling function $\tilde{F}_\chi(t/t_w)$ prove to fairly well agree with the ϕ values for the respective spin concentrations.

Nevertheless, structurally disordered systems in the aging regime at times $t - t_w \sim t_w$ exhibit a sharp decrease in the autocorrelation function $C(t, t_w)$ (Fig. 17a), and its scaling function $\tilde{F}_C(t/t_w)$ (Fig. 19a) in the region of decline can be approximated by the power-law dependence with exponent ϕ_c assuming the values: $\phi_c = 2.59(8)$ for $p = 0.95$, $\phi_c = 2.61(9)$ for $p = 0.8$, $\phi_c = 2.37(10)$ for $p = 0.6$, and $\phi_c = 2.35(10)$ for $p = 0.5$, consistent within the calculation accuracy with the calculated ϕ_χ values for dynamic susceptibility and exponent ϕ. This means that the scaling behavior

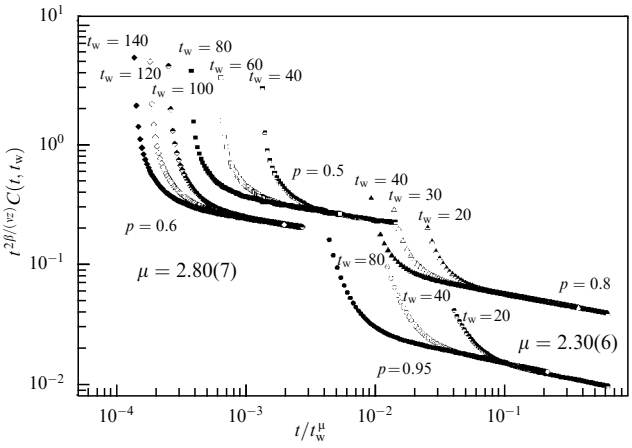

Figure 20. 'Superaging' phenomenon in the scaling behavior of autocorrelation function $t_w^{2\beta/(vz)}C(t, t_w)$ depending on t/t_w^{μ}.

predicted by the renormalization group theory for the correlation function in accordance with relations (47) is manifested as the nonequilibrium behavior of structurally disordered systems up to the aging regime with $t - t_w \sim t_w \gg 1$; in the long-time regime with $t - t_w \gg t_w \gg 1$, pinning of the domain walls on defects accounts for the considerable slowing down of correlation effects, while the autocorrelation function decays with time as a power-law of critical magnetization relaxation.

A subtle analysis of the behavior of the autocorrelation function for structurally disordered systems in the long-time regime with $t - t_w \gg t_w \gg 1$ revealed violation of its simple scaling dependence given by $\tilde{F}_C(t/t_w)$ apparent from the absence of complete coincidence between the data for different t_w (see Fig. 19a). Representation of the scaling dependence for the autocorrelation function in the form $\tilde{F}_C(t/t_w^{\mu})$ provides good coincidence of the data for different t_w at $\mu = 2.30(6)$ for systems with $p = 0.95$ and 0.80 and at $\mu = 2.80(7)$ for systems with $p = 0.6$ and 0.5 (see Fig. 20). Such a case of scaling dependence characterized by exponent $\mu > 1$ is classified in the theory of nonequilibrium processes as 'superaging' phenomenon [2].

Figure 20 demonstrates that the recovery of data collapse for the autocorrelation function in the long-time regime with $t - t_w \gg t_w \gg 1$ by introducing the scaling function $\tilde{F}_C(t/t_w^{\mu})$ destroys the collapse of the same data for $t - t_w \leqslant t_w$ times, suggesting the necessity to use for structurally disordered

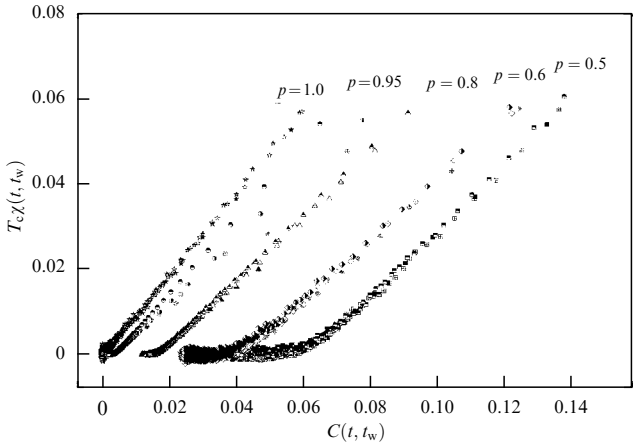

Figure 21. Dependences of susceptibility on the autocorrelation function determining, in accordance with formula (94), the FDR for various spin concentrations p.

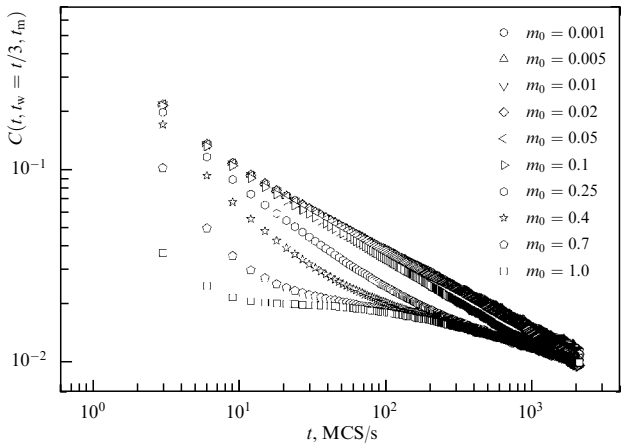

Figure 22. Dependences of autocorrelation function $C(t, t_w = t/3, t_m)$ on observation time t at various initial values of magnetization m_0 for the system with spin concentration $p = 0.8$.

systems a more complicated form of scaling dependence of the autocorrelation function for $t_m \ll t_w < t$ than in relations (47), such as

$$C(t, t_w) = A_C(t - t_w)^{a+1-d/z}\left[\left(\frac{t}{t_w}\right)^{\bar{\theta}-1}\bar{F}_C\left(\frac{t}{t_w}\right) + B_C(p)\tilde{F}_C\left(\frac{t}{t_w^{\mu}}\right)\right] \quad (96)$$

with the functions

$$\bar{F}_C\left(\frac{t}{t_w}\right) \sim \left(\frac{t}{t_w}\right)^{-(\phi+\bar{\theta}-1)} \sim \left(\frac{t}{t_w}\right)^{-2\beta/(z\nu)},$$

$$\tilde{F}_C\left(\frac{t}{t_w^{\mu}}\right) \sim \left(\frac{t}{t_w^{\mu}}\right)^{-\beta/(z\nu)}$$

for $t - t_w \gg t_w \gg 1$ and $B_C(p = 1) = 0$.

At the next stage of research, the authors of Refs [55, 82] calculated the FDR based on relation (93). It follows from Fig. 21 that the C-dependences of $T\chi$ were linear for a 'pure' system over the time range $t - t_w \geqslant t_w \gg 1$ in which the autocorrelation function $C(t, t_w)$ varied and were characterized by the limiting FDR value $X^{\infty} = 0.784(5)$ obtained by determining $X(t_w)$ from relationship (93) for each t_w value. Then, these $X(t_w)$ values underwent linear approximation and extrapolation $X(t_w \to \infty)$ to find the sought limiting FDR value X^{∞}. The limiting value $X^{\infty} = 0.784(5)$ is in excellent agreement with the field-theoretical value $X^{\infty} \simeq 0.78$ obtained in Ref. [46] based on the renormalization group description of nonequilibrium critical dynamics of dissipative model A with the use of ε-expansion. In the case of evolution from a high-temperature initial state, the nonequilibrium critical behavior of the three-dimensional Ising model is characterized by a significantly different limiting FDR value $X^{\infty} = 0.380(13)$ [54].

However, in structurally disordered systems with strong slowing down of correlation effects for times $t - t_w \gg t_w \gg 1$ due to pinning of domain walls on defects, the C-dependences of $T\chi$ exhibit two linear sections (see Fig. 21): one corresponding to a change in autocorrelation function $C(t, t_w)$ for times $t - t_w \sim t_w \gg 1$, the other corresponding to $C(t, t_w)$ values for the long-time stage of evolution with $t - t_w \gg t_w \gg 1$. Clearly, the length of the latter section increases with increasing concentration of defects. The limiting FDR values $X^{\infty} = 0$ correspond to the second sections for all spin concentrations with $p < 1$. At the same time, the analysis of C-dependences of $T\chi$ in the former sections with the use of relation (93) without considering the $C \to 0$ limit shows that application of the linear $X(t_w \to \infty)$ extrapolation procedure to certain $X(t_w)$ leads to $X(p = 0.95) = 0.740(6)$, $X(p = 0.8) = 0.736(6)$, $X(p = 0.6) = 0.726(8)$, and $X(p = 0.5) = 0.726(4)$, close to the mean-field limiting FDR value $X^{\infty} = 0.8$ [46]. Deviations are due to the influence of fluctuation effects and structural defects.

To evaluate the influence of different initial states on the nonequilibrium critical behavior of the structurally disordered Ising model, we constructed the initial states of a system with magnetizations $m_0 = 0.02$, 0.05, 0.10, 0.25, 0.4, 0.7, and 1.0. The behavior of the autocorrelation function and dynamic susceptibility for a system with spin concentration $p = 0.8$ was considered for times t_w depending on observation time t.

By way of example, Fig. 22 presents time dependences of the autocorrelation function for $t_w = t/3$. Aging effects are quite apparent due to the departure of the $C(t, t_w = t/3, t_m)$ dependence from the power-law dependence in the form of a straight line on the double logarithmic scale characterized by the slowing down of correlation and relaxation with the system's age. Figure 22 also demonstrates the enhancement of aging effects with increasing initial magnetization m_0.

For 'pure' systems ($p = 1$) when $t_w = t/3$, the correlation function and susceptibility are described by relations (77). To verify the validity of these scaling forms for disordered systems as well, the scaling functions

$$G_C(tm_0^{\kappa}) = t_w^{2\beta/(z\nu)}C\left(t, t_w = \frac{t}{3}, t_m\right),$$

$$G_{\chi}(tm_0^{\kappa}) = t_w^{2\beta/(z\nu)}\chi\left(t, t_w = \frac{t}{3}, t_m\right)$$

were built from variable $x = tm_0^{\kappa}$ at $\kappa \simeq 2.79$. The graphs demonstrate the collapse of χ susceptibility data at various m_0 in the universal curve corresponding to the scaling function $G_{\chi}(tm_0^{\kappa})$ (see Fig. 23a). However, no such data collapse in the $G_C(tm_0^{\kappa})$ curve is apparent for the autocorrelation function

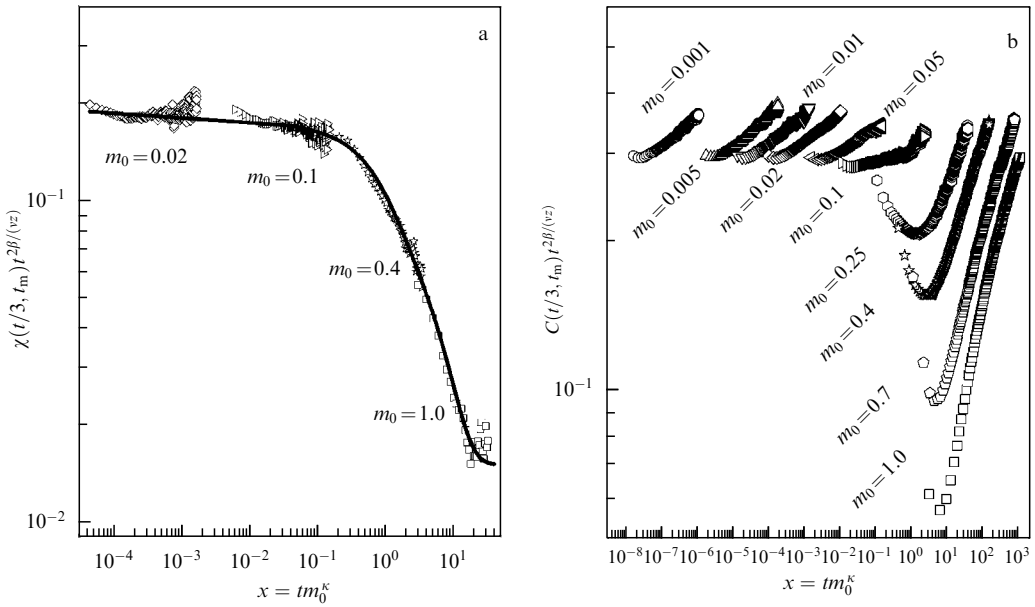

Figure 23. Dependences of scaling functions $t^{2\beta/(z\nu)}\chi(t, t_w = t/3, t_m)$ (a) and $t^{2\beta/(z\nu)}C(t, t_w = t/3, t_m)$ (b) on variable $x = tm_0^\kappa$ for various initial magnetizations m_0 for a system with spin concentration $p = 0.8$.

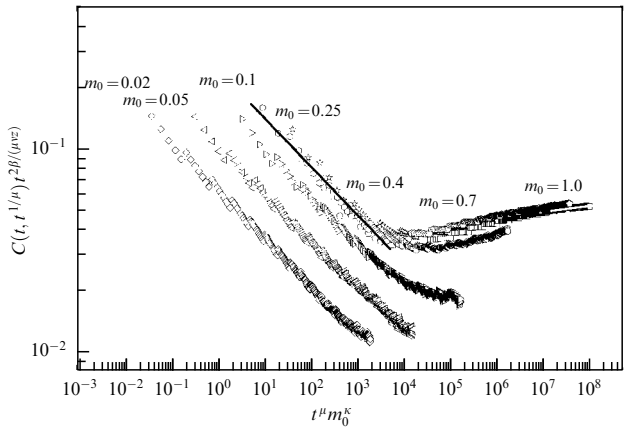

Figure 24. Dependences of scaling function $t^{2\beta/(\mu z\nu)}C(t, t^{1/\mu}, t_m)$ on variable $t^\mu m_0^\kappa$ for different initial magnetizations m_0 for a system with spin concentration $p = 0.8$.

(Fig. 23b), because the behavior of the autocorrelation function and susceptibility in structurally disordered systems with $p < 1$ is significantly different owing to the strong influence of structural defects on the correlation properties of system [82] at the nonequilibrium stage of evolution responsible for 'superaging' phenomenon. Due to this, representation of the autocorrelation function for various m_0 in the form of $t^\mu m_0^\kappa$ dependence of the function $t^{2\beta/(\mu z\nu)}C(t, t^{1/\mu}, t_m)$ for a system with $p = 0.8$ [82] and the superaging exponent $\mu = 2.30(6)$ leads to coincidence of the $m_0 > 0.25$ data in the universal curve (see Fig. 24). Thus, a more complicated scaling dependence

$$C(t, t_w, t_m) \sim t_w^{-2\beta/(z\nu)}\tilde{F}_C\left(\frac{t}{t_w^\mu}, \frac{t}{t_m^{1/\mu}}\right) \tag{97}$$

is realized for the autocorrelation function in the superaging regime with $t \geqslant t_w^\mu$ in the case of structurally disordered systems.

To study the influence of initial states with $m_0 \neq 0$ on limiting FDR values for the system with $p = 0.8$, the time dependence of dynamic susceptibility $\chi(t, t_w, t_m)$ and autocorrelation function $C(t, t_w, t_m)$ at $t_w = t/3$ were calculated for initial states with $m_0 = 0.1$ and 0.4. The calculated parametric C-dependence of $T_c\chi$ shown in Fig. 25 makes it possible to compute the limiting FDR value X^∞ as $C \to 0$ using relation (59). Thus, for the initial state with $m_0 = 0.1$ (Fig. 25a), it was found that $X^\infty = 0.418(29)$, in agreement with the high-temperature X^∞ value 0.413(11); for the initial state with $m_0 = 0.4$, $X^\infty = 0.05(18)$, in agreement, within the calculation accuracy, with low-temperature value $X^\infty = 0$.

Thus, it can be concluded that the nonequilibrium critical behavior of the structurally disordered three-dimensional Ising model with arbitrary initial magnetization m_0 can be divided into two universality subclasses corresponding to high-temperature and low-temperature initial states, each with a characteristic limiting fluctuation–dissipation relation: $X^\infty(m_0 = 0) = 0.413(11)$ for weakly disordered systems and $X^\infty(m_0 = 0) = 0.443(15)$ for strongly disordered systems for $m_0 < 0.25$, and $X^\infty(m_0 = 1) = 0$ for systems with spin concentration $p < 1$ for $m_0 \geqslant 0.25$.

To conclude this section, it is worthwhile to note that numerical studies have revealed the strong influence of defects on nonequilibrium critical dynamics of the three-dimensional Ising model evolving from a low-temperature initial state. It was shown that aging effects heighten with increasing defect concentration. The influence of defects is especially apparent as the marked slowing down of correlation effects in structurally disordered systems, as opposed to 'pure' systems. As a result, the autocorrelation function for times $t - t_w \gg t_w \gg 1$ decays as a power-law of critical magnetization relaxation due to domain wall pinning on defects, while the limiting FDR values determined by domain dynamics in the long-time regime equal zero.

The nonequilibrium critical dynamics of the three-dimensional Ising model undergoes a strong influence of initial states. It was shown that aging effects heighten with increasing initial magnetization m_0 and for $m_0 \geqslant 0.25$ turn

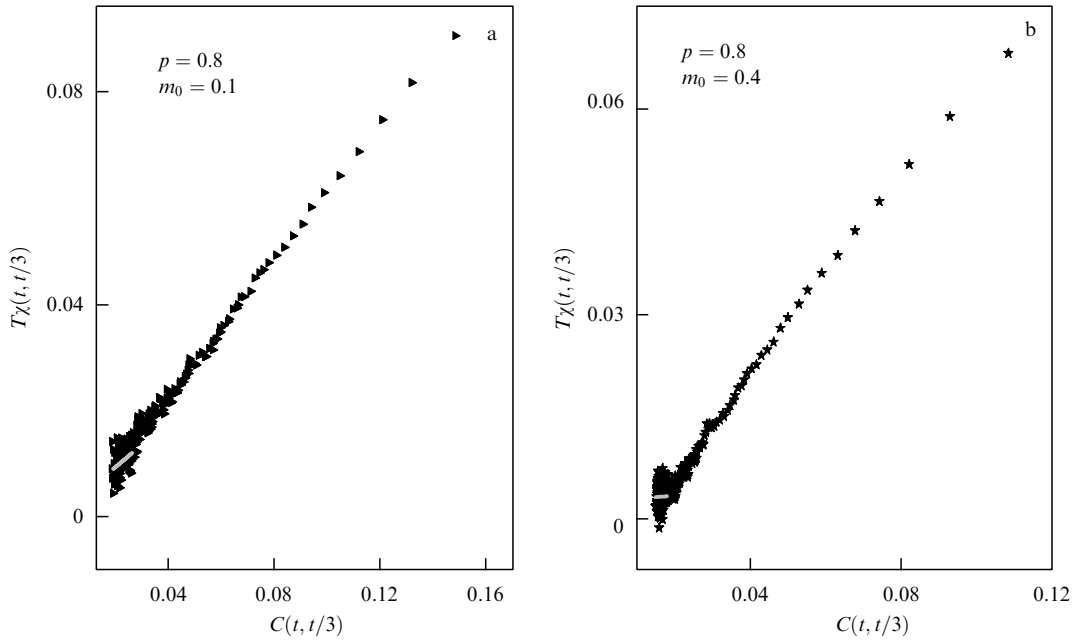

Figure 25. FDR found from $C(t, t/3)$ dependence of $T\chi(t, t/3)$ for initial states with $m_0 = 0.1$ (a) and $m_0 = 0.4$ (b). $X^{\infty} = 0.418(29)$ at $m_0 = 0.1$, and $X^{\infty} = 0.05(18)$ at $m_0 = 0.4$.

into 'superaging' effects in the nonequilibrium behavior of the autocorrelation function.

The critical exponents determining the asymptotic behavior of the autocorrelation function and dynamic susceptibility belong to different universality classes of critical behavior, namely, the critical behavior of 'pure', weakly disordered ($p = 0.95$ and 0.8), and strongly disordered ($p = 0.6$ and 0.5) systems [55, 80–83]. Each of the universality classes of critical behavior may comprise two universality subclasses of nonequilibrium critical behavior corresponding to evolution from high-temperature and low-temperature initial states with characteristic values of the limiting fluctuation–dissipation relation.

5. Observation of memory effects in the nonequilibrium behavior of the three-dimensional Ising model

References [55, 82] were designed to study memory effects made themselves evident in the two-time critical behavior of the autocorrelation function (Fig. 26) at cyclic temperature changes when a system is cooled (quenched) at a certain time of observation $t_1 - t_w \sim t_w$ from the critical temperature T_c to a temperature $T_1 < T_c$ (with a temperature difference $\Delta T = T_c - T_1 > 0$), after which it remains at T_1 during a time interval $\Delta t = t_2 - t_1 = t_w \div 4t_w$. Thereafter, the temperature goes back to T_c.

The results of calculations for systems with spin concentrations $p = 0.8$ and 0.5 (see Fig. 26) at $\Delta T = 1$ and different times $t_w = 20$, 40 MCS/s indicate that the reaction of the system to 'quenching' is characterized by an initial rise in $C(t, t_w)$ compared with its value at T_c, followed by decay of the autocorrelation function determined by 'quenching' temperature $T_1 < T_c$; thereafter, $C(t, t_w)$ tends back to its initial value at the instant of 'quenching' t_1 as the system's temperature returns to critical.

In the case of earlier instant of quenching $t_1 - t_w = t_w$, and a rather long time interval of quenching, $\Delta t = 4t_w$ (Fig. 26a), domain wall pinning on defects prevents the complete recovery of the system's 'memory' about its state at the instant of quenching. An increase in the initial quenching instant, $t_1 - t_w = 2t_w$ and a decrease in the quenching interval to

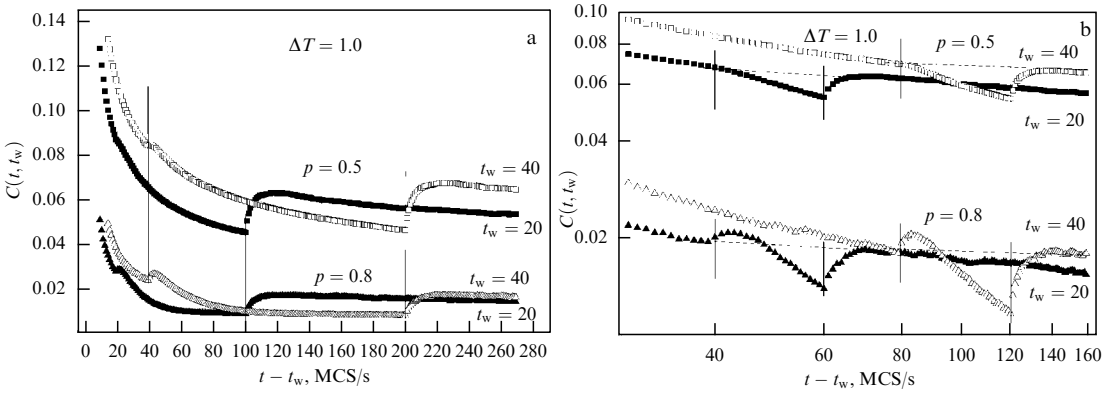

Figure 26. Memory effects in the nonequilibrium critical behavior of autocorrelation function $C(t, t_w)$ for disordered systems with $p = 0.8$ and 0.5 quenched to $\Delta T = 1$ at different stages of evolution with $t_w = 20$ and $t_w = 40$: (a) 'quenching time' $t_1 - t_w = t_w$, quenching time interval $\Delta t = 4t_w$; (b) $t_1 - t_w = 2t_w$, and $\Delta t = t_w$.

$\Delta t = t_w$ promote memory return (Fig. 26b). The removal of data on autocorrelation function values during the period of quenching at T_1 demonstrates the absence of difference between autocorrelation function values at the instant of quenching and upon return to T_c. This correspondence is referred to as the 'memory' effect, being related in our case to both the slower dynamics of the system in the 'aging' regime with $t_1 - t_w > t_w$ and the smallness of the quenching time interval interfering with manifestations of irreversible effects in domain wall dynamics.

Moreover, the amplitude of changes in the autocorrelation function regarded as a response to cooling increases with increasing defect concentration (decreasing spin concentration p) at fixed ΔT and time t_w, because a rise in the concentration of defects in the aging regime leads to heightening the aging effects, i.e., further slowing down of the correlation function with growing t_w (see above).

To explain this phenomenon, it should be borne in mind that a system passing after cooling from the nonmagnetic state at T_c into the magnetized state with $T_1 < T_c$ finds itself in a far-from-equilibrium state. The system's domain structure in this state consists of domains with positive and negative projections of magnetization separated by domain walls. The domain structure of the system changes during equilibration, with the interface component of the domain walls growing with time [84]. The bulk domain fraction rapidly reaches equilibrium state corresponding, while the interface component needs much more time to be equilibrated. The presence of structural defects slows down equilibration, especially that of the interface component of the domain walls.

To sum up, research on the nonequilibrium critical behavior of the three-dimensional Ising model at cyclic temperature changes revealed in the time-dependent behavior of the autocorrelation function in the aging regime the effects of memory about the state of the system at the instant of quenching responsible for restoration of this state after return of the temperature to the critical value at the close of a certain quenching time interval. It was shown that domain wall pinning on defects prevents complete recovery of the system's 'memory' about its state at the instant of quenching.

6. Investigations into aging effects in the two-dimensional XY model

The two-dimensional XY model is one more model demonstrating abnormally slow dynamics. However, unlike the three-dimensional Ising model exhibiting nonequilibrium critical behavior considered in Section 5, it demonstrates abnormally slow behavior not only near the Berezinskii–Kosterlitz–Thouless (BKT) phase transition temperature but throughout the entire low-temperature phase: any temperature in this model is critical, i.e., a continuous cascade of phase transitions takes place [85–88]. The topological Berezinskii–Kosterlitz–Thouless phase transition in the two-dimensional XY model, physically related to the dissociation of coupled vortex–antivortex pairs at the transition point, manifests itself in the form of altered spatial dependence of the correlation function: the exponential decay at high temperatures is replaced by 'long-range' power-law decay in the low-temperature phase. A peculiar feature of XY model behavior is the appearance of rigidity in the low-temperature phase with respect to transverse fluctuations of spin density [85].

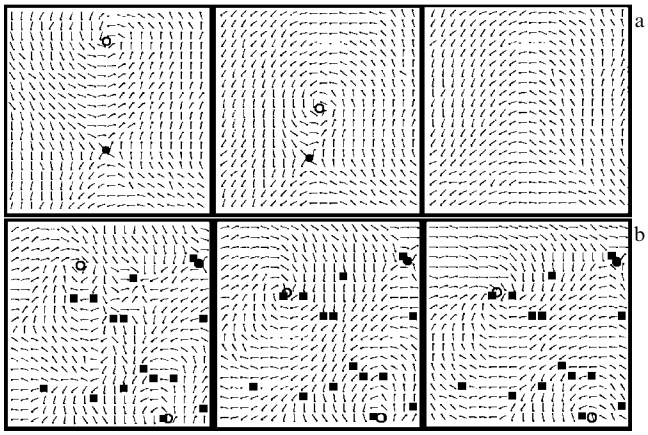

Figure 27. (a) Nonequilibrium process of annihilation of a vortex (○)–antivortex (●) pair at times 300, 400, 500 MCS/s. (b) The nonequilibrium process of vortex excitation pinning on structural defects (■): 250, 400, 2000 MCS/s.

The relevance of two-dimensional XY model research arises from a large number of physical systems whose behavior it describes, including ultrathin magnetic films from transition metal atoms (Co and Ni) deposited onto a nonmagnetic substrate (e.g., from Cu [89]), an important class of planar magnets [85, 89, 90], two-dimensional crystals, superconductor surfaces, superconducting thin films [85, 90], two-dimensional Bose liquids, superfluid helium films [85, 87, 90], Josephson junction arrays, and superconductor–ferromagnetic–superconductor junctions [90–93].

The static properties of the two-dimensional XY model are known fairly well, but the nonequilibrium critical behavior of such systems and the influence of structural disorder on its characteristics remains to be explored. The nonequilibrium critical behavior is expected to exhibit certain specific features described by the two-dimensional XY model of planar magnetic systems related to pinning of vortices and antivortices, as well as vortex/antivortex pairs on structural defects in the low-temperature phase (Fig. 27).

Investigations into aging effects in the two-dimensional XY model are carried out on the assumption of two essentially different initial nonequilibrium states: high-temperature one with $T_0 \gg T_{BKT}(p)$, and low-temperature one with $T_0 = 0$. The system for $T_0 \gg T_{BKT}(p)$ contains a high concentration of free vortex excitations, which allows such a state to be regarded as the initial vortical state in research on nonequilibrium dynamics of the model at quenching temperature $T_s \leqslant T_{BKT}$. In the evolution from a low-temperature initial state with $T = 0$, the key role in dynamics is played by spin-wave excitations. Such a choice of initial states permits the influence of vortex excitations and spin-wave effects on nonequilibrium critical dynamics of the system to be thoroughly investigated.

According to Ref. [9], in the course of the evolution of the two-dimensional XY model from a low-temperature initial state with $m_0 = 1$, the two-time dependence of the autocorrelation function for $T_s \leqslant T_{BKT}$ can be represented in the following scaling form:

$$C(t, t_w) \sim \frac{1}{(t - t_w)^{\eta(T)/2}} \left[\frac{(1+\lambda)^2}{4\lambda}\right]^{\eta(T)/4} \tag{98}$$

for times $t - t_w \gg a^2$, where a is the UV cutoff parameter of a microscopic nature, and $\lambda \equiv t/t_w$, $\eta(T)$ is the critical exponent related to transverse rigidity ρ_s of the system by the following expression:

$$\eta(T) = \frac{T}{2\pi\rho_s(T)}. \tag{99}$$

Two time regimes are distinguished in the nonequilibrium behavior of the autocorrelation function. For times $t - t_w \ll t_w$, this function behaves as

$$C(t, t_w) \sim (t - t_w)^{-\eta(T)/2}, \tag{100}$$

in correspondence with the quasiequilibrium regime of the system's nonequilibrium behavior. For larger times $t - t_w \gg t_w$, a power-law decay of the autocorrelation function is observed:

$$C(t, t_w) \sim t^{-\eta(T)/4}. \tag{101}$$

Transition between the two regimes occurs at $t - t_w \sim t_w$. Evidently, time dependences of the autocorrelation function at different waiting times do not coincide. This phenomenon, called the aging effect [9], is a manifestation of system's age for $t > t_w$.

The two-time dependence of the autocorrelation function $C(t, t_w)$ can be characterized by the generalized scaling form

$$C(t, t_w) = t_w^{-\eta(T)/2} \Phi\left[\frac{\xi(t - t_w)}{\xi(t_w)}\right], \tag{102}$$

where $\xi(t)$ is the correlation length of the system, and $\Phi[\xi(t - t_w)/\xi(t_w)]$ is the scaling function. In the course of evolution from a low-temperature initial state with $m_0 = 1$, the time dependence of the correlation length $\xi(t) \sim t^{1/2}$, whereas in the evolution from a high-temperature initial state with $m_0 \ll 1$, this dependence is modified by vortex interaction effects and takes the form $\xi^2(t) \sim t/\ln t$ [9, 94].

Results of a numerical study of aging effects in the two-dimensional XY model evolving from different initial states and of the influence of quenched structural defects on them are discussed in Sections 6.1 and 6.2.

6.1 Evolution from a high-temperature initial state

Numerical studies of aging effects and FDT violation in a 'pure' two-dimensional XY model and in a structurally disordered model are reported in Refs [9, 95–97] and [97, 98], respectively.

The Hamiltonian of a structurally disordered model can be given as

$$H = -J \sum_{\langle i,j \rangle} p_i p_j \mathbf{S}_i \mathbf{S}_j, \tag{103}$$

where $J > 0$ is the exchange integral, $\mathbf{S}_i$ is a flat classical spin related to the ith site of the two-dimensional lattice, and p_i are occupation numbers: $p_i = 1$ if the ith site contains a spin, and $p_i = 0$ if the site contains a defect.

Systems with spin concentrations $p = 1.0$, 0.9, and 0.8 on a lattice of linear size $L = 256$ were considered. Temperatures T_{BKT} for these spin concentrations were $T_{BKT}(p = 1.0) = 0.893(2)J$ [97, 99], $T_{BKT}(p=0.9) = 0.679(7)J$, $T_{BKT}(p=0.8) = 0.485(4)J$ [97]. To obtain the two-time dependences of the autocorrelation function

$$C(t, t_w) = \overline{\left[\left\langle \frac{1}{pL^2} \sum_i p_i \mathbf{S}_i(t) \mathbf{S}_i(t_w) \right\rangle\right]} \tag{104}$$

and generalized susceptibility

$$\chi(t, t_w) = \overline{\left[\left\langle \frac{1}{pL^2h^2} \sum_i p_i \mathbf{h}_i \mathbf{S}_i(t) \right\rangle\right]}, \tag{105}$$

simulations were undertaken at 16 different waiting times: $t_w = 10$, 20, 30, 40, 50, 100, 250, 500, 1000, 1500, 2000, 3500, 4000, 4500, 5000, and 10,000 MCS/s, and observation times $t - t_w = 50{,}000$ MCS/s. Studies of the two-time dependence of generalized susceptibility were carried out by the small-scale random magnetic field method [9] with the addition of the $\sum_i^N p_i \mathbf{S}_i \mathbf{h}_i$ item to Hamiltonian (103) at the instant of time t_w, choosing the amplitude h of the bimodal random field $h_i = \pm h$ to be equal to 0.04. The application of this method implies separate calculations for each waiting time t_w. Modeling a 'pure' system with $p = 1$ required statistical averaging over 6000 runs, while simulation of a structurally disordered XY model involved averaging over 3000 impurity configurations and 15 statistical runs for each configuration.

The resulting two-time dependences for the autocorrelation function (Fig. 28) explicitly demonstrate the slowing down of relaxation processes with system's 'age' t_w. These aging effects, manifesting themselves at times $t - t_w \simeq t_w$,

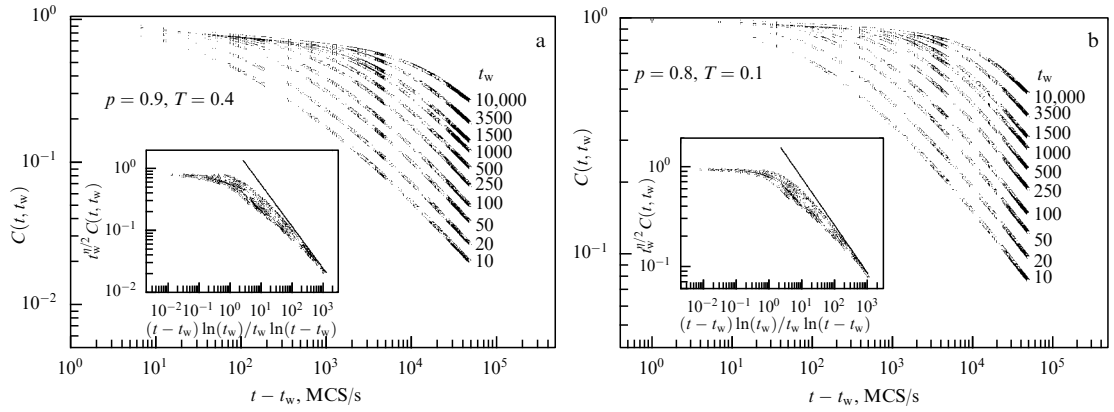

Figure 28. Two-time dependence of the autocorrelation function of a system with $p = 0.9$, $T = 0.4$ (a) and $p = 0.8$, $T = 0.1$ (b) evolving from a high-temperature initial state. The insets show dependences of $t_w^{\eta/2} C(t, t_w)$ on $(t - t_w)\ln t_w/t_w \ln(t - t_w)$ to demonstrate the scaling form (102) of the autocorrelation function.

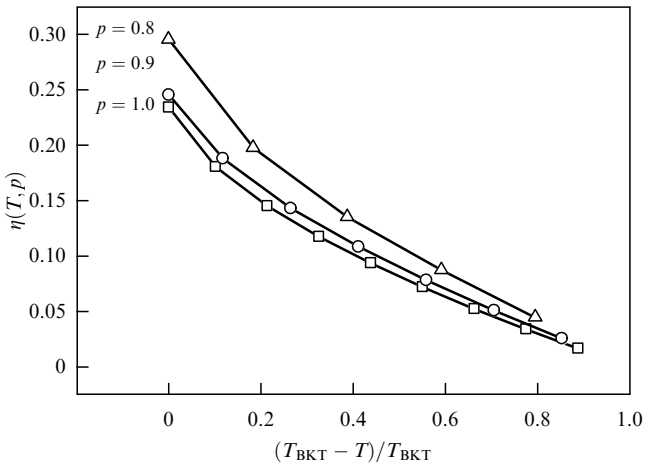

Figure 29. Temperature dependences of the Fisher critical exponent η for different spin concentrations p. Errors are smaller than symbol sizes.

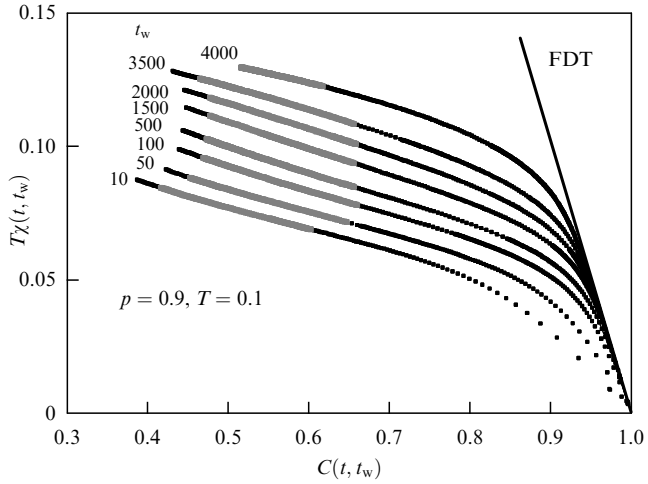

Figure 30. Parametric dependence of susceptibility on the autocorrelation function for the system with spin concentration $p = 0.9$ and temperature $T = 0.1$.

become increasingly more pronounced with increasing concentration of structural defects. For longer observation times, $t - t_w \gg t_w \gg 1$, the behavior of the autocorrelation function is characterized by a faster power-law decay, $C(t, t_w) \sim (t/t_w)^{-c_a}$, than in the aging regime. It was revealed that a rise in defect concentration shifts the onset of the power-law regime to the region of longer observation times.

To characterize the scaling behavior of the autocorrelation function (102), the Fisher critical exponents were calculated for all spin concentrations p and temperatures being considered. To this end, the dimensional dependence $\langle m^2 \rangle \sim L^{-\eta(T,p)}$ was employed. The linear size of the system was chosen to lie in the 4–128 range. The temperature dependences of the calculated Fisher exponents for different p concentrations are presented in Fig. 29, showing that a rise in defect concentration causes an increase in $\eta(T, p)$ values, although the influence of concentrations is much weaker than that of temperature.

To confirm the scaling dependence of autocorrelation function (102), the dependence of $t_w^{\eta/2} C(t, t_w)$ on $(t - t_w) \ln t_w / t_w \ln (t - t_w)$ was constructed. The results shown in the insets to Fig. 28 demonstrate the 'collapse' of the data obtained at the long-time stage of evolution with $t - t_w \gg t_w \gg 1$ for different t_w in the respective $p = 0.9$, $T = 0.4$, and $p = 0.8$, $T = 0.1$ universal curves corresponding to the scaling function $\Phi(\xi(t - t_w)/\xi(t_w))$.

To determine the FDR $X(t, t_w)$ in accordance with relations (86) and (87), generalized susceptibility $\chi(t, t_w)$ (105) was calculated using the data on $\chi(t, t_w)$ and $C(t, t_w)$ to determine their parametric dependence for each fixed t_w (Fig. 30). The limiting FDR value as a universal characteristic of nonequilibrium critical behavior was found based on parametric dependences of $T\chi(t, t_w)$ on $C(t, t_w)$ (Fig. 31) in the $C \to 0$ limit at time sections with $t - t_w \gg t_w \gg 1$, where the scaling dependence for the autocorrelation function (102) is fulfilled. In Figs 30 and 31, these sections are shaded in grey color. $X(t_w)$ values obtained for different waiting times t_w (Fig. 32) were then extrapolated as $t_w \to \infty$, i.e., as $1/t_w \to 0$, to find the limiting FDR value X^∞. Figure 32 illustrates, by way of example, the use of this procedure for obtaining X^∞ values for various temperatures in the low-temperature phase of a system with $p = 0.8$. The resulting temperature dependences of the limiting FDR X^∞ for different spin concentrations are presented in Fig. 33.

The analysis of $X^\infty(p, T \leqslant T_{BKT}(p))$ values thus obtained leads to the conclusion that the influence of structural disorder results in a rise in X^∞ with increasing defect concentration for equal 'quenching' temperatures $T \leqslant T_{BKT}(p)$.

If the temperature dependence of the limiting FDR is given in the form $X^\infty \sim T^\lambda$, the exponent λ for different impurity concentrations assumes the following values: $\lambda(p=1.0) = 1.988(23)$, $\lambda(p=0.9) = 1.848(22)$, and $\lambda(p=0.8) = 1.838(31)$. Extrapolation of temperature dependences for $X^\infty(p, T \leqslant T_{BKT}(p))$ as $T \to 0$ gives $\lim_{T\to 0} X^\infty = 0$ for all impurity concentrations being considered.

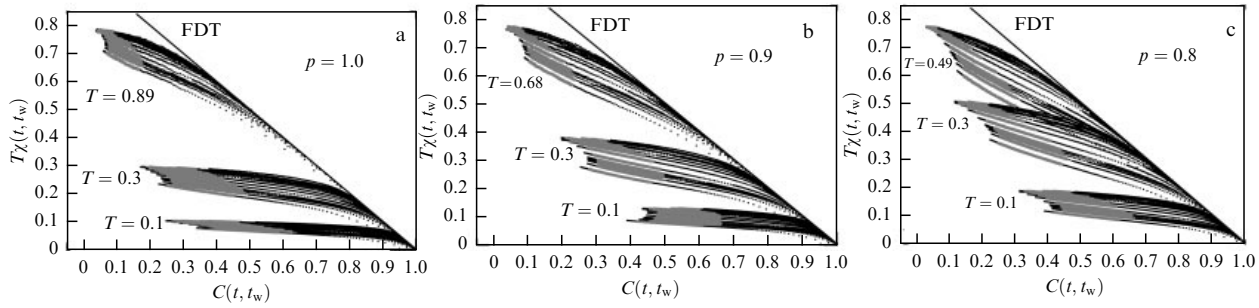

Figure 31. Parametric dependence of susceptibility on the autocorrelation function of the system for different temperatures and spin concentrations in the evolution from the high-temperature initial state. Grey color shades sections with scaling dependence for $C(t, t_w)$.

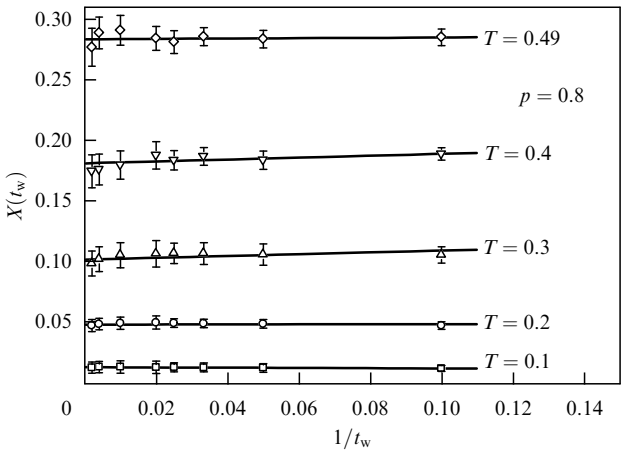

Figure 32. Finding limiting FDR values $X^{\infty}(T)$ for a system with spin concentration $p = 0.8$ by $X(t_w)$ extrapolation as $t_w^{-1} \to 0$.

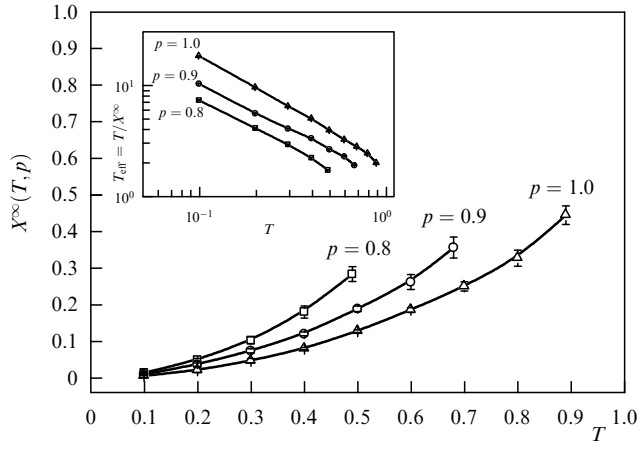

Figure 33. Temperature dependences of the limiting FDR X^{∞} for systems with spin concentrations $p = 1.0$, 0.9, and 0.8 evolving from a high-temperature initial state. The inset shows the dependence of effective temperature $T_{\rm eff}$ of the system on temperature for the same spin concentrations p.

The difference between $X^{\infty}(p = 1.0, T_{\rm BKT}) = 0.444(26)$ at the BKT transition point obtained in Ref. [98] for a 'pure' system and the analytical value $X^{\infty}(p = 1.0, T_{\rm BKT}) = 0.5$ calculated in the vortex-less approximation in Ref. [26] allows the contribution of the vortex dynamics to the FDR to be estimated. The resultant X^{∞} values for structurally disordered systems, $X^{\infty}(p = 0.9, T_{\rm BKT}) = 0.357(29)$, and $X^{\infty}(p = 0.8, T_{\rm BKT}) = 0.284(20)$; they suggest a strong influence of structural defects on nonequilibrium critical behavior of the system.

Reference [100] reports a study of the temperature dependence of FDR for a 'pure' system and $X^{\infty}(T)$ in which the linear dependence $X^{\infty}(T) = 0.5T/T_{\rm BKT}$ was obtained. However, only three time values $t_w = 100$, 300, and 1000 MCS/s were used to find $X^{\infty}(T)$ when extrapolating to $t_w \to \infty$ in Ref. [100]. We used more than ten t_w values ranging from 10 to 10,000 MCS/s for such extrapolation to control the passage of $X(t, t_w)$ to the universal scaling regime and to correctly perform the limiting transition to determining $X^{\infty}(T)$. Crossover effects in the behavior of C dependence of $T\chi$ (hence, the $X(t, t_w)$ dependence) manifest themselves in the high-temperature region close to $T_{\rm BKT}(p)$, as clearly demonstrated in Fig. 31.

It follows from the above that the two-dimensional XY model for the effective temperature $T_{\rm eff}(T \leqslant T_{\rm BKT}) = T/X^{\infty}(p)$ predicts the power-law $T_{\rm eff}(p) \sim T^{1-\lambda(p)}$ type dependences presented in the inset to Fig. 33.

It can also be concluded that the relaxation dynamics of the system in the BKT phase markedly slow down with decreasing temperature, which facilitates strengthening of aging effects. The presence of structural defects in the system also leads to further heightening of the aging effects.

6.2 Evolution from a low-temperature initial state. Superaging effects

Spin-wave excitations exert the most pronounced influence on aging effects in the two-dimensional XY model evolving from a low-temperature initial state with $m_0 = 1$. These excitations manifest themselves first and foremost as peculiarities of the two-time dependence of the autocorrelation function

$$C(t, t_w) = \left[\left\langle \frac{1}{pL^2}\sum_i p_i \mathbf{S}_i(t)\mathbf{S}_i(t_w)\right\rangle\right] - \left[\left\langle \frac{1}{pL^2}\sum_i p_i \mathbf{S}_i(t)\right\rangle\left\langle \frac{1}{pL^2}\sum_i p_i \mathbf{S}_i(t_w)\right\rangle\right], \quad (106)$$

in which, in contrast to that in the case of evolution from a high-temperature initial state, the important role is played by the second constituent $C_{mm}(t, t_w)$ of the autocorrelation function.

Functions $C(t, t_w)$ for the two-dimensional XY model with spin concentrations $p = 1.0$, 0.9, and 0.8 were calculated for different quenching temperatures in the low-temperature phase with $T_s \leqslant T_{\rm BKT}(p)$. Figure 34 demonstrates, as an example, the autocorrelation functions for $p = 1.0$ and $p = 0.8$ at temperatures $T = T_{\rm BKT}(p)$ and $T = 0.1$. The aging effects, manifested through the dependence of the autocorrelation function on the system's 'age' t_w at observation times $t - t_w \sim t_w$, are characterized by correlation slowing down with age. It also follows from Fig. 34 that a rise in defect concentration (decrease in spin concentration p) strengthens aging effects. To recall, for a high-temperature initial state, correlation slows down to the same extent as in the case of a low-temperature initial state at one order of magnitude longer observation times.

The influence of defects is especially apparent as the strong slowing down of correlation effects in structurally disordered systems, compared with those in a 'pure' system. We attribute these marked changes in the behavior of the autocorrelation function to cluster fragmentation coming about in the course of evolution of the two-dimensional XY-model from a low-temperature initial state in which one large cluster at $m_0 = 1$ breaks down into smaller ones. Introducing defects into the system results in abnormal slowing down of cluster fragmentation [101], as illustrated by the plots for two constituents of the autocorrelation function in formula (106), $C_{ss}(t, t_w)$ and $C_{mm}(t, t_w)$, presented in Figs 35a, b for a 'pure' system and a system with spin concentration $p = 0.9$, respectively. The graphs show that, for 'pure' and structurally disordered systems, the values of $C_{ss}(t, t_w)$ and $C_{mm}(t, t_w)$ constituents begin to coincide for observation times $t - t_w \geqslant t_w$, which leads to their cancellation in the complete autocorrelation function, even if cancellation in the structurally disordered systems occurs at longer observation

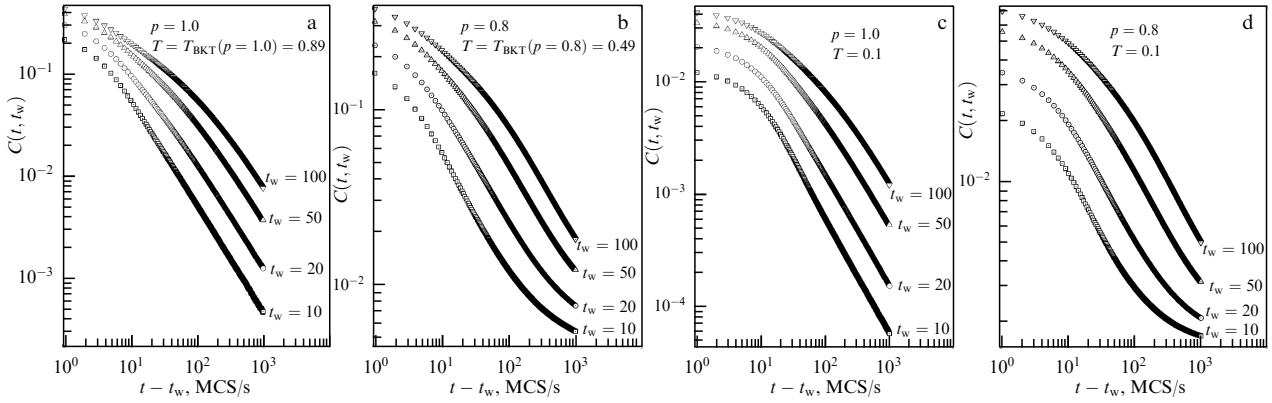

Figure 34. Nonequilibrium dependence of autocorrelation function $C(t, t_w)$ on observation time $t - t_w$ for systems with $p = 1.0$ and $T = T_{BKT} = 0.89$ (a), $p = 0.8$ and $T = T_{BKT} = 0.49$ (b), $p = 1.0$ and $T = 0.1$ (c), $p = 0.8$ and $T = 0.1$ (d) for various t_w times in the course of evolution from a low-temperature initial state.

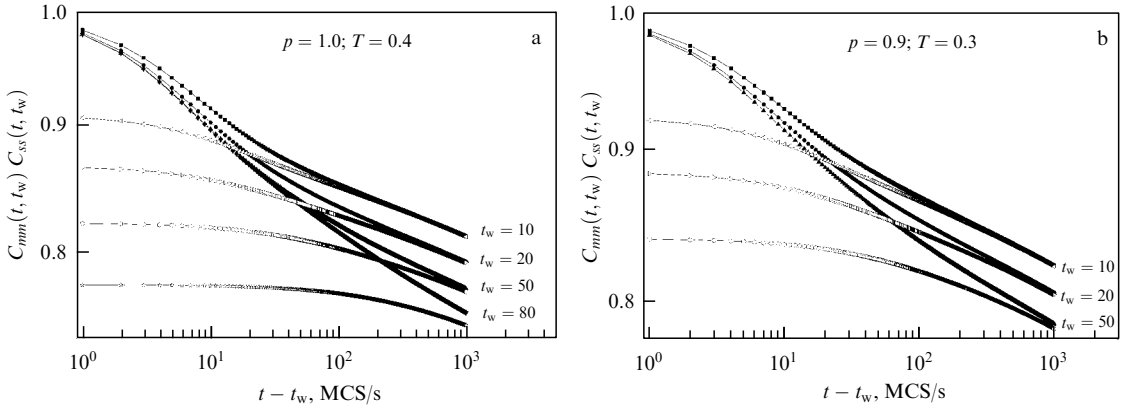

Figure 35. Comparison of time dependences of contributions to autocorrelation functions $C_{ss}(t, t_w) \sim [\langle S(t)S(t_w)\rangle]$ and $C_{mm}(t, t_w) \sim [\langle S(t)\rangle\langle S(t_w)\rangle]$ for spin concentrations $p = 1.0$ (a) and $p = 0.9$ (b).

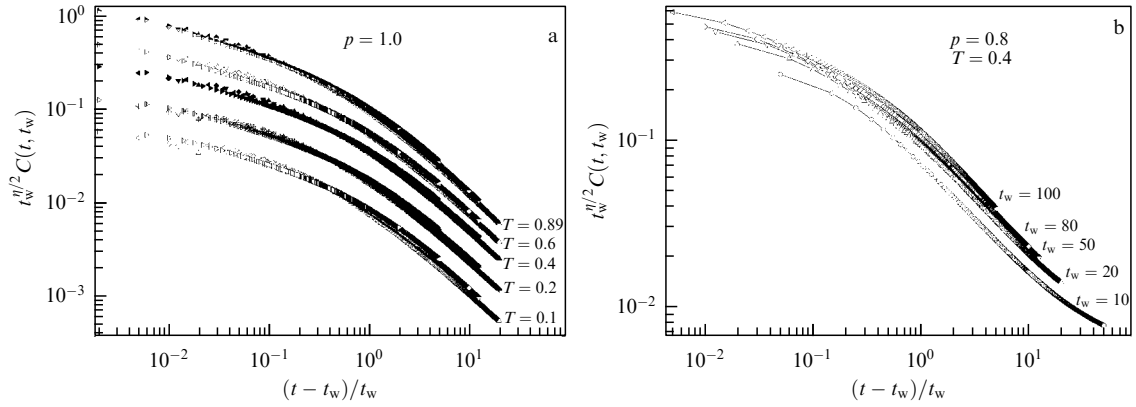

Figure 36. Scaling dependences of autocorrelation function $t_w^{\eta/2} C(t, t_w)$ on $(t - t_w)/t_w$ in systems with $p = 1.0$ (a) and $p = 0.8$ (b), demonstrating 'collapse' of different t_w data for a 'pure' system and its absence for a structurally disordered system.

times than in the 'pure' system. These effects reflect marked differences in the nonequilibrium behaviors between the two-dimensional XY model and the three-dimensional Ising model, arising from the absence of spontaneous magnetization in the former that is inherent in the latter.

To confirm the generalized scaling dependence of the autocorrelation function given by expression (102), $(t-t_w)/t_w$ dependences of $t_w^{\eta/2} C(t, t_w)$ were derived. Figure 36 showing results for the 'pure' system ($p = 1.0$) demonstrates the 'collapse' of the data for different t_w in the universal curves corresponding to the temperatures indicated in the figure panels and fitted by the scaling function $\Phi[\xi(t - t_w)/\xi(t_w)]$ (102) and the absence of a similar 'collapse' for the structurally disordered system with $p = 0.8$. A more complicated form of scaling dependence of the autocorrelation function than that in Eqn (102) was supposed to be realized

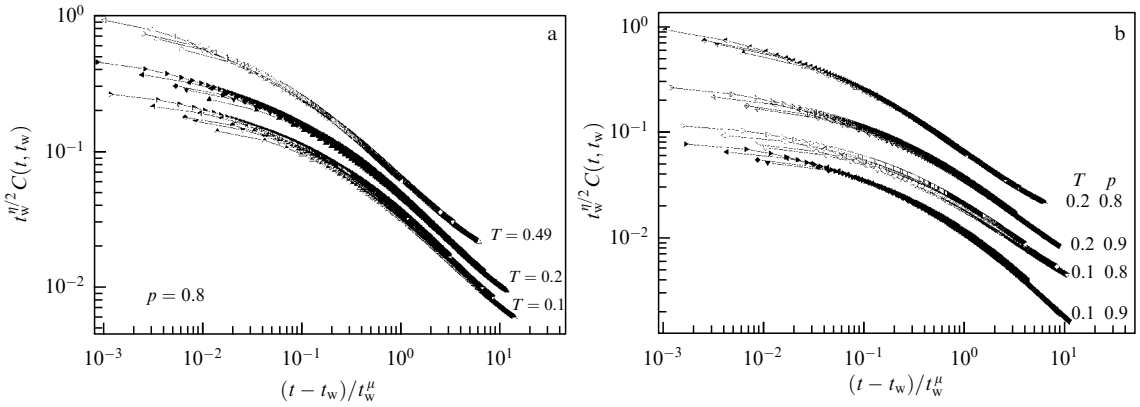

Figure 37. 'Superaging' effect in the scaling behavior of autocorrelation function $t_w^{\eta/2}C(t,t_w)$ depending on $(t-t_w)/t_w^{\mu}$ exemplified by systems with $p = 0.8$ (a) and $p = 0.9$, $p = 0.8$ (b) for various temperatures, which evolve from a low-temperature initial state.

for the structurally disordered two-dimensional XY model. Based on this assumption, the scaling function $\Phi[(t-t_w)/t_w^{\mu}]$ was proposed with exponent μ to be found from the requirement of data 'collapse' for the $(t-t_w)/t_w^{\mu}$ dependence of $t_w^{\eta/2}C(t,t_w)$ at various t_w. Figure 37 illustrates the realization of this procedure for a system with $p = 0.8$ at various temperatures. It was revealed that the exponent $\mu \simeq 1 + \eta(T,p)$ is associated with the 'collapse' of the data for structurally disordered systems. This case of scaling dependence on waiting time with exponent $\mu > 1$ is regarded as 'superaging' phenomenon.

To conclude this section, it is worthwhile to note that numerical studies of nonequilibrium behavior of the two-dimensional XY model revealed significant differences in the behaviors of systems evolving from different initial states. These differences are attributable to the small role of high-energy vortex excitations in system's dynamics during relaxation from the low-temperature initial state with $m_0 = 1$; indeed, its dynamics are governed only by low-energy spin-wave excitations. Vortex excitations and their interactions play the key role in systems evolving from a high-temperature initial state with $m_0 \ll 1$. The nonequilibrium behavior of the two-dimensional XY model exhibits aging effects and FDT violations at quenching temperatures corresponding to the entire low-temperature phase of the XY model. It was shown that the presence of structural defects enhances manifestations of aging effects and produces superaging effects in the case of evolution from a low-temperature initial state.

7. Aging effects in the nonequilibrium behavior of multilayer structures

The currently known peculiarities of nonequilibrium critical dynamics provide a basis for the adequate interpretation of experimental data obtained for Co/Cr-based multilayer structures [13]. Reference [13], designed to investigate the relaxation of magnetization, revealed magnetic aging effects in a Co(0.6 nm)/Cr(0.78 nm) magnetic superstructure. The nanoscale periodicity in these magnetic multilayer structures produces mesoscopic effects of spatial spin correlation with slow relaxation dynamics of magnetization upon quenching the system in the nonequilibrium state. Unlike bulk magnetic systems, where slow dynamics and aging effects manifest themselves near the critical point, magnetic superstructures with nanoscale periodicity make it possible to prolong the relaxation time by virtue of effects associated with an increased characteristic correlation length of spin–spin correlations. Due to this, aging and nonergodicity effects can be observed in multilayer magnetic structures within a wider temperature range than in bulk systems.

Reference [102] reports a numerical MC study of the specific features of nonequilibrium behavior of a multilayer magnetic structure made from ferromagnetic films separated by a nonmagnetic metal layer. The magnetic films had linear sizes $L \times L \times N$ and imposed periodic boundary conditions in the film plane. A structure with the magnetic film thickness $N = 3$ was considered. The value of the exchange integral J_1 determining interactions between the neighboring spins inside a ferromagnetic film was chosen to be $J_1/(k_B T) = 1$, and film–film interactions were defined by the quantity $J_2 = -0.3J_1$. The negativeness of J_2 reflects the fact that the thickness of the nonmagnetic interlayer in multilayer structures with giant magnetic resistance is chosen such that the long-range and oscillating Ruderman–Kittel–Kasuya–Yosida (RKKY) interactions between the spins of ferromagnetic layers had an effective antiferromagnetic character [103]. This interaction aligned magnetizations of the neighboring ferromagnetic layers oppositely to each other.

The magnetic properties of Fe, Co, and Ni-based ultrathin films in contact with a nonmagnetic metal substrate are most adequately described by the Heisenberg anisotropic model [104, 105] specified by the Hamiltonian

$$H = -\sum_{\langle i,j \rangle} J_{ij}\left[\mathbf{S}_i \mathbf{S}_j - \Delta(N) S_i^z S_j^z\right] - h\sum_i S_i^x , \qquad (107)$$

where $\mathbf{S}_i = (S_i^x, S_i^y, S_i^z)$ is the three-dimensional unit vector in the ith site, $\Delta = 0.7$ is the anisotropy parameter for Co ferromagnetic films with monolayer thickness $N = 3$, and h is an external magnetic field. The form and parameters of the Hamiltonian are chosen such that it corresponds to a multilayer Co(0.6 nm/Cr) structure in which ultrathin Co films undergo spontaneous magnetization $\mathbf{m}$ in the film plane xy at subcritical temperatures.

At the first stage of the study, equilibrium characteristics of the multilayer structure were calculated to determine ferromagnetic phase transition temperature T_c in magnetic films, and T_N characterizing realization of the antiferromagnetic configuration of film magnetizations in the structure due to J_2 negativeness (Fig. 38). To determine critical temperatures more precisely, structures with differ-

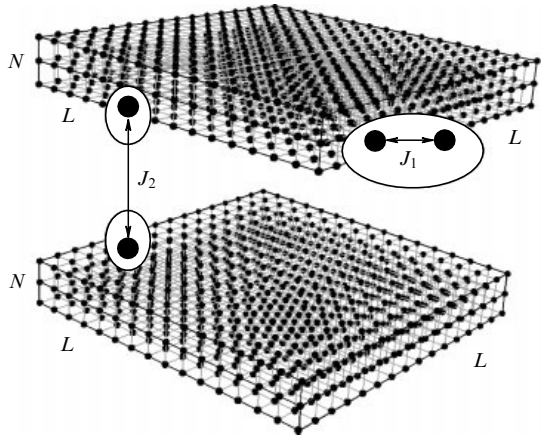

Figure 38. Model of a three-layer structure, $N = 3$, $J_2 = -0.3J_1$.

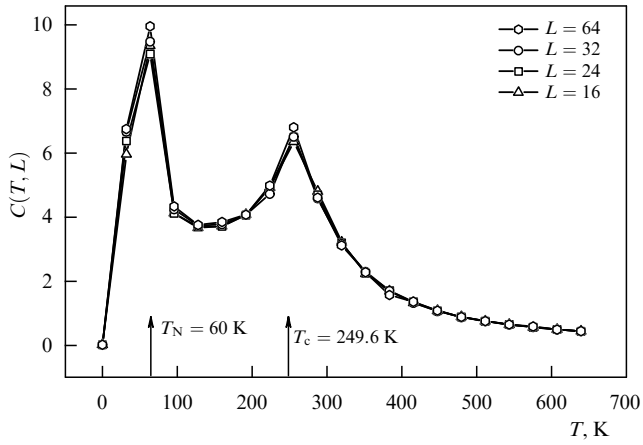

Figure 39. Temperature behavior of heat capacity $C(T, L)$ for lattices of various size L.

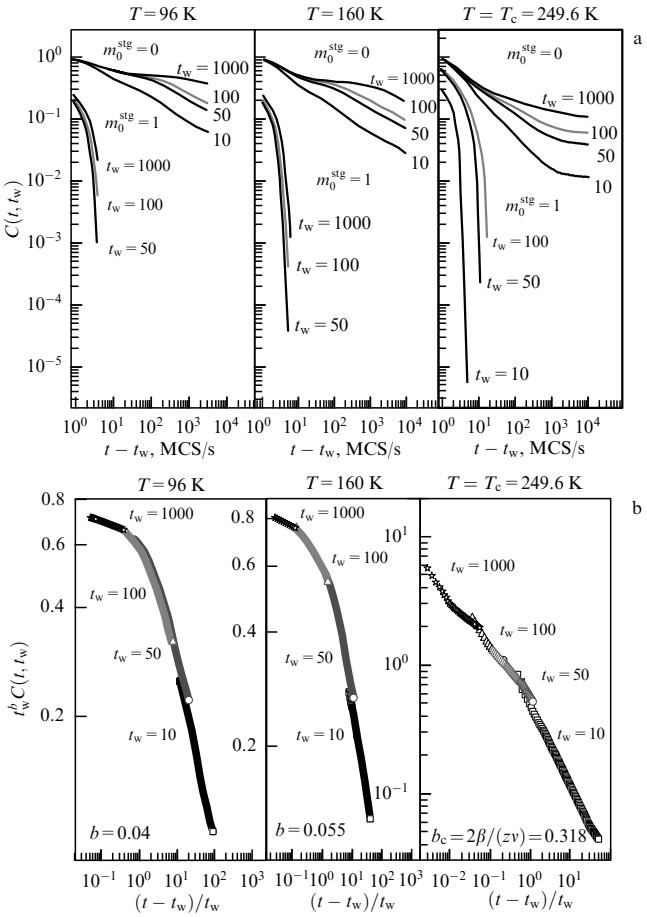

Figure 40. Dependences of autocorrelation function $C(t, t_w)$ on observation time $t - t_w$ in the course of evolution from different initial states with $m_0^{stg} = 0$ and $m_0^{stg} = 1$ (a) and its scaling function $F(t/t_w) = t_w^b C(t, t_w)$ on $(t - t_w)/t_w$ at $m_0^{stg} = 0$ (b) for quenching temperatures $T_s = 96$ and 160 K and $T_s = T_c = 249.6$ K.

ent linear sizes of the films ($L = 16$, 24, 32, 64) were considered. Such characteristics as 'staggered' magnetization $\mathbf{m}_{stg} = \mathbf{m}_1 - \mathbf{m}_2$, where $\mathbf{m}_1$, $\mathbf{m}_2$ are the film magnetizations; 'staggered' susceptibility $\chi_{stg} = [\langle \mathbf{m}_{stg}^2 \rangle - \langle \mathbf{m}_{stg} \rangle^2]/(TN_s)$, where N_s is the number of spins in the film; heat capacity $C_h = [\langle E^2 \rangle - \langle E \rangle^2]/(T^2 N_s)$, and Binder cumulant $U_4 = (3 - \langle m^4 \rangle / \langle m^2 \rangle^2)/2$ were calculated.

The analysis of the temperature dependence of these thermodynamic quantities in films of different linear size L makes it possible to unambiguously characterize the type of phase transformations in a multilayer structure and determine critical temperatures T_c and T_N [40, 41]. To enhance the physical correspondence of the temperature dependences of the above characteristics to the Co/Cr system, the temperature scale was set through the exchange interaction integral $J_1 = 4.4 \times 10^{-14}$ erg corresponding to cobalt. By way of example, Fig. 39 presents the temperature dependence of heat capacity with two characteristic peaks corresponding to $T_N = 60$ K ($k_B T_N / J_1 = 0.19$) and $T_c = 249.6$ K ($k_B T_c / J_1 = 0.78$). To recall, these critical temperatures for the model multilayer structure are in excellent agreement with $T_N = 53$ K and $T_c = 225$ K measured in experiment [13] for the Co/Cr structure.

The next stage of the study was designed to examine the nonequilibrium behavior of the multilayer structure at quenching temperatures T_s equaling critical temperature $T_c = 249.6$ K and temperatures $T_s = 96$ and 160 K being within the $T_N < T_s < T_c$ range. The autocorrelation function was calculated for the evolution of the system from a high-temperature initial state created for $T_0 \gg T_c$ with reduced 'staggered' magnetization $m_0^{stg} = 0.05$ and from a low-temperature initial state with $m_0^{stg} = 1$. Characteristics were averaged over 1000 runs.

The plots in Fig. 40 demonstrate the presence of aging effects in the system, i.e., the abatement of correlation effects over time t_w. Aging effects arise in multilayer structures not only at $T_s = T_c$ as in bulk systems but also at quenching temperatures $T_s < T_c$. Evidently, evolution from both low-temperature and high-temperature initial states is associated with a time-related correlation slowing down corresponding to the sense of aging. It should also be noted that, correlation times in the course of system's evolution from a high-temperature initial state are two–three orders of magnitude more than those in the evolution from a low-temperature initial state at the same t_w values.

In the aging regime for $t - t_w \sim t_w \gg 1$, the two-time dependence of the autocorrelation function is characterized by the scaling form

$$C(t, t_w) \sim t_w^{-b} F_C\left(\frac{t}{t_w}\right), \qquad (108)$$

where exponent b at quenching temperature $T_s = T_c$ is expressed via critical exponents: $b = 2\beta/(z\nu)$. The scaling function $F_C(t/t_w)$ in formula (108) is the homogeneous function of argument t/t_w, being characterized at the long-time stage of evolution with $t - t_w \gg t_w \gg 1$ by the power-law decay:

$$F_C\left(\frac{t}{t_w}\right) \sim \left(\frac{t}{t_w}\right)^{-c_a} \tag{109}$$

with exponent $c_a = d/z - \theta'$ in the course of evolution from a high-temperature initial state at $T_s = T_c$ and $c_a = 1 + d/z + \beta/(z\nu)$ in the case of evolution from a low-temperature initial state at $T_s = T_c$. At quenching temperatures $T_s \neq T_c$, exponents b and c_a in formulas (108) and (109) are already unrelated to critical exponents of the system of interest.

To verify the validity of the scaling form (108) for the data on the autocorrelation function, t/t_w dependences of $t_w^b C(t, t_w) = F_C(t/t_w)$ were constructed with the choice of b values such that the data for different t_w fall, if possible, into a single curve for $t/t_w \gg 1$. By the example of the autocorrelation function obtained for evolution from a high-temperature initial state, the collapse of the data on $t_w^b C(t, t_w)$ and different t_w is seen in the universal curve (see Fig. 40) corresponding to the scaling function $F_C(t/t_w)$ at $T_s = T_c = 249.6$ K with the exponent $b_c = 2\beta/(z\nu) = 0.318(8)$, at $T_s = 96$ K with $b = 0.04(1)$, and at $T_s = 160$ K with $b = 0.055(10)$.

The evaluation of aging effects in the behavior of the autocorrelation function was supplemented by modeling conditions under which aging effects in the relaxation properties of magnetization were revealed for the Co/Cr structure [13]. To this effect, a rather strong magnetic field was applied in the film plane ($h = 100J_1$) at instant t_w for a short time during relaxation of 'staggered' magnetization of the structure evolving from a low-temperature initial state at quenching temperature T_s. Removal of the field gave rise to isothermal relaxation of 'staggered' magnetization and its slow return to the relaxation curve characterizing the nonequilibrium behavior of the structure in the absence of the magnetic field ($h = 0$). The regions within which magnetization first relaxed and thereafter recovered following magnetic field withdrawal to its unperturbed value at $h = 0$ were analyzed at waiting times $t_w = 10$, 50, 100, and 1000 MCS/s and quenching temperatures $T_s = 96$ and 160 K, and $T_s = T_c = 249.6$ K. Figure 41 graphically demonstrates manifestations of aging effects in the relaxation of film magnetization in a multilayer structure, i.e., relaxation slowing down with growing t_w.

The theory of nonequilibrium processes predicts the following scaling dependence for the magnetization behavior (in our case 'staggered' magnetization):

$$m_{stg}(t, t_w) \sim t_w^{-a} F_m\left(\frac{t}{t_w}\right), \tag{110}$$

where exponent a at quenching temperature $T_s = T_c$ is expressed via critical exponents: $a = \beta/(z\nu)$.

The proposed t/t_w dependences of $t_w^a m_{stg}(t, t_w)$ (see Fig. 41) confirmed the scaling form (110) and distinguished the t_w-independent function $F_m(t/t_w)$ where there is an adequate choice of exponent a for each quenching temperature T_s. The figure shows that the 'collapse' of the data in the curve common for all t_w takes place not only at the critical temperature with $T_s = T_c$ but also for $T_s < T_c$.

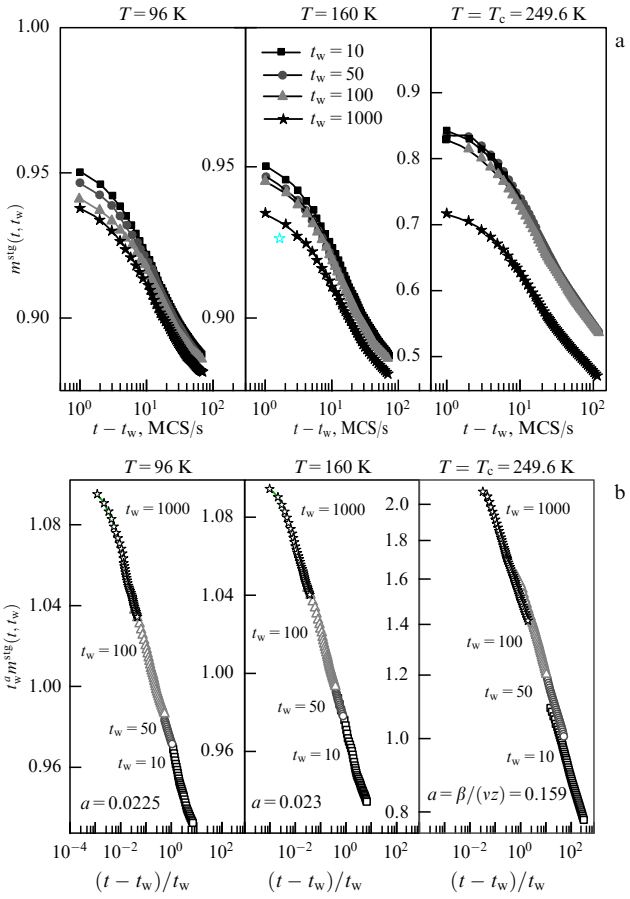

Figure 41. Relaxation of 'staggered' magnetization $m^{stg}(t, t_w)$ from the low-temperature initial state with $m_0^{stg} = 1$ (a) and the dependence of its scaling function $t_w^a m^{stg}(t, t_w)$ on $(t - t_w)/t_w$ (b) for quenching temperatures $T_s = 96$ and 160 K, and $T_s = T_c = 249.6$ K.

The following values for the exponent a were obtained: $a_c = \beta/(z\nu) = 0.159(5)$ at $T_s = T_c = 249.6$ K, $a = 0.022(7)$ at $T_s = 96$ K, and $a = 0.025(7)$ at $T_s = 160$ K. It follows from the comparison of a and b values that equality $b = 2a$, consistent with the ratio of these exponents at the critical temperature, holds within the calculation accuracy. Moreover, aging effects in the relaxation behavior of magnetization in our model multilayer structure are in excellent agreement with those observed in the Co/Cr experiment [13].

To sum up, investigations and calculations of two-time dependences of the autocorrelation function and 'staggered' magnetization by Monte Carlo methods revealed aging effects in the nonequilibrium critical behavior of multilayer magnetic structures not only at $T_s = T_c$ but also in a wide quenching temperature range $T_s < T_c$. Clearly, such nonequilibrium effects should be taken into consideration in practical applications of multilayer magnetic structures as components of spintronic devices with a giant magnetic resistance effect.

8. Conclusions

This review deals with characteristic features of the nonequilibrium critical behavior of far-from-equilibrium macroscopic systems. Special emphasis is laid on the methods for renormalization group and numerical descriptions of model statistical systems, such as the three-dimensional Ising model

and two-dimensional XY model. Processes of the critical relaxation of pure and structurally disordered systems exposed to the influence of abnormally strong fluctuation effects accompanying ordering processes in solids during second-order phase transitions are considered. The current upsurge of interest in such systems comes from predicted and observed aging effects associated with their slow evolution from a nonequilibrium initial state and violations of the fluctuation–dissipation theorem.

Results of numerical studies of the nonequilibrium critical behavior of the three-dimensional Ising model presented in this review give evidence of FDT violations and strong aging effects in the two-time behavior of the correlation and response functions. They show that limiting FDR values characterizing the degree of system departure from equilibrium and FDT violation satisfy inequality $X^{\infty} < 1$ and depend on the universality class of nonequilibrium critical behavior to which they belong: one of these classes corresponds to the high-temperature, and the other to the low-temperature initial state of the system. The concept of threshold initial magnetization m_0^{th} separating these two universality classes falling in the $0.1 < m_0^{\text{th}} < 0.4$ range was introduced.

Numerical research revealed the strong influence of structural defects on nonequilibrium critical behavior of the three-dimensional Ising model. Specifically, a rise in defect concentration results in the strengthening of aging effects manifested as the slowing down of correlation and relaxation processes in structurally disordered systems, in contrast to 'pure' systems. Nonequilibrium initial states begin to increasingly more strongly influence peculiar features and characteristics of the system's evolution. For example, in the case of evolution from a high-temperature initial state with magnetization $m_0 \ll 1$, the influence of defects is manifested in quantitative changes to universal characteristics of nonequilibrium critical behavior, such as critical exponents and the limiting FDR $X^{\infty}(p)$.

It was shown that the presence of structural defects results in setting new $X^{\infty}(p)$ values, with $X^{\infty}(p)$ for strongly structurally disordered systems being higher than $X^{\infty}(p)$ for weakly disordered systems, which, in turn, is higher than $X^{\infty}(p = 1)$ for a 'pure' three-dimensional Ising model. For evolution from a low-temperature initial state with $m_0 = 1$, the autocorrelation function for times $t - t_{\text{w}} \gg t_{\text{w}} \gg 1$ decreases as a power-law of critical magnetization relaxation due to domain wall pinning on structural defects, while limiting FDR values determined by the domain dynamics in the long-time regime become equal to zero. In this case, the two-time scaling dependence of the autocorrelation function was found to obey relations of the 'superaging' theory suggesting enhanced influence of the system's 'age' (the time of onset of t_{w} measurement) determined by the power-law dependence t_{w}^{μ} with exponent $\mu > 1$. The values of this exponent were shown to differ for weakly ($\mu = 2.3(1)$) and strongly ($\mu = 2.8(1)$) disordered Ising models. Investigations into the influence of initial magnetization m_0 on peculiarities of the nonequilibrium critical behavior of the disordered three-dimensional Ising model demonstrated an enhancement of aging effects with increasing m_0 that turn into 'superaging' effects in the autocorrelation function behavior for $m_0 \geqslant 0.25$.

A comprehensive analysis of the nonequilibrium critical dynamics of the three-dimensional Ising model revealed that critical parameters determining the asymptotic behavior of the autocorrelation function and response function belong to different universality classes of critical behavior, namely the critical behavior of 'pure', weakly disordered, and strongly disordered systems. Each of these classes can be subdivided into two universality subclasses of nonequilibrium critical behavior corresponding to the system's evolution from high-temperature and low-temperature initial states with limiting FDR values characteristic for each of them.

Research on the nonequilibrium critical behavior of the three-dimensional Ising model at cyclic temperature variations demonstrated that the time-related behavior of the autocorrelation function in the aging regime exhibits effects of memory about the state of the system at the instant of quenching responsible for the recovery of this state following the return of the temperature to the critical value after the system resides for some time in the 'frozen' state. Domain wall pining on structural defects was shown to prevent the complete recovery of 'memory' about the system's state at the instant of 'quenching'.

When preparing conditions of experiments for the study of critical behavior of different systems and analysis of the experimental data, it is important to take into consideration not only critical slowing down effects but also aging effects that markedly strengthen the critical slowing down effects as the 'sample' age t_{w} increases and underlie the influence of the system's initial states. The presence of structural defects and the increase in their concentration enhance the influence of aging effects.

The review includes results of descriptions of nonequilibrium behavior of one more important statistical system, the two-dimensional XY model providing a basis for research on phase transitions and critical events in such physical systems as ultrathin magnetic films, planar magnets, superfluid thin films, and two-dimensional crystals.

A specific feature of the XY model is the abnormally strong spatial and temporal correlation between the system's states throughout the entire low-temperature phase for $T \leqslant T_{\text{BKT}}$ characterized by power-law decline. It allows the slow dynamics of the two-dimensional XY model to be observed not only near the critical point but also over the entire low-temperature $T \leqslant T_{\text{BKT}}$ range. The numerical description of the nonequilibrium behavior of the two-dimensional XY model as opposed to that of the three-dimensional Ising model is complicated by correlation and relaxation times one or two orders of magnitude longer than those inherent in the latter system, even taking into account the finite-dimensional effect.

Peculiarities of the influence of initial states and structural defects on characteristics of the two-time behavior of response and autocorrelation functions for the two-dimensional XY model were considered and the FDR calculated. One of the factors underlying the influence of initial states is the different time dependence of the correlation length $\xi(t)$. In the course of evolution from a low-temperature initial state, the correlation length $\xi(t) \sim t^{1/2}$, whereas in the case of a high-temperature initial state, this dependence is modified by vortex interaction effects and assumes the form $\xi^2(t) \sim t/\ln t$. In the latter case, the key role is played by high-energy vortex excitations and their interaction. This type of initial state was shown to be associated with the enhancement of aging effects parallel to the increase in structural defect concentration. The behavior of the autocorrelation function for long observation times $t - t_{\text{w}} \gg t_{\text{w}} \gg 1$ was shown to be characterized by a faster decline in the power-law regime than in the aging

regime. The onset of the power-law regime was shown to be shifted toward the longer observation time region with increasing defect concentrations.

Calculations of limiting FDR values $X^{\infty}(p, T \leqslant T_{\mathrm{BKT}}(p))$ for the two-dimensional XY model gave evidence that the influence of structural disorder is responsible for their increase with growing defect concentrations. The temperature dependence of the limiting FDR can be given in the form $X^{\infty} \sim T^{\lambda}$, with the exponent $\lambda(p)$ taking the following values for different impurity concentrations: $\lambda(p = 1.0) = 1.988(23)$, $\lambda(p = 0.9) = 1.848(22)$, and $\lambda(p = 0.8) = 1.838(31)$. Extrapolation of the temperature dependences obtained for $X^{\infty}(p, T \leqslant T_{\mathrm{BKT}}(p))$ as $T \to 0$ gives $\lim_{T \to 0} X^{\infty} = 0$ for all impurity concentrations.

In the evolution of the two-dimensional XY model from a low-temperature initial state, the key role in the influence on model dynamics is played by low-energy spin-wave excitations. The strong influence of structural defects on the nonequilibrium behavior of the autocorrelation function manifests itself in the considerable slowing down of correlation effects in structurally disordered systems in comparison with those in a 'pure' XY model. These pronounced changes are related to cluster fragmentation, i.e., the breakdown of a single large cluster into a few smaller ones. The introduction of defects into the system leads to the abnormal slowing down of cluster fragmentation as confirmed by results of detailed studies on autocorrelation function behavior. In this case, the two-time scaling dependence of the autocorrelation function obeys relations of the 'superaging' theory, and the power-law increase in the influence of the system's age t_{w} is characterized by the exponent $\mu = 1 + \eta(T, p) > 1$, where $\eta(T, p)$ stands for the temperature- and spin concentration-dependent critical exponent related to transverse rigidity of the system.

The review provides evidence that the intriguing features of nonequilibrium behavior manifest themselves in the properties of magnetic superstructures composed of alternating Co/Cr nanoscale magnetic and nonmagnetic layers not only near the critical temperature T_{c} of ferromagnetic ordering in films, but also within a wide temperature range with $T \leqslant T_{\mathrm{c}}$. The nanoscale periodicity stipulates the appearance in these multilayer magnetic structures mesoscopic effects of the spatial spin correlation with slow magnetization relaxation dynamics during quenching of the system in the nonequilibrium state.

It is worthy of note that critical properties of an ultrathin cobalt film on the chromium substrate in a Co(0.6 nm)/Cr(0.78 nm) magnetic superstructure showing experimentally observable aging effects [13] are adequately described by the two-dimensional XY model taking account of finite-dimensional effects [89]. The influence of nonequilibrium aging effects should be taken into consideration in practical applications of multilayer magnetic structures as components of spintronic devices with the giant magnetic resistance effect.

Acknowledgments

This study was partially supported by the Russian Science Foundation (project 14-12-00562), the Russian Foundation for Basic Research (grant 17-02-00279), and a grant MD-6024.2016.2 established by the President of the Russian Federation. Calculations were carried out using resources of the Supercomputer Center of Lomonosov Moscow State University and the Joint Supercomputer Center of the Russian Academy of Sciences.

References

1. Cugliandolo L F, in *Slow Relaxation and Nonequilibrium Dynamics in Condensed Matter* (Les Houches, École d'Ete de Physique Theorique, Vol. 77, Eds J-L Barrat et al.) (Berlin: Springer, 2003) p. 371
2. Henkel M, Pleimling M *Non-Equilibrium Phase Transitions* Vol. 2 (Heidelberg: Springer, 2010)
3. Afzal N, Pleimling M *Phys. Rev. E* **87** 012114 (2013)
4. Ehlers G *J. Phys. Condens. Matter* **18** R231 (2006)
5. Berthier L, Kurchan J *Nature Phys.* **9** 310 (2013)
6. Vincent E et al. *Lect. Notes Phys.* **492** 184 (1997)
7. Bouchaud J P et al., in *Spin Glasses and Random Fields* (Directions in Condensed Matter Physics, Vol. 12, Ed. A P Young) (Singapore: World Scientific, 1998) p. 443
8. Calabrese P, Gambassi A *J. Phys. A* **38** R133 (2005)
9. Berthier L, Holdsworth P C W, Sellitto M *J. Phys. A* **34** 1805 (2001)
10. Pleimling M, Gambassi A *Phys. Rev. B* **71** 180401(R) (2005)
11. Gambassi A *Eur. Phys. J. B* **64** 379 (2008)
12. Drovosekov A B et al. *JETP Lett.* **88** 118 (2008); *Pis'ma Zh. Eksp. Teor. Fiz.* **88** 126 (2008)
13. Mukherjee T, Pleimling M, Binek Ch *Phys. Rev. B* **82** 134425 (2010)
14. Prudnikov V V et al. *JETP* **106** 1095 (2008); *Zh. Eksp. Teor. Fiz.* **133** 1251 (2008)
15. Prudnikov V V et al. *JETP* **110** 253 (2010); *Zh. Eksp. Teor. Fiz.* **137** 287 (2010)
16. Prudnikov V V et al. *JETP* **105** 371 (2007); *Zh. Eksp. Teor. Fiz.* **132** 417 (2007)
17. Prudnikov V V et al. *Phys. Rev. E* **81** 011130 (2010)
18. Prudnikov V V et al. *Prog. Theor. Phys.* **117** 973 (2007)
19. Prudnikov P V, Medvedeva M A *Prog. Theor. Phys.* **127** 369 (2012)
20. Rosov N, Hohenemser C, Eibschütz M *Phys. Rev. B* **46** 3452 (1992)
21. Calabrese P, Gambassi A *Phys. Rev. E* **66** 066101 (2002)
22. Calabrese P, Gambassi A *Phys. Rev. B* **66** 212407 (2002)
23. Prudnikov V V, Prudnikov P V, Purtov A N, Mamonova M V *JETP Lett.* **104** 776 (2016); *Pis'ma Zh. Eksp. Teor. Fiz.* **104** 797 (2016)
24. Cugliandolo L F, Kurchan J, Peliti L *Phys. Rev. E* **55** 3898 (1997)
25. Godréche C, Luck J M *J. Phys. Condens. Matter* **14** 1589 (2002)
26. Calabrese P, Gambassi A *J. Phys. A* **38** R133 (2005)
27. Godréche C, Luck J M *J. Phys. A* **33** 9141 (2000)
28. Cugliandolo L F, Kurchan J, Parisi G *J. Physique* **4** 1641 (1994)
29. Lippiello E, Zannetti M *Phys. Rev. E* **61** 3369 (2000)
30. Mayer P et al. *Phys. Rev. E* **68** 016116 (2003)
31. Chatelain C *J. Phys. A* **36** 10739 (2003)
32. Chatelain C *J. Stat. Mech.* P06006 (2004)
33. Abriet S, Karevski D *Eur. Phys. J. B* **41** 79 (2004)
34. Janssen H K, Schaub B, Schmittmann B *Z. Phys. B* **73** 539 (1989)
35. Hohenberg P C, Halperin B I *Rev. Mod. Phys.* **49** 435 (1977)
36. Oerding K, Janssen H K *J. Phys. A* **28** 4271 (1995)
37. Oerding K, Janssen H K *J. Phys. A* **26** 3369 (1993)
38. Oerding K, Janssen H K *J. Phys. A* **26** 5295 (1993)
39. Jaster A et al. *J. Phys. A* **32** 1395 (1999)
40. Prudnikov V V, Vakilov A N, Prudnikov P V *Fazovye Perekhody i Metody Ikh Komp'yuternogo Modelirovaniya* (Phase Transitions and Methods of Their Computer Simulation) (Moscow: Fizmatlit, 2009)
41. Prudnikov V V, Prudnikov P V, Vakilov A N *Teoreticheskie Metody Opisaniya Neravnovesnogo Kriticheskogo Povedeniya Strukturno-neuporyadochennykh Sistem* (Theoretical Methods for the Description of Nonequilibrium Critical Behavior of Structurally Disordered Systems) (Moscow: Fizmatlit, 2013)
42. Vasil'ev A N *Field Theoretic Renormalization Group in Critical Behavior Theory and Stochastic Dynamics* (Boca Raton, FL: Chapman and Hall. CRC, 2004); Translated from Russian: *Kvantovopolevaya Renormgruppa v Teorii Kriticheskogo Povedeniya i Stokhasticheskoi Dinamike* (St. Petersburg: Izd. PIYaF, 1998)
43. Pelissetto A, Vicari E *Phys. Rep.* **368** 549 (2002)
44. Prudnikov V V, Prudnikov P V *JETP* **95** 550 (2002); *Zh. Eksp. Teor. Fiz.* **122** 636 (2002)
45. Folk R, Holovatch Yu, Yavorskii T *Phys. Usp.* **46** 169 (2003); *Usp. Fiz. Nauk* **173** 175 (2003)
46. Calabrese P, Gambassi A, Krzakala F *J. Stat. Mech.* P06016 (2006)
47. Janke W *Lect. Notes Phys.* **739** 79 (2008)

48. Prudnikov V V, Prudnikov P V, Pospelov E A *J. Phys. Conf. Ser.* **510** 012015 (2014)
49. Prudnikov V V, Prudnikov P V *J. Phys. Conf. Ser.* **510** 012020 (2014)
50. Prudnikov P V et al. *Prog. Theor. Exp. Phys.* 053A01 (2015)
51. Ferrenberg A M, Landau D P *Phys. Rev. B* **44** 5081 (1991)
52. Ricci-Tersenghi F *Phys. Rev. E* **68** 065104(R) (2003)
53. Godrèche C, Krzakala F, Ricci-Tersenghi F *J. Stat. Mech.* P04007 (2004)
54. Prudnikov P V, Prudnikov V V, Pospelov E A *JETP Lett.* **98** 619 (2013); *Pis'ma Zh. Eksp. Teor. Fiz.* **98** 693 (2013)
55. Prudnikov V V, Prudnikov P V, Pospelov E A *J. Stat. Mech.* 043303 (2016)
56. Guida R, Zinn-Justin J *J. Phys. A* **31** 8103 (1998)
57. Krinitsyn A S, Prudnikov V V, Prudnikov P V *Theor. Math. Phys.* **147** 561 (2006); *Teor. Mat. Fiz.* **147** 137 (2006)
58. Harris A B *J. Phys. C* **7** 1671 (1974)
59. Kamilov I K, Murtazaev A K, Aliev Kh K *Phys. Usp.* **42** 689 (1999); *Usp. Fiz. Nauk* **169** 773 (1999)
60. Murtazaev A K, Kamilov I K, Babaev A B *JETP* **99** 1201 (2004); *Zh. Eksp. Teor. Fiz.* **126** 1377 (2004)
61. Birgeneau R J et al. *Phys. Rev. B* **27** 6747 (1983)
62. Mitchell P W et al. *Phys. Rev. B* **34** 4719 (1986)
63. Rosov N et al. *Phys. Rev. B* **37** 3265 (1988)
64. Slanič Z, Belanger D P, Fernandez-Baca J A *Phys. Rev. Lett.* **82** 426 (1999)
65. Prudnikov V V, Prudnikov P V, Fedorenko A A *Phys. Rev. B* **62** 8777 (2000)
66. Prudnikov V V, Vakilov A N *JETP Lett.* **55** 741 (1992); *Pis'ma Zh. Eksp. Teor. Fiz.* **55** 709 (1992)
67. Prudnikov V V, Vakilov A N *JETP* **76** 469 (1993); *Zh. Eksp. Teor. Fiz.* **103** 962 (1993)
68. Pelissetto A, Vicari E *Phys. Rev. B* **62** 6393 (2000)
69. Ballesteros H G et al. *Phys. Rev. B* **58** 2740 (1998)
70. Parisi G, Ricci-Tersenghi F, Ruiz-Lorenzo J J *Phys. Rev. E* **60** 5198 (1999)
71. Hasenbusch M, Pelissetto A, Vicari E *J. Stat. Mech.* P11009 (2007)
72. Schehr G, Paul R *Phys. Rev. E* **72** 016105 (2005)
73. Schehr G, Paul R *J. Phys. Conf. Ser.* **40** 27 (2006)
74. Heuer H-O *Phys. Rev. B* **42** 6476 (1990)
75. Heuer H-O *J. Phys. A* **26** L341 (1993)
76. Wiseman S, Domany E *Phys. Rev. Lett.* **81** 22 (1998)
77. Wiseman S, Domany E *Phys. Rev. E* **58** 2938 (1998)
78. Prudnikov V V et al., in *Trudy Seminara po Vychislitel'nym Tekhnologiyam v Estestvennykh Naukakh* (Proc. of the Seminar on Computation Technologies in Natural Sciences) Issue 1 *Vychislitel'naya Fizika* (Computational Physics) (Ed. R R Nazirov) (Moscow: Izd. KDU, 2009) p. 240
79. Prudnikov V V et al. *Vestn. Omsk. Univ.* (2) 101 (2012)
80. Prudnikov V V, Prudnikov P V, Pospelov E A *JETP* **118** 401 (2014); *Zh. Eksp. Teor. Fiz.* **145** 462 (2014)
81. Prudnikov V V et al. *Phys. Lett. A* **379** 774 (2015)
82. Prudnikov V V et al. *JETP Lett.* **102** 167 (2015); *Pis'ma Zh. Eksp. Teor. Fiz.* **102** 192 (2015)
83. Prudnikov V V, Vakilov A N, Talashok D V *JETP Lett.* **100** 675 (2014); *Pis'ma Zh. Eksp. Teor. Fiz.* **100** 760 (2014)
84. Bray A J *Adv. Phys.* **43** 357 (1994)
85. Berezinskii V L *Nizkotemperaturnye Svoistva Dvumernykh Sistem s Nepreryvnoi Gruppoi Simmetrii* (Low-temperature Properties of Two-dimensional Systems with Continuous Symmetry Group) (Moscow: Fizmatlit, 2007)
86. Berezinskii V L *Sov. Phys. JETP* **32** 493 (1971); *Zh. Eksp. Teor. Fiz.* **59** 907 (1970)
87. Kosterlitz J M, Thouless D J *J. Phys. C* **6** 1181 (1973)
88. Kosterlitz J M *J. Phys. C* **7** 1046 (1974)
89. Vaz C A F, Bland J A C, Lauhoff G *Rep. Prog. Phys.* **71** 056501 (2008)
90. Korshunov S E *Phys. Usp.* **49** 225 (2006); *Usp. Fiz. Nauk* **176** 233 (2006)
91. Bulaevskii L N, Kuzii V V, Sobyanin A A *JETP Lett.* **25** 290 (1977); *Pis'ma Zh. Eksp. Teor. Fiz.* **25** 314 (1977)
92. Buzdin A I, Bulaevskii L N, Panyukov S V *JETP Lett.* **35** 178 (1982); *Pis'ma Zh. Eksp. Teor. Fiz.* **35** 147 (1982)
93. Buzdin A I, Bujicic B, Kupriyanov M Yu *JETP* **74** 124 (1992); *Zh. Eksp. Teor. Fiz.* **101** 231 (1992)
94. Bray A J, Briant A J, Jervis D K *Phys. Rev. Lett.* **84** 1503 (2000)
95. Lei X W, Zheng B *Phys. Rev. E* **75** 040104(R) (2007)
96. Prudnikov V V et al. *Phys. Met. Metallogr.* **115** 1186 (2014); *Fiz. Met. Metalloved.* **115** 1254 (2014)
97. Prudnikov P V, Popov I S *J. Phys. Conf. Ser.* **510** 012014 (2014)
98. Prudnikov P V, Prudnikov V V, Popov I S *JETP Lett.* **101** 539 (2015); *Pis'ma Zh. Eksp. Teor. Fiz.* **101** 596 (2015)
99. Weber H, Minnhagen P *Phys. Rev. B* **37** 5986(R) (1988)
100. Abriet S, Karevski D *Eur. Phys. J. B* **37** 47 (2004)
101. Popov I S, Prudnikov P V, Prudnikov V V *J. Phys. Conf. Ser.* **681** 012015 (2016)
102. Prudnikov V V, Prudnikov P V, Purtov A N *Vestn. Omsk. Univ.* (3) 33 (2016)
103. Prudnikov V V, Prudnikov P V, Romanovskii D E *JETP Lett.* **102** 668 (2015); *Pis'ma Zh. Eksp. Teor. Fiz.* **102** 759 (2015)
104. Prudnikov P V, Prudnikov V V, Medvedeva M A *JETP Lett.* **100** 446 (2014); *Pis'ma Zh. Eksp. Teor. Fiz.* **100** 501 (2014)
105. Prudnikov P V et al. *J. Magn. Magn. Mater.* **387** 77 (2015)